THE UNIVERSITY OF OKLAHOMA

GRADUATE COLLEGE

INTERACTION EFFECTS OF WIND-BLOWN PROXIMATE FLAMES FROM BURNING WOOD CRIBS

A DISSERTATION

SUBMITTED TO THE GRADUATE FACULTY

in partial fulfillment of the requirements for the

degree of

DOCTOR OF PHILOSOPHY

BY

JOE RIOS

Norman, Oklahoma

1966

INTERACTION EFFECTS OF WIND-BLOWN

PROXIMATE FLAMES FROM BURNING

WOOD CRIBS

APPROVED BY

DISSERTATION COMMITTEE

ACKNOWLEDGMENTS

The writer wishes to express his sincere gratitude to the many persons who have assisted in the analysis, laboratory work, and evaluation stages of this study.

Thanks are extended to all those who assisted in the preparation of this dissertation.

The continual encouragement and assistance offered by the author's committee chairman, Dr. C. M. Sliepcevich, is especially appreciated. The suggestions by other members of the doctoral committee were also helpful.

My sincere appreciation is extended to Dr. Omer A. Pipkin and Dr. J. Reed Welker for the many helpful discussions during the course of this study.

The invaluable ideas and assistance during the design and assembly of the combustion tables and photographic equipment provided by Mr. H. M. Bradbury, the important contributions made by Mr. J. Morrison and his associates of the University of Oklahoma Research Institute Shop at various instances during the fabrication of the equipment and apparatus and the help offered by Messrs. J. Turpin and G. Bradley during the assembly of the test setup are appreciated.

Thanks are also extended to the writer's fellow graduate students: Messrs. M. Ghaffarzadeh, A. N. Koohyar, K. Huffman, and P. Mody for the hours spent helping gather the experimental data, and to Mr. M. D. Nasta who carried out several of the calculations.

The financial assistance provided by the Ford Foundation during the writer's graduate study and the sponsorship of this dissertation by the University of Oklahoma Research Institute is fully appreciated.

And, finally, the writer wishes to express his gratitude to those who have contributed in any way to this task and whose effort may have been inadvertently overlooked.

Joe Rios

TO

My wife Eva and our children, Sinia, Joe R. and Sigfredo R.

TABLE OF CONTENTS

Page

APPENDICES

LIST OF TABLES

Table | Page

LIST OF ILLUSTRATIONS

INTERACTION EFFECTS OF WIND-BLOWN PROXIMATE FLAMES FROM BURNING WOOD CRIBS

CHAPTER I

INTRODUCTION

The occurrence of uncontrolled, and usually unexpected, burning of combustible materials presents a great number of economic and social problems. The concern for these problems is not new. In fact, fireproofing dates back farther than 400 B.C. (69). In modern times, the problems of suppression and prevention have been the concern of various private and government organizations. Some $20 million are spent annually in the United States in fire-related research and development, of which no more than $1 million is directed towards fundamental research (69). The remainder is directed mainly to work of an applied nature. Yet, the above $20 million only represents about 0.4 per cent of the total annual cost of fire in this nation, or about 1.3 per cent of the annual cost of direct physical damage.

Besides the economic aspect, the social problems are also of great magnitude. The loss of life (which in the

United States numbers about 11,500 annually), the care for the injured, the unemployment that destruction of a factory or industry creates, the indirect effect and losses to others, such as increase in the cost of insurance, losses caused by interruption of business due to the reduction in the supply of materials or products to other regions, destruction of parks and recreational areas, etc., are a few of them.

In certain cases, the occurrence of an unexpected fire has been beneficial, particularly when it has helped clear certain sites or eliminate slum areas or condemned structures. These examples indicate instances in which fire could be put to good use. Yet, the application of fire techniques under controlled conditions is hindered because the degree of control required cannot be ascertained until a more fundamental knowledge of fire behavior is available.

A large body of knowledge concerning fire prevention and suppression techniques exists at the present time, and it keeps increasing every day. In recent years, a greater emphasis has been placed on fundamental research since it, for a long time, had been neglected in comparison with research of an applied nature. Flames from solid, liquid and gaseous fuels have been studied with a greater emphasis being placed on obtaining information and correlating those variables which will provide a basic understanding of the behavior and characteristics of the fire. This information should provide a better base for determining standards, codes and methods of fire suppression and prevention.

Small laminar flames, mostly from gaseous fuels, have been analyzed extensively. Most of the studies have dealt with the temperature distribution in the flame, the kinetics of the chemical reactions and spectroscopic analyses of the flames.

The flames from gaseous fuels are frequently of the "jet" type, i.e., the initial momentum of the gas leaving the burner is high compared with the buoyancy forces acting on the flame. The flames are known as "buoyant" when the buoyant force causing the hot gases to rise is large in comparison with the momentum of the fuel leaving the source.

The rate of burning of flames from gaseous burners is controlled by the rate of fuel supply and, therefore, the flames are termed "controlled flames." The flames from liquid and solid fuels are mostly of the "uncontrolled" type in which the rate of burning is determined mainly by the characteristics of the fuel and those of the surroundings.

The studies of flames from gaseous fuels have comprised both "premixed" and "diffusion" type of flames. In the "premixed" flames, the fuel is mixed with the oxidizer prior to entering the combustion zone; in the diffusion flame the oxidizer necessary for combustion is obtained from the surroundings by eddy or molecular diffusion at and within the reaction zone. The flames from liquid and solid fuels burning freely are of the diffusion type.

Lately, the emphasis on basic research has centered around larger fires. This interest is prompted by the immediate applicability of the results to fires involving dwellings, forests, fuel tanks, etc. These fires are of a turbulent nature. Their behavior is usually described in terms of gross, readily measurable physical parameters.

Since actual scale tests of this nature are difficult and expensive, the testing is in most cases performed on a smaller scale or model. Several papers available in the literature deal with the problem of modeling of fires, i.e., interpreting and extending the information obtained on the small scale to the full sized phenomena and vice versa.

Studies of fires in still air have been carried out by a large number of experimenters. Most of these tests have simulated or modeled the burning of buildings and forests. Due in part to these applications, a great number of tests have been carried out with solid fuels (mostly wood).

In the early tests, wind was considered a nuisance and experimental techniques avoiding or minimizing the effect of wind were usually utilized (17, 33, 80, 8, 46). Recently, however, the effect of wind on buoyant diffusion flames has been the subject of several papers appearing in the literature. In almost any actual case, the wind will influence the behavior of the flame.

Most of the experiments have been concerned with the analysis of single fires. A few have considered flames from

multiple sources. The multiple fire problem is complex and for initial analysis, simplified models have been utilized. Much of this work will be considered in detail later.

When the sources are distant from each other, each fire can be considered as a single flame and analyzed as such. However, as the separation distance decreases the flames interact with each other.

At this point, it is well to distinguish between the terms "interaction" and "merging" as used in this work. Consider several sources arranged in a certain pattern and spaced at a considerable distance from each other compared with the dimension of each individual source. As the spacing is reduced, each flame will start influencing the surrounding ones even before they touch each other. These effects will be termed "flame interactions." As the spacing is reduced further each flame starts touching the adjacent ones. This point is considered the onset of merging. From this point on, the degree of merging varies as spacing diminishes until, for closely spaced sources, full merging of the fires occurs. Thus, "merging" is included within the range of flame "interactions."

It is probably correct to say that most of the experimental data and analyses available for multiple fires are for the case of flame merging. There seem to be few results available for the interaction effects prior to merging. The data available are essentially from tests involving unsteady

burning under calm conditions. However, the action of the wind is expected to have some influence on flame interactions. Such questions as how the wind velocity profile is altered by the first encounter of the wind with a flame and how subsequent encounters are affected, how the inclination of the individual flames by wind is influenced, how the individual burning rates are modified, how the spatial temperature distributions of the surroundings at ground level and in the downwind plume are established, and many others, remain to be investigated.

It is the purpose of this work to seek answers to these questions on a foundation of simple models, dimensional analysis and experimentation.

As a first step in this direction, the case of the interaction of the wind on two proximate fires burning one downwind of the other has been chosen for investigation because of its geometrical simplicity. Furthermore, this situation, as a model, may apply to certain large-scale fires, for example, forest fires and the backfires utilized to fight them.

CHAPTER II

BACKGROUND AND RESEARCH OBJECTIVES

This chapter commences with a general introduction to the nature of fire research and is followed by a presentation of the previous work related to the more basic aspects of multiple fires and interaction effects. A discussion of the objectives of the present work and the selection of fuels concludes the chapter.

General

Fire played an important role in the areas of philosophy, mythology, religion, and alchemy of ancient civilizations. It was once classed with air, earth, and water, as one of the four elements making up the universe. Much of the advancement in modern technology has been due to the harnessing of combustion processes and their utilization in various industrial and chemical processes. The concern about the uncontrolled occurrence of fires has centered mostly on their damaging aspects. Such a concern is a very old one indeed. Thus, it is not surprising to find that the earliest work concerning fire dealt with the treatment of combustible materials to reduce their vulnerability. Gay-Lussac (30)

probably carried out the first systematic investigation of the fireproofing of cellulosic materials about 1821. Preliminary observations of small flames date as far back as about 1600 (28). Since then, a great deal of the work reported in the literature has been concerned with prevention, suppression and fireproofing techniques. These techniques have been utilized in many instances for the creation of codes, regulations, standards, and procedures to limit and combat the fire hazard. Thus, although hundreds of papers are available in the literature covering practically every aspect of fire research, their usefulness in basic research is limited by their applied and sometimes specific nature. However, they provide a good background and a starting point for certain areas of research.

Lately, more attention has been given to the quantitative description of flames. Small laminar flames, both of the diffusion and premixed types have been the subject of a great number of investigations. The composition and temperature fields within the flame have been analyzed on various occasions. Flame appearance, size, and radiation characteristics have been measured and described. The development of new experimental techniques has greatly aided the analysis of small laminar flames. Since the results derived from the study of such flames are not directly applicable to the present work, they will not be discussed further, but the reader is referred

to the works of Lewis and von Elbe (45), Gaydon (31), Gaydon and Wolfhard (32), Pyrodynamic Journals (61), International Symposium on Combustion Series (39), Fuel (29), Combustion and Flame (11), and Fire and Research Abstracts and Reviews (21), for a thorough presentation of the subject. Also, a recent book by Fristrom and Westenberg (28) presents a comprehensive treatment of one dimensional, laminar, premixed gaseous flames with emphasis being placed on a detailed description of experimental techniques and methods of data analysis. Two additional books with a much broader coverage are those of Fenimore (20) and of Williams (83). Additional publications on the subject are listed in an appendix in reference (28).

Freely burning turbulent flames, due to the complexity of the flow processes within the flame and surroundings, have been analyzed in almost every case in terms of the gross properties of the flame. A great amount of work on such flames has been carried out in Great Britain and Japan. A summary of the history of fire research and present work being done in these countries can be found in the works of Lawson (44) and Kinbara (43). In the United States, several agencies have been and are still contributing to the effort. A listing of them and the projects in which they are involved can be found in the Directory of Fire Research in the United States (14). In addition, Brown (7) summarizes the work presently being done on forest fire research in the United States, and

Robertson (63) summarizes that being done by the National Bureau of Standards. A summary of forest fire research projects being carried out in Canada is listed in the Directory of Forest Fire Research Projects (15). A survey of the projects listed reveals that, although the number of such projects is considerable, only a small fraction deals with studies in basic research.

Related Previous Work

Most previous studies have considered single flames from solid, liquid and gaseous fuels. The multiple fire problem is complex and initial analysis has been based on simple models. The need for an understanding of this problem arises from the catastrophic nature of the conflagration and the firestorm to which it is closely related. Both are multiple fires phenomena inasmuch as several fuel units (houses, trees, etc.) are burning simultaneously; however, a conflagration is characterized by a moving fire front driven by a strong wind while a firestorm is an area fire in which most of the available fuel over the area is ignited and burns simultaneously. While the conflagration ignites new fuel ahead of it leaving smoldering ashes in its wake, the very strong inflow of air at the periphery of a firestorm prevents it from spreading outwardly. Conflagrations are common occurrences in forest fires. They have originated in the past in cities after a strong earthquake, from a grass

or forest fire sweeping in from the surroundings, or from a small fire. Firestorms occur rarely in peacetime. One could probably occur as a result of a severe earthquake. During wartime, fire-bomb raids or a nuclear attack can cause firestorms under the proper conditions. Examples of such occurrences during wartime are the destructive fires which resulted after the attacks on the cities of Hamburg, Dresden, Nagasaki and Hiroshima in World War II.

The production of multiple fires on a large scale for purposes of investigation is prohibitively expensive. Researchers thus far have had to rely on information obtained from small laboratory or field fires to predict and correlate the phenomena of mass fires with the awareness that such an extrapolation is liable to possess large deviations.

The available literature on multiple fires is limited. Thomas, et al. (76) reported on the onset of merging of flames for two different configurations: two rectangular fuel beds, and four square fuel beds. Each fuel bed was made up of 1 foot square burners supplied with town gas and with the space between and surrounding the burner filled in to provide a flat surface in the plane of the burners. Putnam and Speich (58, 60) have analyzed a number of flame arrays utilizing gas burners operating under conditions such that the flames were buoyancy controlled. The purpose was to establish considerations for a model utilizing gaseous fuels, in which case the burning rate is independent of heat feedback into

the fuel. It was determined that in order to insure the attainment of turbulent-buoyancy controlled flames a Reynolds number, based on the size of the orifice and the properties of the fuel gas, had to exceed a value of 5000 and a Froude number defined as (Q_o^2/gd_o^5) should have a value not exceeding 8000.* Q_o is the volume flux of fuel through a single source, g is the gravitational acceleration and d_o is the diameter of the orifice. This model was to be utilized in investigating the parameters which are significant in the merging of a number of individual fires into a mass fire. The data obtained were analyzed and presented from two different viewpoints--considering the total flame source as a series of small or point sources of fuel, and considering the total flame source on an area basis.

Later on, Putnam and Speich (59) pursued further their study of multiple flames of various array patterns. Different classes of flames were produced and the increase in flame length of a single source was measured. The flames were classified as acting as a single-point source, area source, line source, and a number of individual sources. Point and area-

---

*The nomenclature used throughout the discussion of the work of other authors has been kept essentially the same as presented in the various papers. Although in some instances, different symbols are used to represent the same variable, it was decided not to alter the original nomenclature in order to facilitate referring to the original work by someone interested in more detailed discussion.

source flames were exposed to cross-winds. Dual sources were utilized to determine the distance at which two buoyancy-controlled turbulent diffusion flames originating at essentially point sources merge. In addition, experiments on the merging of two multiple source arrays were carried out.

In the extension of the above work by Putnam (57), area- and line-source fires exposed to various cross winds were considered. Both the flame height and the horizontal extent of the flame were measured and related to the unblown height. For a point source he found (for $V^2/gL^* > 0.2$)

$$L_{sv}/L^* = 0.45\ (V^2/gL^*)^{-1/4} \qquad (1)$$

and

$$L_{sh}/L^* = 0.60\ (V^2/gL^*)^{1/6} \qquad (2)$$

For line fires he found

$$L_{sv}/\bar{L}^* = (1+4\ V^2/g\bar{L}^*)^{-1/2} \qquad (3)$$

and the ratio of horizontal flame projection to flame height to be

$$L_{sh}/L_{sv} = 1.4\ (V^2/g\bar{L}^*)^{1/2} \qquad (4)$$

where L_{sv} and L_{sh} are the height and the horizontal projection of the blown flame respectively. L^* is the height of a single isolated flame with no wind, $\bar{L}^*$ is the height of array with no wind, V is the wind velocity and g is the gravitational acceleration.

Burning rates of a fuel bed of 4 kg of wood observed as a single pile and as a complex of two piles with varying separations were reported by Strasser and Grumer (68). As

a result of their observations, they concluded that radiative heat transfer between proximate fires augments the burning rate to a much lesser extent than convective heat transfer.

Countryman (12) has described outdoor experiments on a much larger scale than laboratory fires (plots up to 2,200,000 sq. ft. in size were used). The plots were prepared using different fuel types classed as fine fuels, heavy fuels and mixed fuels. In addition, a two-story wooden frame house was also burned. Several of the plots were arranged in the form of multiple piles simulating urban conditions.

Waterman, et al. (80) have also analyzed the coalescence of convective columns, in this case from freely burning fires. Laboratory experiments with liquid fuel fires and with wood crib fires, as well as larger-scale field experiments, were considered. Their tests indicated that coalescence is a function not only of the proximity of the fires, but also of the total number of fires. A criterion for coalescence based upon a rapid change in the total burning rate of each array coinciding with a transition from coalesced to non-coalesced fires is presented. It was found that the burning rate tended to increase as the space between the cribs was increased until a transition point was reached at which time the burning rate suffered a sudden drop in magnitude. The scaling law for coalescence was presented as

$$\left(\frac{\text{distance between cribs}}{\text{crib dimension}}\right)_{peak} = 0.069\ (nR_s)^{0.4} \quad (5)$$

where

n = number of cribs

R_s = burning rate of a single crib

The burning rate at transition, R_{peak}, was given as

$$R_{peak} = 1.56\ (nR_s) \quad (6)$$

The fires for these studies were burned under as calm conditions as possible with respect to wind disturbances. In addition, the arrays were set on fire so that all the combustible material reached a fully involved state simultaneously.

Huffman (38) has pursued further this study utilizing square and circular cell patterns in which various liquid fuels (acetone, normal-hexane, cyclohexane, benzene and napalm test solvent) were burned. The burning rate data for all the fuels were successfully brought into a single correlation by introducing the burning rate function, BRF, defined as

$$BRF = \dot{m}''\left(\frac{\Delta H_v}{\Delta H_c}\right)\left(\frac{\dot{m}''_{peak}}{\dot{m}''}\right) \quad (7)$$

and plotting it against the parameter $S/D\left(\dot{m}''_s\right)^{-q}$

where

$\dot{m}''$ = burning rate per unit area of burner surface for fuel cells in the array.

$\dot{m}''_{peak}$ = burning rate per unit area of burner surface for fuel cells in the array at the onset of merging

$\dot{m}''_s$ = burning rate per unit area of burner surface of a single cell

ΔH_v = latent heat of vaporization of the fuel

ΔH_c = lower heat of combustion of the fuel (product water in vapor state)

q = exponent

s = spacing between centers of the cells in the square array; radius of the circular array

D = length of the side of the square cells; diameter of the circular cells

The foregoing comprises the work that has been done on multiple fires. As can be seen, the amount of analysis and experimental work available is limited. Furthermore, the interactions between the flames from nearby-fires and wind have not been given adequate attention.

Most of the work that has been reported in the literature has been done utilizing single flames. Almost every important parameter has been considered; some of them rather crudely and some in great detail.

Among those of importance for this work is that of flame inclination. An immediately noticeable effect of wind on a flame is the inclination of the latter from the vertical and toward the downwind direction. Undoubtedly, this interaction is a very complex one. Nevertheless, in recent years, theories based on simplified models aimed at a quantitative description of this effect have appeared in the literature.

The first of the theories seems to be that presented by Hamada (34) in 1952 in trying to correlate the action of the wind on flames from burning wooden residential structures. Pipkin and Sliepcevich(55) recently proposed a similar correlation based on a limited number of experiments in which small-size natural gas flames were observed in a small-scale wind tunnel. They assumed that the envelope of the flame could be represented by a cylindrical surface. Upon being blown by the wind, the cylindrical surface would tilt to a position determined by an equilibrium of the forces of buoyancy, wind pressure, and the momentum of the fuel. This work was further revised by Welker, et al. (82) resulting in a satisfactory correlation of the data.

Welker carried out further work along this line (81), utilizing liquid fuels (methanol, acetone, normal hexane, cyclohexane and benzene) that were burned in circular and rectangular burners of various sizes (7 circular burners ranging in size from 1 inch to 24 inches, and 4 channel burners 5 feet long and ranging in width from 2 to 8 inches) mounted flush with the floor of the test section of a wind tunnel.

Anderson and Rothermel (2) have considered a correlation of the flame bending angle in terms of the momentum of the airstream and of the momentum of the convection column as

$$\tan \theta = \frac{\text{momentum of air stream}}{\text{momentum of convection column}} \qquad (8)$$

where θ is the angle of inclination of the flame from the vertical. They evaluated the momentum ratio by assuming it to be proportional to the ratio of the energy rate per unit area of the airstream to the equivalent unit energy release rate of the fire. Their data showed good correlation within the range of 25 to 60 degrees of inclination, with no evidence of dependence upon moisture content or species of pine needles used.

Flame height and horizontal projection of wind blown flames were measured by Putnam (57) from which bending angles can be obtained (see p. 13) in terms of the Froude number V^2/gL^* or $V^2/g\bar{L}^*$.

Another parameter of importance, which has been measured by various experimenters, is the burning rate. In the case of gaseous fuels the supply of combustible material to the flame is independent of heat-feedback to the fuel. Thus, the burning rate can be varied by the experimenter. In most cases its metering has been carried out by means of calibrated orifices. On the other hand, with liquid and solid fuels, the burning rate is determined by the amount of energy available through the feedback mechanism from flame and surroundings to the unburned fuel.

In those cases, where a given amount of liquid fuel has been burned without supplying additional fuel to the burner while the burning process was going on, the burning rate has been evaluated as the mass of liquid fuel initially available divided by the total time it took to burn it, i.e.

the total burning time. In some cases, the depth of the liquid fuel has been utilized in lieu of its mass (17). In other cases, the level of the liquid has been noted at various times during the burning process. In the latter two instances, a burning rate has been determined in terms of what has been called "the mean-burning-velocity." It is defined and measured as the depth of liquid fuel which has burned divided by the burning time considered. This mean-burning-velocity has also been called the liquid level regression rate.

Extensive measurements on the rate of burning and the temperature distribution beneath the surface of burning liquids had been carried out by Khudyakov (1945) (41), Burgoyne and Katan (1947) (9), Katan (1949) (40), Williams-Leir (1951) (84), Khudyakov (1951) (42), and Spalding (1953) (67).

An overflow system was utilized by Rasbash, et al. (1956) (62) to maintain the level of the liquid fuel constant at 2.00 cm below the top of the combustion vessel, during their experiments with alcohol, benzene, gasoline and kerosine. Volume replacement was utilized for the measurement of burning rate. Some tests were for the purpose of checking the volume replacement method. In these tests the quantity of fuel consumed was obtained from the difference in the weight of the fuel before and after the flaming had occurred.

In 1957, Blinov and Khudyakov (4) published the results of their work on fires burning from the surface

of liquid fuels. Gasoline, tractor kerosine, diesel oil, and solar oil were burned in cylindrical burners of diameters ranging from 3.7 mm to 22.9 meters. The broad range of diameters covered made this work significant. Their data showed three burning regimes present for the pan sizes involved. Laminar flames were present at the burners having diameters less than 3 cm and the burning rate (measured in terms of the liquid level regression rate) decreased with increasing diameter in this regime. As pan diameters increased from 3 cm to 10 cm, the flame structure started to change from laminar to turbulent. This regime was considered as a transition one. The burning rate kept decreasing and leveled off at about 10 cm. From this burner size on, and until about 130 cm, the burning rate increased with increasing pan diameters. At about 130 cm a fully turbulent flame structure was already established. For diameters larger than 130 cm, the burning rate was not influenced by changes in burner size.

In a review of Blinov and Khudyakov's work, Hottel (36) discussed a semiquantitative description of the burning rate behavior obtained. Since the burning rate is determined by the fuel vaporization rate, which in turn depends upon the heat transfer to the liquid fuel, he was able to provide some explanations by considering the mechanisms which contribute to the heat feedback in the laminar, transition, and turbulent regimes. He assumed the heating rate, given by q, to be the sum of components due to conduction from the pan rim, convection from the flame, and flame radiation, denoted

as q_1, q_2, and q_3 respectively. The vaporization rate per unit of surface would be given by

$$\frac{q}{\pi d^2/4} = \frac{q_1+q_2+q_3}{\pi d^2/4} \tag{9}$$

or

$$\frac{q}{\pi d^2/4} = \frac{4k(T_f-T_b)}{d} + U(T_f-T_b) + \sigma F(T_f^4-T_b^4)(1-e^{-\varkappa d}) \tag{10}$$

where

q = heat transfer rate to the fuel

k = conduction co efficient

U = convection coefficient

d = diameter of burner

T_f = absolute flame temperature

T_b = absolute fuel temperature

σ = Stefan-Boltzmann constant

F = geometrical view factor that the liquid has of the flame

$\varkappa$ = Beer's law extinction coefficient of the flame to allow for increasing opacity with thickness

Blinov and Khudyakov commented on the reduction of the energy transfer by conduction through the rim and by convection from the flames for large diameters and attributed the constancy of burning rate for turbulent combustion to the irradiation rate per unit of the liquid fuel surface becoming predominant and independent of burner diameter. From Equation (10) it is apparent that, at large diameters, the conduction

of heat through the rim is negligible, the convection from the flames is constant and the radiation from the flames is dominant and nearly constant because αd is large. With decreasing diameters approaching intermediate sizes, the magnitude of the radiation term decreases faster than the conduction term increases so that a minimum rate is obtained. As the burner size further diminishes the conduction term predominates over the radiation term, causing the burning rate to increase.

In 1959, Emmons (17) reported the results of experiments on the burning of acetone and methyl alcohol utilizing circular pans varying in size from 1/4 inch to 10 inches. The pans were made from a flat brass plate with a brass rim 1/4 inch deep and sharp at the upper edge. The burning rate was determined by filling the pan 3/4 full and noting the time required to burn all of the fuel. In other words, unsteady burning rates were obtained. He found that when the pans were set flush with the table top surrounding the burner, the results obtained were in agreement with those of Blinov and Khudyakov for the pan sizes 4 inches to 10 inches; however, for smaller sizes the data disagreed and a continuously decreasing burning rate was obtained as the diameter of the burner was decreased. When Emmons set the pans on top of the table, exposing in this way the rim of the burners, the burning rates obtained for the smaller diameter showed closer agreement with the ones of Blinov and Khudyakov. At first it was supposed that radiation directly from the flames to the

exposed rim was responsible for the burning rate increase observed, but experiments in which the rim was shielded from the radiation showed no change in the burning rate behavior. This result led Emmons to postulate a four-step mechanism by which heat was transferred in the simple conduction term proposed by Hottel. In this mechanism, radiation from the flames heats the surrounding table top, the inducted air receives energy from the table top by convection, similarly, the pan rim is heated through convection by the induced air moving toward the flame, and finally the energy received by the rim is transferred (by conduction) to the liquid fuel. A variation in any of the above steps in the transfer mechanism outlined would account for the variability of burning rate results obtained for the small pan sizes. Emmons also reported the effect that blackening the bottom of the pans with lampblack had on the burning rate. He found about a 7 per cent increase in burning rates for acetone and none for methyl alcohol after blackening the pans.

Burgess, et al. (8), in extending the work of Blinov and Khudyakov, carried out experiments with butane, normal hexane, benzene, liquid hydrogen and unsymmetrical dimethylhydrazine burning in trays up to 8 feet in diameter outdoors. The liquid level was adjusted to be nearly flush with the rim of the burner. They reported liquid regression rates as a function of the ratio of the heat of combustion to the effective heat of vaporization, i.e. the heat of vaporization at the boiling point plus the integrated heat capacity of the fuel from

ambient temperature to the boiling point. The results on the burning rate behavior as a function of pan diameters were formally similar to those reported by Blinov and Khudyakov.

Magnus (46) measured burning rates for gasoline and ethanol burning in tanks varying in size from 12 to 120 cm. His interest in that investigation was prompted by problems involving fires in storage tanks. The burning rate was measured by means of a hydraulic balance made up of a hydraulic cylinder upon which the test tank rested. The cylinder was connected to a manograph, giving instantaneous readings of the weight of the fuel in the tank. In the case of the larger tanks, the fuel regression was obtained by observing the liquid level at specified time intervals. He found that the specific burning rate of the liquid fuels (unit volume per unit time per unit area) increased with increasing diameters. In addition, it was found that burning rate does not precisely represent rate of heat release. He also reported on the effect of freeboard height (height of burner rim above the fuel surface) on the burning rate. The effect was found to be a complex one involving, in addition, the fuel composition and the ratio of freeboard height to burning surface area.

Fons (25) presented the results of a series of laboratory experiments in which normal-hexane and cyclohexane were burned in circular pans ranging from 0.22 to 11.94 inches in diameter. An overflow system similar to that used by Rasbash, et al. (62) was utilized. The level of the fuel was kept at 0.220 inch below the lip of the burner. His data

showed a trend similar to that obtained by Blinov and Khudyakov, even though a water-cooled burner, to prevent heat conduction down the metal rim to the fuel, was utilized.

Hirst and Sutton (35) have made measurements of the rate of consumption of fuel from the liquid surface of isododecane and aviation kerosine burning in a diffusion flame in a low pressure surrounding. They were interested in obtaining information regarding the behavior of fires in aircraft flying at high altitude. In a portion of their experiments, the effect of air flows (supplied from below the burner) on burning rate was investigated. The fuel consumption rate was found to be independent of air flow above a certain lower flow limit. Vitiation experiments, aimed at determining its effect on burning rate were also conducted. Consumption rates were measured when the incoming air was mixed with nitrogen in varying proportions. The total gas flow was kept constant. The fuel consumption rate was found to decrease with increasing proportions of nitrogen in the mixture, until a point was reached at which extinguishment of the flame occurred. Regarding the effect of pressure, it was found that the relationship between the fuel consumption rate and the pressure of the surroundings was approximately the same for each burner. It was expressed as $C \sim p^{0.46}$ where C denotes consumption rate and p the pressure. The relationship between the radius of the burner, r, and the consumption rate was found to be approximately the same at each pressure and given by $C \sim r^{1.5}$.

In the case of solid fuels, two methods have been used for the determination of the burning rate. In some cases, the weight of the fuel prior to combustion has been obtained and the time required for its consumption has been noted. This method was used mostly during the early experiments. In most cases, however, the burning rate has been obtained by weighing the material either continuously or at specified time intervals.

Two techniques exist at present to carry out experiments involving solid fuels. Both make use of a fuel bed made either of randomly distributed combustible material (pine needles, twigs, excelsior, etc.) or a neat arrangement of the material in a particular pattern (usually in the form of a crib of wood sticks). In one technique, the fuel is ignited throughout as nearly simultaneously as possible. The burning process in this case is a non-steady one involving three stages. The initial (or ignition) stage involves the buildup of the fire and corresponds to a gradually increasing rate of weight loss. It is followed by the so-called active stage where the burning rate is a maximum and relatively uniform for a certain period. The final stage (or decay) corresponds to the exhaustion of the volatiles and subsequent flame extinguishment, followed ultimately by complete extinction. Measurements are generally made during the stage where the burning rate is constant.

In the second technique, a long fuel bed (a crib made of wood sticks formed by placing the sticks in tiers

with a particular spacing between sticks) is ignited at one end. The fire propagates through the crib. The three stages are also present but in this case the buildup and decay stages are of a very short duration compared with the stage of constant burning rate. In the initial tests carried out by Fons (26), who was the first one to develop this steady state technique, the crib was moved into the fire thus keeping the flame in a fixed position on the combustion table. The advantage of this procedure lies in the fact that the instrumentation can remain stationary and the data can be collected while the fire is burning at a steady rate. Fons was mainly interested in rate of spread and therefore no provision was made for the direct weighing of the fuel during its combustion.

In certain instances, the mass per unit area of combustible material has been used to convert the spread velocity to a rate of weight loss (78, 27).

The experiments carried out by Fons, et al. (26) by means of the steady-state technique showed that the rate of combustion expressed in BTU/sec tended to decrease linearly with an increase in the specific gravity of the wood used in the cribs.

Thomas (75) has reviewed the results of experiments on fires in single compartments or enclosures. The data showed that, for relatively low ventilation, the burning rate is proportional to the air flow. The burning rate data were correlated in terms of an air flow factor given by $A\sqrt{H}$ where A is the area and H the height of the opening

of the enclosure. In the case of relatively large openings, i.e., well-ventilated fires, the burning rate was found no longer to increase proportionately to A/H. Rather the burning rate tended to a constant value for a given fire load (total quantity and disposition of combustible material). In this case the burning rate increased in proportion to the exposed surface of the fuel.

Thomas, Webster and Raftery (78) have utilized direct weighing of the fuel in their experiments on flame heights from wood cribs burning on a square horizontal base (side of crib varying in length from 25 to 152 cm) and also inside enclosures (size of the cribs used was 91.5 and 61 cm on the side).

A dynamometer of the resistance strain gage type was used by Gross (33) for the purpose of obtaining a continuous weight record in his experiments on the burning of cross piles of wood (Douglas fir). Conventional platform scales were also used with the larger size of piles. The rate of weight loss curve obtained illustrated the three characteristic stages previously discussed, i.e., ignition, active and decay periods. The effects of the characteristics of the floor surrounding the base of the pile on the burning rate were investigated by utilizing a highly-reflective aluminum foil surface and a highly absorptive carbon-blacked surface. It was found that the maximum burning rate was not appreciably changed by the character of the surface. It was also noticed that the maximum values of the

product $Rb^{1.6}$, where R is the maximum burning rate expressed in per cent per sec and b is the width of the sticks of square cross section, were all equal to about 0.62.

Fons, et al. (27), in re-evaluating and extending the information presented in (26), described experiments carried out with cribs burning under steady-state conditions. The duration of the steady-state was found to depend upon the initial buildup time and available length of crib. The time to reach steady burning, after ignition at one end had taken place, depended upon such factors as spacing, density, size, and moisture content of the wood sticks.

In experiments on air flows into uncontrolled fires carried out by Strasser and Grumer (68), burning rate was measured by a continuous weighing device made of a scale modified to accommodate a force transducer whose calibrated output was recorded on a strip chart recorder. Ordered and unordered arrays of blocks of wood (pine and Douglas fir) of various sizes were burned. Simultaneous ignition at all points in the fuel was used. Experiments in which generated winds of about 5 mph and 20 mph were blown into the fires at various heights were performed. An increase in the burning rate was observed only when the wind blew directly on the fuel bed. When the wind blew into the flame or thermal column above it, the maximum burning rate was a little less than in still air; this characteristic was regarded as resulting from interference of the air stream with the efflux of products of combustion from the bed. Based on the data

obtained the authors indicated that the fire column over a burning fuel bed seems to have little influence on the burning rate; only the air flow into the fuel bed increases the burning rate.

In 1964, Byram, et al. reported the results of experiments to determine the effect of size of burning area on the rate of burning (10). This work was an extension of experiments by Fons, et al. (27). Square cribs constructed of 1/4 inch sticks of white fir and conditioned to a moisture content of 10.1 per cent were used. Each crib had a stick spacing of 3/4 inch and a height of 3.1 inches. The crib width varied from 0.2 feet to 1.28 feet. The weight loss of the crib while burning was determined by means of a direct reading balance. Simultaneous ignition of all the portions of the crib was used thus resulting in unsteady burning. The burning rate was determined from the slope of the weight loss curve during the period when rate of weight loss was nearly constant.

A device incorporating a strain gauge system was used by Eggleston, et al. (16) for the determination of the weight loss rate in their experiments with cubical models made of hardwood and used to scale building fires. The burning of the models was conducted in essentially still air.

Anderson (2) measured rate of weight loss of a mat-type array of ponderosa and white pine needles burning in still air using strain gauge force ring transducers.

Thus far, the discussion on burning rate has dealt with the experimental techniques used and of a qualitative description of the results obtained during various experiments. In what follows, an outline of the quantitative presentation of the data which have been utilized in these experiments will be presented.

In 1956, Rasbash, et al. (62) made use of a relation postulated by Spalding (67) for predicting rates of burning of liquids in natural convection. The rate of burning obtained by using this relation was in good agreement with the value obtained for one of the liquid fuel fires of Rasbash's tests. The empirical relation postulated by Spalding is

$$\frac{\dot{m}_x C_p}{k} = 0.45 B^{3/4} \left(\frac{g x^3}{\alpha} \right)^{1/4} \qquad (11)$$

where

$\dot{m}$ = average mass flow per unit area from the liquid surface

C_p = specific heat at constant pressure of air at room temperature

k = thermal conductivity of air at room temperature

α = thermal diffusivity of air at room temperature

g = gravitational acceleration

x = dimension of the surface

B = transfer number calculable from the properties of the fluid and given by

$$\frac{h_{a,o}-h_a+Hm_o/r}{\lambda+h_o-h}$$

where

$h_{a,o}$ = enthalpy of air at fuel evaporation temperature

h_a = enthalpy of air

h_o = enthalpy of fuel at evaporation temperature

h = enthalpy of fuel

H = heat of combustion of fuel

m_o = oxygen concentration of environment

λ = heat of vaporization of fuel at evaporation temperature

r = stoichiometric ratio, mass of oxygen per unit mass of fuel

This equation is based on the supposition that all the heat transfer takes place by conduction and convection through the vapor zone. The equation predicts a reduction of burning rate per unit area as the linear dimension of the burning surface increases. This result is contrary to the behavior observed with liquid fuels burning in open pans (84, 41, 4, 40, 62, 81). Rasbash ascribed this contradictory result to the importance of radiation to the surface of the fuel. A model of forest fire spread presented in (69) seemed* to indicate that an increase in burning rate per unit area causes a smaller value of depth** of flaming zone.

---

*The cause and effect may be hard to separate.

**The depth of the flaming zone refers to the horizontal distance of penetration of the flame into the crib in the direction of propagation of the flame.

In this model, the only effective mechanism of energy feedback was assumed to be that of radiation from the burning solids alone. In the case of <u>forced</u> convection, Spalding (67) correlated his data adequately by the empirical equation

$$\frac{\dot{m}''d}{\mu} = 0.53B^{3/5}\left(\frac{Ud}{\nu}\right)^{1/2} \qquad (12)$$

where μ= dynamic viscosity

U = velocity of gas stream

d = diameter

ν = kinematic viscosity of the gas stream

Fons (25) correlated his data from burning liquid fuels in terms of a relation similar to equation (11). In his case, the correlation equation used is

$$\frac{\dot{m}''}{\nu_a \rho_a g} = kB^m\left(\frac{gd^3}{\nu_a^2}\right)^n \qquad (13)$$

which held for all burning regimes (laminar, transition, and turbulent) depending upon the value of the exponent n (n increased with diameter of the burner from about 0.25 for the 3 inch pan to about 1.0 for the 12 inch diameter pan). In the above equation, d is the diameter of the vessel, m and n are exponents, B is the same transfer number mentioned before, ν_a is the kinematic viscosity of air, ρ_a is the mass density of air, $\dot{m}''$ is the burning rate per unit area, g is the gravitational acceleration and k is a constant of proportionality.

Thomas (73), who was interested in correlating the height of the flames, obtained by a simple dimensional analysis

the relationship

$$\frac{L}{D} = f\left(\frac{Q^2}{gD^5}\right) \tag{14}$$

which relates the height of the flame to the volumetric flow of fuel and the fire diameter. In this relationship L is the length of the flame, D is the diameter of the burner, g is the gravitational acceleration and Q is the fuel volumetric flow rate. Thomas (74), in extending the work presented in references (73, 78) presented a more formal derivation of the above relationship. The quantity Q^2/gD^5 is obtained experimentally in terms of the burning rate per unit area, $\dot{m}''/\rho_a\sqrt{gD}$ where ρ_a is the density of the surrounding air. Utilizing Fon's data and his own, Thomas presented a relation for the burning rate in terms of the size of the fire as

$$L/D = 42\left(\frac{\dot{m}''}{\rho_a\sqrt{gD}}\right)^{0.61} \tag{15}$$

for fires burning under a calm condition from nearly radially symmetrical fuel beds.

Thomas also utilized the same functional relationship to correlate the data obtained by Blinov and Khudyakov (4) for liquid fuel fires, Putnam and Speich (58) for gaseous fuel fires and Broido and McMasters (6), Étienne (18) and Faure (19) for large scale wood fires. The data covered a range of L/D from about 0.01 to 100 and of $\dot{m}''/\rho_a\sqrt{gD}$ of 10^{-5} to 100.

Experiments involving flames issuing from an enclosure through windows were also considered. Cribs made from sticks

of square cross section of sizes 1/2, 1 and 2 inches square and ranging in height from 4 to 16 inches were burned inside 2 and 3 feet cubical enclosures. The data were correlated in the same manner. The resulting expression was

$$L = 400\, \dot{m}_w^{2/3} \quad \text{for } 1.5 < L/D < 4 \tag{16}$$

where

$\dot{m}$ = burning rate of the crib per unit length of strip, in cgs units (the enclosure's opening was considered as a line source lying on a horizontal plane containing the top of the enclosure)

Thomas also presented some data involving fires burning under the action of the wind. In these cases, the above relation for L/D was extended to include the wind effect. It is assumed that

$$L/D = f\left(\frac{\dot{m}''}{\rho_a\sqrt{gD}},\ \frac{U^2}{gD}\right) \tag{17}$$

A statistical analysis of the data yielded the correlation

$$L/D = 70\left[\frac{\dot{m}''^2}{\rho_a^2 gD}\right]^{0.43}\left[\frac{U^2}{gD}\right]^{-0.11} \tag{18}$$

where U is the wind velocity. The factor U^2/gD is a form of the Froude number. In the above relationship the length of the flame shows a stronger dependence upon burning rate than upon wind velocity.

The results of the experiments of Byran, et al. on the effect of the size of burning area on the burning rate

(see page 29) were correlated in terms of the dimensionless groups $\frac{\dot{m}''D}{\nu_a \rho_a}$ and $\frac{gD^3}{\nu_a^2}$; the resulting correlation indicating that

$$\frac{\dot{m}''D}{\nu_a \rho_a} \sim \left(\frac{gD^3}{\nu_a^2}\right)^n \tag{19}$$

where $n \sim 1/4$. The burning rate per unit area $\dot{m}''$ was found to vary as the minus 1/4 power of the crib width D in the range of crib sizes used. In the above relationship, ν_a and ρ_a are the kinematic viscosity and density of air respectively and g is the gravitational acceleration.

Anderson and Rothermel (2) used the same type of functional relation used by Thomas (78) in analyzing the fires from mat-type of fuel beds of ponderosa and white pine needles burning under both calm and windy conditions.

The rate of spread is a parameter characteristic of spreading fires, i.e. moving along a front. Rate of spread and burning rate are interdependent. Rate of spread studies date as far back as 1916-17, when Show (66) investigated rate of spread from small test fires. As a result of his observations, he concluded that fires burning under conditions favorable to rapid spread tend to burn with acceleration, while slower-burning fires tend to burn at a steady rate. He also concluded that the rate of spread could be expressed as a function of the square of the wind velocity. Curry and Fons continued the work of Show in 1933 and 1934 (13). They reported on the rate of spread

of surface fires utilizing ponderosa pine type (small trees) of California as fuel. Six primary factors were recognized as important to rate of spread studies in their work, viz; (1) fuel size and arrangement; (2) moisture content of the fuel; (3) air supply (wind movement); (4) slope of the ground; (5) the tendency of fires to burn at an increasing rate with time; and (6) size of the fire. The rate of perimeter increase, which is a measure of the size of the fire, was measured in tests involving various conditions of the other variables when a fire starting at essentially a point source on the ground spread with time. The influence of moisture on rate of perimeter increase and of wind on the rate of perimeter increase was described as linear with the slopes of the lines varying with the time factor. (This observation is contrary to the conclusion of Show on the effect of the wind. The disagreement was explained by Curry and Fons to be apparently due to intercorrelation between the wind and moisture). With low wind speeds, the maximum rate of spread was soon attained. With higher wind velocities, the period required to attain maximum rate of spread increased, indicating a longer time required to reach steady state. The effect of slope on rate of spread was found to be curvilinear and largely dependent for its influence upon the occurrence of winds in the direction of the slope.

Experiments similar to those of Curry and Fons in still air were conducted later by Fons (23) in a wind tunnel in which air velocity was controlled. A description of the

results of these experiments was presented by Fons (22). In this reference the analytical development for the rate of spread was based on the theory that the flame propagation can be expressed as successive ignitions of adjacent fuel particles and that its rate of spread is thus governed by the time required to raise the successive fuel particles to ignition. Additional models on fire-front propagation and forest-fire spread have been presented in reference (69).

Later experiments carried out by Fons, et al. (27) with wood cribs burning under steady-state conditions showed that during steady-state burning, the rate of fire spread through the crib was constant. The cribs for these tests were 5.5 inches high, 9.25 inches wide and 35.5 inches long, and were made of nominal 1/2 inch square sticks of white fir with a spacing between sticks in each tier of 1.25 inches. An increase in the specific gravity of wood was found to decrease the rate of spread of the fire through the crib. The rate of spread increased rapidly with decreasing moisture for specific gravity values less than 0.45 and moisture content less than 10 per cent, whereas above these values the rate of spread approached a constant value.

Additional data from cribs of various widths and heights and containing wood of various densities, fuel size and moisture content showed that for a propagating model, in which the depth of the flaming zone was allowed to assume a natural value, the ratio of D/d_o (the depth of flaming zone to initial thickness of fuel) was approximately 10.5 for each fire. In general, it

was found that the data from propagating flame models and stationary flame models could be correlated by the same dimensionless groups.

McCarter and Broido (47) have indicated the importance of radiative energy to the fire propagation rate. Their experiments with wood cribs made of 1/2 inch square western hemlock sticks arranged in several ordered arrays and burning under steady-state conditions indicated that the flames above such crib fires are of considerably less importance to fire spread than is usually assumed. They pointed out that any radiation transfer of importance in elevating unburned fuel to the temperature of ignition seems to originate mainly within the solid combustion zone and represents a small fraction of the total emitted radiation. Their cribs were supported from the unburned end in the air thus avoiding the conduction of heat into the ground. Although this arrangement resulted in a propagation rate nearly 50 percent larger than when the crib was burned resting on a flat insulated base, the increase was primarily a result of achieving unrestricted air flow underneath rather than eliminating conduction into the ground. Countryman (12) has also commented, based on his experiments, that it appears unlikely that radiation from the flames above the fuel bed is a very important factor in fire spread.

The effect of stick size and stick spacing on the rate of spread of crib fires has been studied by Byram, et al. (10). Stick sizes ranging from 0.25 inch to 1.0 inch and spacings ranging from 0.5 inch to 5.0 inches were considered. The

data showed that rate of spread varied approximately as $d_o^{-0.6} s^{0.9}$ for their experiments where d_o is the stick size and s the stick spacing. Fons, et al. (24) also analyzed the effect of fuel size on rate of fire spread in cribs but for a single spacing of 1 1/4 inches. His results indicated that rate of spread varies inversely as the 1/2 power of stick size.

The effects of moisture content on the rate of fire spread have been reported by Anderson (1, 2). Ponderosa pine and western pine needles artificially packed in a random manner so as to provide a mat-type fuel bed 3 inches deep, 18 inches wide and 8 feet long, were used for Anderson's tests. The rate of spread in still air was found to decrease linearly with moisture content increase within the range of 5 to 15 per cent fuel moisture investigated. The rate of spread under windy conditions was found to be an exponential function of the wind speed for ponderosa pine needles and a power function of the wind speed for white pine.

Several mathematical models on firespread through a fuel bed have been presented and discussed by Hottel, et al. in reference (37).

Another physical parameter which has been extensively analyzed is that of flame length. It is appropriate at this point to differentiate between the terms flame length and flame height. In the early studies where the effect of air currents was usually avoided, flame height and flame length were used interchangeably. However, with the recent interest

in studying fires under the action of the wind it has become necessary to distinguish between the two. The term flame length is the distance from a point at the base of the flame (in most cases, the center of the burner area) to the tip of the flames (averaged over a period of time). The flame height is given by the vertical projection of the flame length. Flame lengths have been obtained experimentally by visual and/or photographic means. Yokoi (85, 86) estimated flame lengths by regarding the distance from the base of the flame to the point along the center line of the flame at which the average temperature had fallen to 500°C as the flame length.

Blinov and Khudyakov (4) reported flame height measurements obtained by burning liquid fuels in pans of various sizes. The flame height to diameter of burner, L/D, showed a continuous decrease as pan size increased until the condition of fully turbulent flow in the flame was attained, at which point the ratio L/D leveled off and remained at a value of about 1.7.

As discussed previously, Thomas (73) suggested a functional equation of the form

$$L/D = f\left(\frac{Q^2}{gD^5}\right) = f_1\left(\frac{\dot{m}''^2}{\rho_a{}^2 gD}\right) \qquad (20)$$

for correlating flame height data. Thomas, Webster and Raftery (78) carried out experimental measurements of flame heights and used a similar relationship in correlating

the information obtained. They burned cribs of spruce sticks arranged on a square horizontal base of size D. Varying the amount of wood and the design of the crib yielded a range of mass burning rates. The heights of the flame were, in each case, measured from the base of the crib. The mean flame heights were recorded photographically. The exposure time was greater than the short period of fluctuation in heights of the flames. Their results, as well as those of Gross (33) on the burning of cubical cribs of Douglas fir and of Fons, et al. (24) on the spread of a burning zone along a long wood crib of white fir, were presented as L/D plotted against $(\rho Q)^2/D^5$. (The data of Fons, et al. were plotted using an equivalent square base defined by $D = (D_c D_w)^{1/2}$ where D_c is the width of the crib and D_w the measured length of the flame zone in the direction of flame spread along the crib. The results where the flame height was less than three times the larger of either D_c or D_w were excluded). The data were all in very good agreement even though Gross' values of flame height ratio tend to be about 20 per cent larger. It was suggested by Thomas, et al. that the difference is due mainly to a difference between visual and photographic measurements since Gross' flame heights were obtained visually. Heights of flames from burning cribs inside enclosures with one of the sides of the crib completely open, and also of flames from strips of hanging fabric (cotton) were also reported.

Hirst and Sutton (35) reported on the heights reached by flames from isododecane and kerosine fuels burning at

reduced pressures. The flame heights were measured by means of a graduated scale located adjacent to the side of the flames.

Experiments to determine the flame length from wood crib fires burning under the action of the wind were carried out by Thomas and Scott (77). The crib was ignited completely throughout. It was used to represent the instantaneous conditions of a moving burning zone in a fire spreading on a wide front. The data obtained were correlated as

$$L\left[\frac{g\rho_a}{\dot{m}'^2}\right]^{1/3} = 70\left[\frac{U\rho_a^{1/3}}{\dot{m}'^{1/3}g^{1/3}}\right]^{-0.21}\left[\frac{\dot{m}'}{g\rho_a^2 D^3}\right]^{0.06} \qquad (21)$$

where ρ_a = density of surrounding air (taken as 1.3×10^{-3} g/cc)

g = gravitational acceleration

D = length of the burning zone in the direction of fire spread

U = wind velocity

$\dot{m}'$ = rate of burning per unit length of fire front

If the left hand side is denoted by L' and the first parentheses in the right by U', it was found that plotting $L'U'^{0.21}$ against $D^3/\dot{m}'^2$ resulted in a linear relation. When extrapolated to a value of $L'U'^{0.21}$ corresponding to zero value of D, i.e. a line fire, it gave $L'U'^{0.21} = 55 \pm 5$ which can be used to predict the flame length with little loss of accuracy provided the value of D does not exceed $20\ (\dot{m}')^{2/3}$, where $\dot{m}'$ is in lb/ft-sec and D is in feet.

The maximum heights of flames above the level of the fuel bed were found to correlate approximately as

$$H\left[\frac{g\rho_a^{\,2}}{\dot{m}''^{\,2}}\right]^{1/3} = 38\left[\frac{U\rho_a^{\,1/3}}{(\dot{m}'')^{1/3}g^{1/3}}\right]^{-0.69} \qquad (22)$$

where H = flame height.

Gross (33) has also reported visual measurements of the maximum height attained by flames from burning cross piles of Douglas fir.

Thomas (74), in extending the analysis presented in references (73, 78) obtained a linear plot on log-log coordinates when L/D was plotted as a function of $\frac{\dot{m}''}{\rho_a\sqrt{gD}}$. The correlations obtained have been discussed previously on page 34.

Fons, et al. (27) utilized a relation similar to that of Thomas, et al. (78) to correlate the data on flame lengths of fires propagating at a steady rate through cribs of wood. Measurements of the depth of flaming zone in the direction of spread, D, and of the length of the flame, L, were made from time-lapse motion pictures. The cribs utilized were of various widths and heights and contained wood of various densities, fuel sizes, and moisture contents. These crib parameters were assumed to be important only in their effect on the rate of burning per unit area, $\dot{m}''$, which was calculated by the relation

$$\dot{m}'' = \frac{\dot{m}''R}{D} \qquad (23)$$

where $\dot{m}''$ = mass of fuel burned per unit area

R = rate of fire spread

The resulting correlation showed

$$L/D = 4.5\left[\frac{C(\dot{m}'')^2}{\rho_g gD}\right]^{0.43} \qquad (24)$$

where

ρ_g = density of the gas in the flaming zone (a value 0.019 lbm/cu ft was assumed)

C = weight of gas produced per unit weight of solid fuel

Fons pointed out that, since the exponent 0.43 is in agreement with the value obtained in reference (78) for line fires which were burned with and without the action of wind, the functional power relation between flame length and modified Froude number, $\frac{\dot{m}''}{\rho_a\sqrt{gD}}$, is independent of wind. The length of flames for values of D/W_b, where W_b is the width of crib, was also found to be correlated in terms of the energy liberation rate per unit length of fire front as

$$L = 0.74\ (H\dot{m}''R)^{2/3} \qquad (25)$$

where H = heat of combustion (lower heating value).

Putnam and Speich (58, 60), in analyzing their experiments with gaseous fuel burners, regarded a deviation from the straight line obtained when the relation

$$L/d_o = 29\left(\frac{Q_o^2}{gd_o^5}\right)^{1/5} \qquad (26)$$

was plotted in log-log coordinates as an indication of a change in the character of the flame from a buoyancy-controlled to a thrust controlled (or jet) flame. In the above relation, L is the length of the flame, d_o is the diameter of the nozzle port, g is the gravitational acceleration and Q_o is the volume flux of injected fuel. These experiments were aimed at developing a model for studies of mass fires. The use of gaseous fuels provided a convenient method of varying the burning rate independent of heat feedback from the flames.

In an extension of the above work, Putnam and Speich (59) and also Putnam (57) reported the heights of flames attained with various gas burner arrangements. They included information obtained with point- and area-source flames, as well as with line fires exposed to cross winds.

The analyses of the convection currents above fires has had its roots in the analysis of the convective motion in the atmospheres and in the studies of plumes. In the atmosphere, whenever air at any point is hotter than the surrounding air, the heated air rises and unheated air must flow in below to replace it. The early studies of such movements were usually related to meteorological investigations. The behavior of plumes from sources of heat on the ground has also been considered. Such knowledge is of

interest in pollution studies; probably for this reason, the usual interest has been in predicting the height reached by the plume above ground. In this region, far removed from the source, the usual practice is to assume a constant density for the plume.

Mathematical representation of convection currents (thermal jets) rising from concentrated sources of heat (point and horizontal lines) were presented by Schmidt (65) in 1941. He applied Prandtl's mixing length theory of momentum and heat transfer to his analysis. The results obtained predicted the spreading out of the heated column so that both the distribution of temperature and of upward velocity are similar at all heights (though not the same distribution). Further, the width of the column increases uniformly with height above the source so that the heat is contained within a wedge if the heat source is a line, or a cone if it is a point. Another prediction was that the distributions of temperature and velocity assume the forms calculated by Schmidt. He made experimental measurements of the distribution of temperature and velocity at various heights above a concentrated source of heat and found close agreement between theoretical and experimental observations.

In 1952, Rouse, et al. (64), unaware of Schmidt's analysis, deduced Schmidt's results regarding the spreading out of the column with height using only the assumption of similarity of temperature and velocity distributions at all heights. Rouse's treatment could not give information

about the distribution of temperature across the thermal jet; the latter was obtained experimentally.

Bosanquet, et al. (5), Priestley (56), and Sutton (70) have presented theories for predicting plume heights. The results predicted have been of the same order as those determined experimentally by Bosanquet, et al. and Ball (3). Priestley's theory seems to represent best the data obtained experimentally. Morton, Taylor, and Turner (52) have also developed theories of convective flow and applied them to the prediction of the height to which smoke plumes will rise. The studies have been extended to the case of a moist atmosphere (48) and to chimney effluents (50, 49).

Murgai and Emmons (53) have analyzed the properties of a turbulent convection column and have presented a method of solution for the case of a stratified atmosphere.

Recently, and in regard to convection currents above fires, the interest has shifted to the zone just above and also within the flaming zone. In this case, the usual assumption of constant density for the region removed from the source breaks down. Further complications arise due to a lack of knowledge as to how the combustion process is coupled with the movement of entrained air.

Yokoi (85), by non-dimensionalizing the equations of momentum and heat balance as applied to a cross section of flow perpendicular to the vertical upward current from a circular heat source, has arrived at two dimensionless relations,

$$\bar{w} = \frac{w r_o^{1/3}}{\left(\frac{Qg}{c_p \rho \theta_o}\right)^{1/3}} = f_1(r/r_o, z/r_o) \qquad (27)$$

and

$$\Theta = \frac{\Delta\theta r_o^{5/3}}{\left(\frac{Q^2 \theta_o}{c_p^2 \rho^2 g}\right)^{1/3}} = f_2(r/r_o, z/r_o) \qquad (28)$$

called the dimensionless upward velocity and dimensionless excess temperature, respectively. In these relations w is the upward velocity, $\Delta\theta$ is the excess temperature* at any point in the current, θ_o is the absolute temperature of the surrounding air, c_p and ρ are the specific heat and density of the gas in the current, g is the gravitational acceleration, r_o is the radius of the heat source, r and z are coordinates of a point in the convection current, and Q is the heat quantity conveyed by the current per unit time. The function f_1 and f_2 are determined experimentally. Yokoi carried out measurements of the temperature distribution in the convection current from circular and rectangular heat sources. The observations obtained are discussed on page 54.

Faure (19) has described an experimental setup, using heated circular plates of 50 and 100 cm, where convection

---

*Excess temperature is the difference between the temperature in the fire zone and ambient temperature at a point sufficiently removed from the effect of the flame.

currents were made visible by means of feathers. Smoke generators, magnesium oxide powder, thistledown, and lycopodium dust are among other methods utilized by various other experimenters in attempting to observe and measure the flow conditions at a heated source.

An analytical model which described the variation with altitude of the composition, temperature and velocity of the gases within a plume above a large free-burning fire has been formulated by Nielsen and Tao (54). The model includes the effects of combustion, composition variation and radiation losses from the hot gases.

In a paper by Morton (51) the modifications that must be made to theories dealing with weakly buoyant plumes for a satisfactory treatment of strongly buoyant plumes were discussed.

Two parameters closely related to the convective flow of the flame are the upward velocity of the gases in the flame and the rate of air entrainment by the flame.

In 1945, Taylor (71) suggested that the rate at which fluid is entrained into a heated plume be taken as proportional to the vertical velocity on the axis of the plume, i.e. $v = \alpha w$ where v is the velocity of entrainment at a certain height and w is vertical velocity along the axis at the same height. The entrainment constant α was found experimentally to have a value of 0.16. This relationship was later adopted by Morton, Taylor and Turner (52), Morton (50) and Thomas, et al. (78).

In 1956, Rasbash, et al. (62) determined the upward velocity of flames for alcohol, benzene, gasoline and kerosine fires from cinematographic records. The results were correlated by an equation of the form

$$V = a\ell + bt + c \tag{29}$$

where a, b, and c are constants, ℓ is the height above the liquid surface, t the time of burning, and V the velocity of fluctuation of the flame tips. Values of a, b, and c are tabulated in the paper for the fuels used. For all the flames the effect of height on upward flame velocity was reported as significant, the velocity increasing as the height increased.

In a subsequent paper, Thomas (74) extended Taylor's assumption (which applied strictly to plumes where the density difference is small) to buoyant turbulent flames where density variations can not be neglected and assumed the relation

$$v \sim w(\rho_{f\ell}/\rho_o)^{1/2} \tag{30}$$

to apply to flames. $\rho_{f\ell}$ is the flame density due to temperature rise of the gas and ρ_o that of the surrounding fluid. Using a nominal flame temperature of 1290 °K and an ambient temperature equal to 290 °K, the expression reduces to

$$v = 0.075\ w \tag{31}$$

This relation was assumed to apply up to tip of the flame. In the same paper, Thomas, utilizing the data of Rasbash, et al. (62) obtained the following relationship for the

upward velocity of the instantaneous flame tip along the central vertical axis, w_t:

$$w_t = 0.36\ (2g\theta_{fl}z_t/T_o)^{1/2} \tag{32}$$

where g = gravitational acceleration

θ_{fl} = temperature rise at the flame zone

z_t = height of the flame tip

T_o = absolute temperature of the surrounding air

If the flame zone is treated as a region of uniform temperature, i.e. θ_{fl} = constant and the average flame height is denoted by L, for the case of low exit velocities from the burner, the above relation reduces to

$$\bar{w}_L \sim (gL)^{1/2} \tag{33}$$

where $\bar{w}_L$ is the mean upward velocity. To account for differently shaped flames, a shape factor F was suggested. Its inclusion resulted in

$$\bar{w}_L \sim (gL)^{1/2}\ F(L/D) \tag{34}$$

where the bar denotes the mean value over the whole flame height and F is shown as a function of the ratio L/D.

In 1964, Strasser and Grumer (68) reported experiments carried out to determine the characteristics and magnitudes of air flows into uncontrolled fires. Experiments were carried out using a buoyant helium plume to avoid temperature gradients in the laboratory. The flow of fine lycopodium dust into the plume was photographed with a movie camera. Profiles of helium-air composition within the plume were also

determined. A value of the order of 5.4 to 6.5 cm/sec was obtained for the inflow velocity of air. Measurements of the air flow near fires of liquid benzene, xylene and methanol as well as with ordered and unordered arrays of wood blocks were also carried out. The observed air flows were about equal to the air flows required for stoichiometric burning. A quantitative treatment of air flow was developed based on a study of pressure drop through packed tubes. The agreement between the predicted air velocities and the experimentally determined values was fairly good.

Thomas, et al. (76) have also measured the flow of air into flames. Thistledown was used as a tracer to measure the flow in their studies. Flames from ethyl alcohol and wood fires 91 cm in diameter were considered. They found the total quantity of air influx below the mean flame height to be one order times the stoichiometric requirements, with a substantial part of the air flowing upwards around the flame. The total flow also exceeded that estimated from entrainment theory and measurements of flame tip velocity.

Nielsen and Tao (54) in their development of a model for plumes above fires assumed that the entrainment of air into the plumes is proportional to the mass velocity, i.e., the product of density and velocity. The relationship used for the velocity in the vertical direction, at a point where the density of the fire in the plume is ρ and where the inflow velocity of air is u, was

$$v = - \alpha u \frac{\rho}{\rho_a} \tag{35}$$

The flame temperatures in the luminous flames of different kinds of burning forest fuel were measured by Fons (22) using chromel-alumel thermocouples held at several points in the flame. The average temperature so measured was found to be approximately 1500°F.

The flame temperature of liquid fuel fires has been measured by Rasbash, et al. (62) by means of the Schmidt method and also with a disappearing filament optical pyrometer.

Magnus (46) reported temperature measurements using thermocouples, in and above the flame zone as well as below the liquid surface.

In Yokoi's work (85), referenced previously in connection with the discussion on convection above heat sources, measurements of the gas temperature in the flaming zone were made using bare chromel-alumel and copper-constantan thermocouples. Flames from alcohol burning in circular vessels ranging in radii from 3.3 to 37.5 cm were utilized. A burner composed of little wicks in alcohol lamps placed within a circle of a certain radius was also used. It was found that: 1) the horizontal temperature distributions at any height in the upward currents from the circular heat sources of various radii could be represented by one curve in dimensionless coordinates z/r_o and r/r_o, and 2) two kinds of domain as to the temperature distribution were obtained.

In the domain nearer the source of heat ($z/r_o < 2.5$), the horizontal distribution of temperature had the shape of a plateau and the hot current did not spread horizontally as widely as it rose. In the upper domain ($z/r_o > 2.5$), the horizontal temperature distribution was like that from the upward current originating at a point heat source. The current spread widely as if started from a point heat source located at the center of the circular vessel. The vertical temperature distribution of the upward current from the circular heat source in the domain far from the source was found to be correlated well by

$$\Theta = 9.115\left(\frac{z}{r_o}\right)^{-5/3} \tag{36}$$

where z = height from the base of the flame

r_o = radius of the circular vessel

In the domain near the heat source

$$\Theta \sim 1.6 \tag{37}$$

The arguments for a circular heat source were extended to rectangular heat sources. In this case, three domains were postulated. In the first one, directly above the source, the temperature varied little with height; above it, in the second domain, the vertical temperature distribution was similar to the case of the upward current from a line heat source; and at the top, in the last domain, the temperature was similar to the case of the upward current from a point heat source. A correlation of values obtained

for several rectangular sources was presented. The results obtained were applied to the calculation of temperatures above a burning wooden house, making, in addition, corrections for the influence of radiation.

Fons, et al. (26) have also measured the horizontal distribution of temperature at several heights in the convection column and the change in temperature up the central axis of the column for fires from wood cribs burning at a steady rate. The temperature readings were obtained with thermocouples.

Hirst and Sutton (35), in the course of their experiments on diffusion flames from isododecane and kerosine burning at reduced pressures, made measurements in the carbon-free part of the flame and in the liquid with a platinum-platinum rhodium thermocouple. It was found that the liquid quickly attained thermal equilibrium and that the temperature gradient at the edge was the same as in the centre. The temperature in the liquid usually became constant for depths between 10 and 20 mm.

Anderson (1) has reported on the measurement of vertical temperature gradients in the flame and convection column of fires from mat-type fuel beds of ponderosa and white pine needles. (Chromel-alumel and iron-constantan thermocouples were used for the measurements.) He found that, although the rates of spread were nearly the same in the two fuels, the temperature distribution was considerably different. He stated that the reason for the difference in temperature

profiles was related to the differences in amount of volatilized material from the beds of fuel.

Another parameter related to temperatures at the flaming zone is flame radiation. Thomas (75) reviewed the results of measurements of radiation from flames inside single compartments open on one side. The maximum radiation at the center of the opening was shown to correlate in terms of the rate of burning per unit area of fuel surface within the range of the experiments considered.

Fons, et al. (26) plotted irradiance to the side of a fire at an angle of 20° from the horizontal and at a radius of 14 feet from the source against rate of combustion and obtained a good correlation.

Reference (69) presented a discussion on radiative transport problems associated with a model of fire spread in a forest.

Fons (25) attributed the increase in the exponent of Equation (13), (see page 33), from 0.25 to 1.0, to the radiation from the flame to the liquid surface for large diameter burners (> 5 inches in diameter) due to the increase in the height of the flame and the corresponding increase in emissivity, especially for fuels that burn with sooty flames.

Measurements of the radiant flux from the burning of cross piles of wood were carried out by Gross (33) with a multiple junction total radiation thermopile. It was mounted horizontally at a distance of 160 times the stick width used in the pile and at a height equal to 60 times the

stick width. A plot on logarithmic coordinates of the maximum radiant intensity as a function of the maximum burning rate was fitted well by a straight line of unit slope.

Experiments of McCarter and Broido (47) have indicated the importance of the radiation from the embers in elevating the unburned fuel to combustion temperatures. These experiments, carried out with western hemlock cribs under conditions of negligible conduction losses, showed that about 43 per cent of the heat of combustion was radiated, 55 per cent convected and about 2 per cent uncombusted. Experiments in which the embers were quenched using water, gave an amount of radiated heat of 21 per cent and convected heat of 44 per cent. It was also found that a nearly complete array of radiation measurements over the imaginary sphere surrounding the fire was necessary to obtain a valid integration of the total radiation rate.

Objectives of the Present Study

The purpose of this study was to analyze further aspects of the phenomena of multiple fires. As pointed out previously the interest in this kind of fires is due to the greater destructive capacity possessed by multiple units of fuel burning simultaneously as compared to a single unit of fuel.

The knowledge obtained from studies of mass fires eventually will lead to a better understanding of the conflagration and firestorm and of the behavior of planned multiple ignitions. The studies of multiple fires thus

far have dealt mainly with the condition of flame merging under calm conditions. When wind has been considered, it was under conditions in which the fire could be treated as a single flame. In most cases multiple fires will occur in units of fuel separated by a certain distance and under the action of the wind. This study has investigated experimentally the behavior of two proximate fires under windy conditions. At the present time, the description of the behavior of proximate fires is mainly of a speculative nature since no experimental attempt seems to have been carried out before to obtain data on them. The major parameters considered were burning rate, rate of spread and flame inclination. In addition, temperatures in the wake gases of the flames and radiation to a point downstream were measured. An attempt was made to explain the behavior observed and to correlate the data obtained in terms of the gross properties of the fires.

Several single fires using the same type of fuel were burned in order to establish a basis for comparison of the behavior of proximate fires and single fires.

Fuel Selection

A solid fuel was chosen because it was felt that it is more representative of the character of the combustible material which will be found burning under conditions of multiple ignition. In addition, liquid and gaseous fuels present certain peculiar problems. Obtaining a wide and

sufficiently long flame from a single port burner utilizing a gaseous fuel and emerging at a low velocity, so that the flame does not act as a jet, is difficult. Buoyant diffusion flames from liquid fuels burning in shallow pans possess the unique characteristic of flame trailing* (81). Obtaining a suitable flame from a solid fuel also presents problems. One of the problems in using solid fuels for the production of buoyant diffusion flames involves flame reproducibility. Exerting great care in the design and production of the fuel configuration seemed to be the answer. Another problem is that of determining the burning rate or weight loss of the fuel as it is consumed. In addition, since with a solid the fire front usually moves through the fuel, the relative movement of the flame with respect to the surroundings causes certain problems related to the positioning of instruments used to gather the data. A discussion of these problems and their solution are presented later.

Wood was chosen as the solid fuel for this study because of the availability of data in the literature with which to compare the data obtained, the ease of handling of wooden configurations, the direct relationship with forests and the close relationship with building materials. In addition, experiments carried out by Strasser and

---

*Flame trailing is the extent to which the flame "spills over" the downwind side at the surface of the burning pool.

Grumer (68) have indicated that, of various solid fuels tested (charcoal, bituminous coal, treated bituminous coal and wood), wood gave the highest burning rate and attained equilibrium combustion in the shortest time. Southern yellow pine (Pinus Palustris) was chosen because of its higher content of volatiles, thus assuring longer burning times. It was conditioned to a moisture content of about 10 per cent, which is close to its equilibrium content in normal atmospheres. Some preliminary tests were carried out on improvised combustion surfaces in a wind tunnel test section (described later) in order to determine the fuel size, geometry and the minimum length and width requirements of the fuel bed best suited for these experiments.

The first problem considered was that of the arrangement of the solid fuel to provide a uniform flame zone and rate of advance. Slats 1/8 inch by 2 inches and of different lengths were assembled with the 2 inches side positioned vertically and with various spacings between the slats. It was found that when they burned, the fire tended to advance faster along the pieces used to join and hold them together. The same condition occurred when pieces about 2 inches long and having square cross-sections of both 1/2 inch and 3/4 inch on a side were cemented in a vertical position on top of a 1/8 inch thick piece of wood and burned. These tests were discontinued because it was apparent that the fire tended to spread faster along certain portions of the fuel bed unless the configuration was

such that it provided a more homogeneous volume distribution of the fuel. Consideration was then given to wood cribs which have been utilized previously by others. Briefly, these cribs are prepared by joining together alternate layers of sticks of square or rectangular cross-section in order to form a fuel bed. Initial tests showed that the flaming zone and rate of spread were more uniform than with the arrangements described above. Nevertheless, as discussed in the following, additional improvements were made.

Since one of the principal objectives of this study was to investigate the behavior of proximate fires produced by burning two cribs simultaneously while maintaining the flame front of each at fixed positions, it was necessary to provide a means for advancing each crib into the flame front. To do so, while at the same time being able to bring the two flame fronts into close proximity, it was necessary to resort to the use of cribs articulated in sections which could be fed continuously from beneath onto the combustion table of the wind tunnel test section by means of a continuous conveyor arrangement composed of the cribs themselves (see Figure 7). A crib was initially made from rectangular sections about 3-3/4 inches wide composed of sticks 3/4 inch square and with a stick size to spacing ratio of 1:1. The sections were joined by stapling airplane wires to the bottom of the sections parallel to the direction of crib movement. These wires were wrapped around a shaft turned by an electric motor.

In this way, fuel could be continuously fed into the fire zone at a rate corresponding to that of consumption, so that the burning region remained at a fixed position. This technique was tried and worked satisfactorily except for the movement of ashes out of the burning zone; the ashes tended to accumulate at the burning zone since the combustion table itself was stationary. To resolve this problem a piece of asbestos cloth was stapled to the underside of the moving crib so that the ashes would remain on the cloth and would therefore move at the same rate as the crib. This arrangement was tested and found to work satisfactorily.

It was noted that the burning zone advanced more rapidly along the exposed sides of the crib than in the interior of the crib. By covering the sides of the crib with asbestos cloth, it was found that the burning zone then advanced more rapidly in the interior rather than the sides. Finally, by providing 1/4 inch, square holes* in the cloth directly opposite the open spaces in the crib, it was possible to achieve a uniform advance of the burning zone across the full width of the crib. Figure 1 gives an indication of the pronounced effect exerted by the cloth.

Various tests were carried out to determine which width of crib would yield a flame whose bending was

---

*Because of the difficulty of cutting these holes without leaving ragged edges, the asbestos cloth was sprayed with contact cement diluted with equal parts of acetone and toluol (ratio of cement to diluent of 3:1). The cement stiffened the cloth sufficiently to permit punching clean holes.

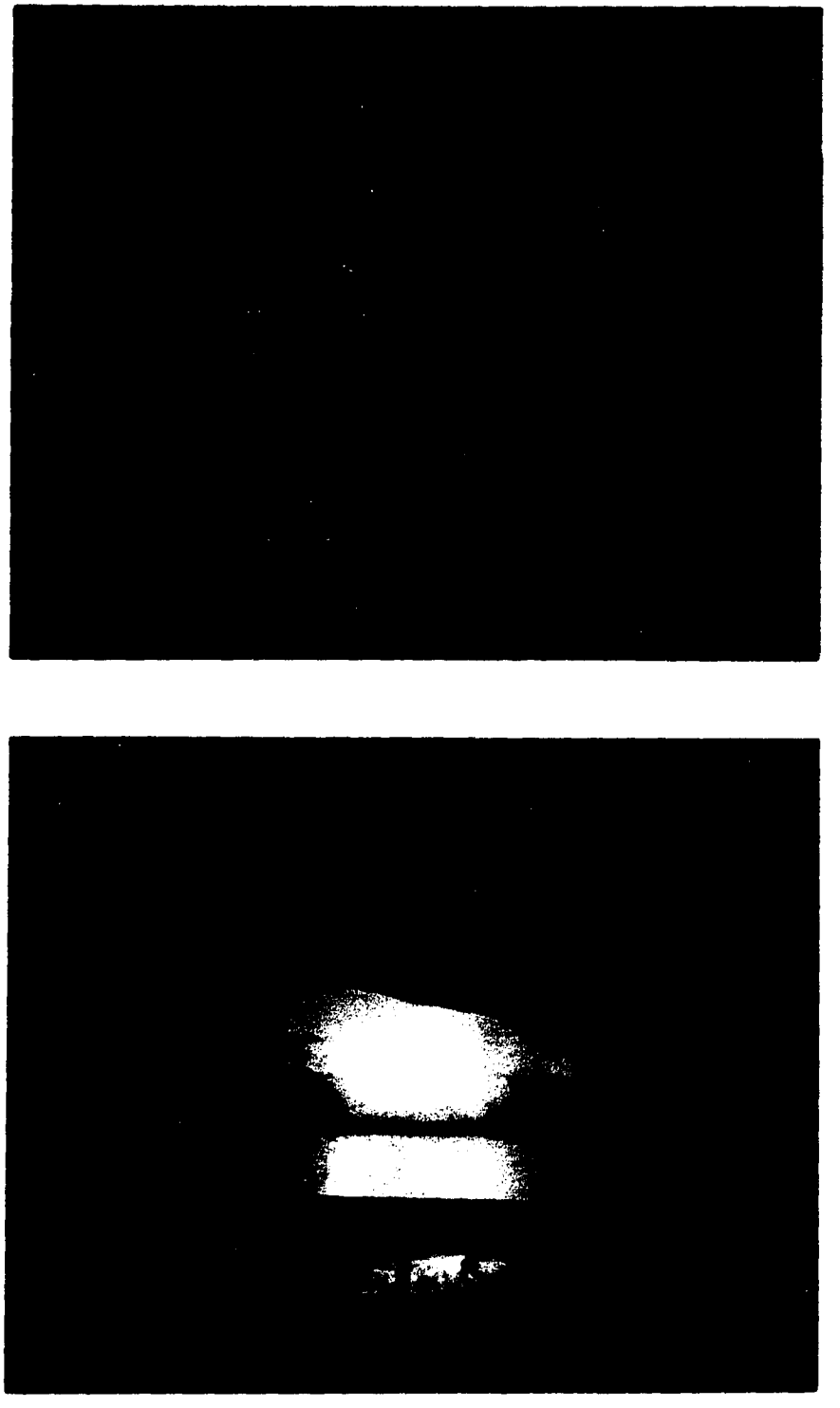

Figure 1. A Piece of Crib Burning Under the Action of the Wind and Showing in A) the Side Effect for the Uncovered Side; in B) the Side Effect for the Side Covered With a Piece of Asbestos Cloth

essentially independent of crib width and would generate a downstream temperature distribution at any elevation which would be essentially uniform across the full width of the tunnel, so that the temperature gradients were restricted to the vertical and longitudinal directions. A width of 3 feet was found to be satisfactory. Tests were also carried out to determine the size of stick and proper spacing to achieve a convenient length of flame (about 2 to 3 feet) and a convenient rate of spread. It was found that 1/2 inch square sticks spaced at 1 inch intervals were convenient. The length of crib which could be handled satisfactorily in the test section was 8 feet.

CHAPTER III

EXPERIMENTAL FACILITIES AND EQUIPMENT

Wind Tunnel Facility

The tests were carried out at the Flame Dynamics Laboratory Low Speed Wind Tunnel of the University of Oklahoma Research Institute. This facility was originally designed and constructed at the Research Institute for the purpose of analysis and investigation of buoyant diffusion flames from burning liquid pools. Construction and design details are given in a thesis by R. A. Milburn (1965). Modifications of the original design were made during the construction stage to accommodate flames from burning solids as well. A description of this facility and of the modifications made is the subject of the discussion that follows.

a) General

The wind tunnel consists mainly of a dynamic test section and associated wind producing and calming devices, a static test room, and an observation and instrumentation room. Figure 2 shows an exterior view of the facility. A schematic plan layout of the facility is shown in Figure 3. It shows the location of the blower, the flow straightening section, the dynamic test section, the observation and instrumentation room, and the static test room.

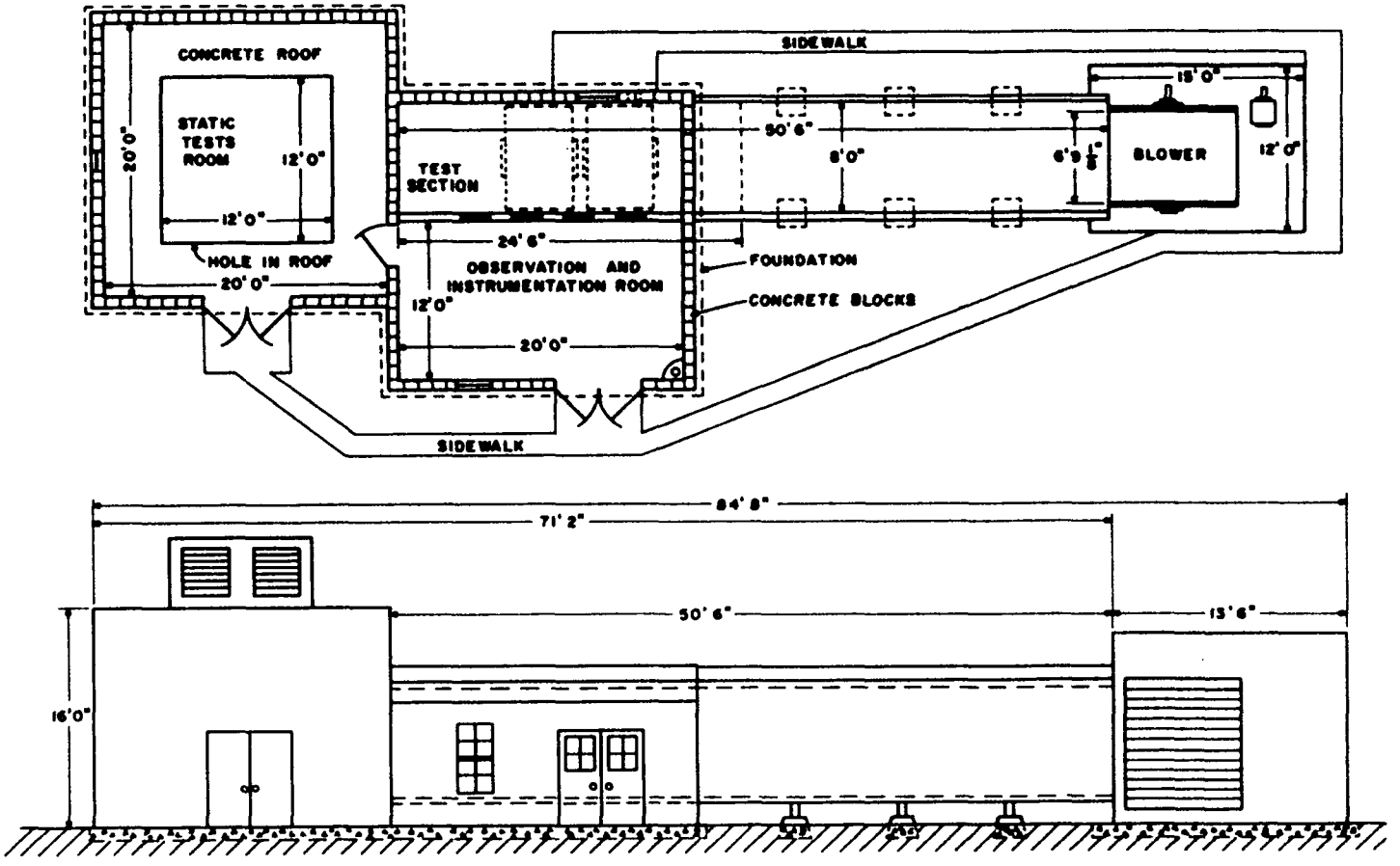

Figure 3. Layout of the Flame Wind Tunnel

b) Wind Producing Section

The wind producing device consists of a 103,000 CFM (at 1 inch of water head) blower driven by a 50 HP motor. The blower and motor rest on a concrete pad and are protected from the weather by a wooden housing covered with asbestos shingles. The blower has variable inlet vanes to control the air flow rate through the tunnel. These are controlled remotely from the observation and instrumentation room. The blower inlets are protected against the effect of gustiness in the prevailing winds.

The calming section extends about 29 feet from the blower to the inlet of the test section. Its cross section measures 8 feet by 8 feet. Several screens (14 x 18 mesh size) and two sections of honeycomb structure located in the straightening section and perpendicular to the flow provide a smooth parallel flow in the test section. Their positions are shown in Figure 4. The profiles of velocity variation as measured by a hot wire anemometer probe (to be described later) are shown in Figure 5 for velocities of 16.8, 11.3, 3.5, and 0.55 ft/sec. Figure 6 is a time exposure of tufted yarn spaced at one foot intervals across the entrance of the test section. It shows physically what the flow pattern looked like. The photograph is a 30 second exposure with the wind speed at the maximum obtainable (about 23 ft/sec). The outside wind velocity was 18 ft/sec from the south with gusts to 25 ft/sec.

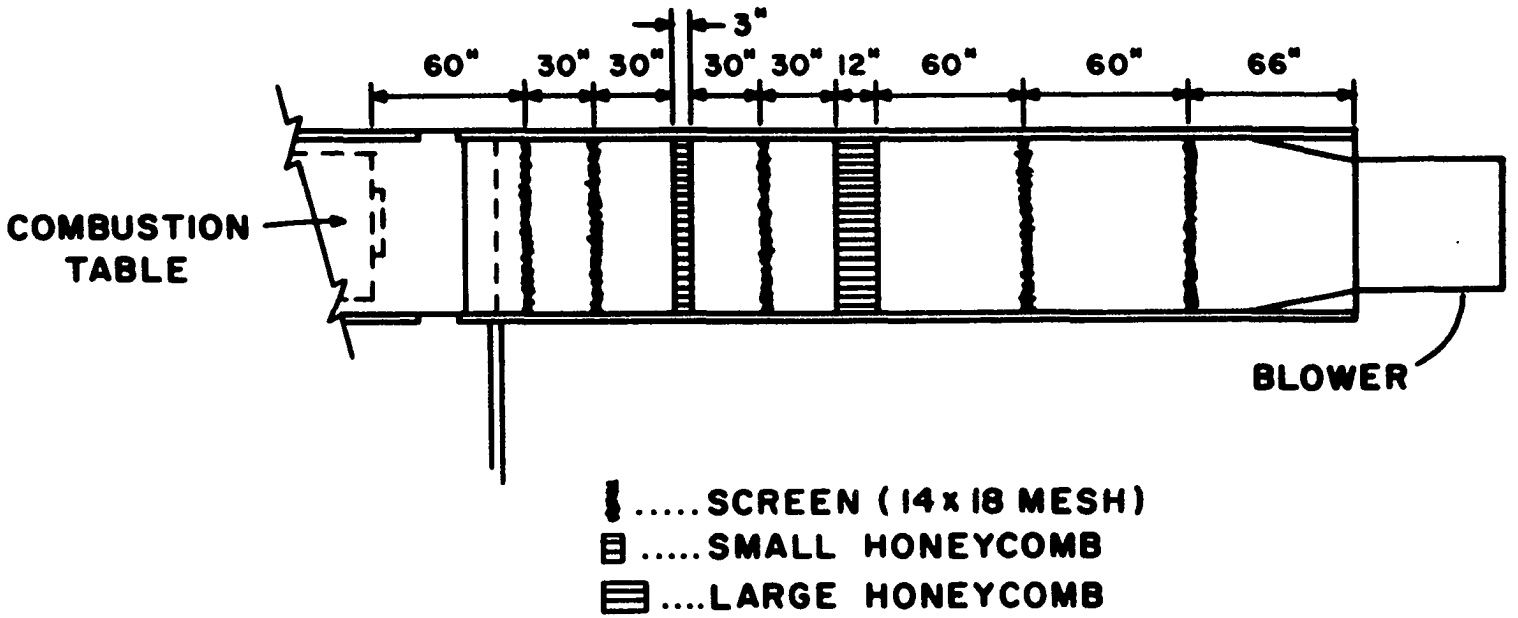

Figure 4. Location of the Screens and Honeycomb Structure in the Straightening Section

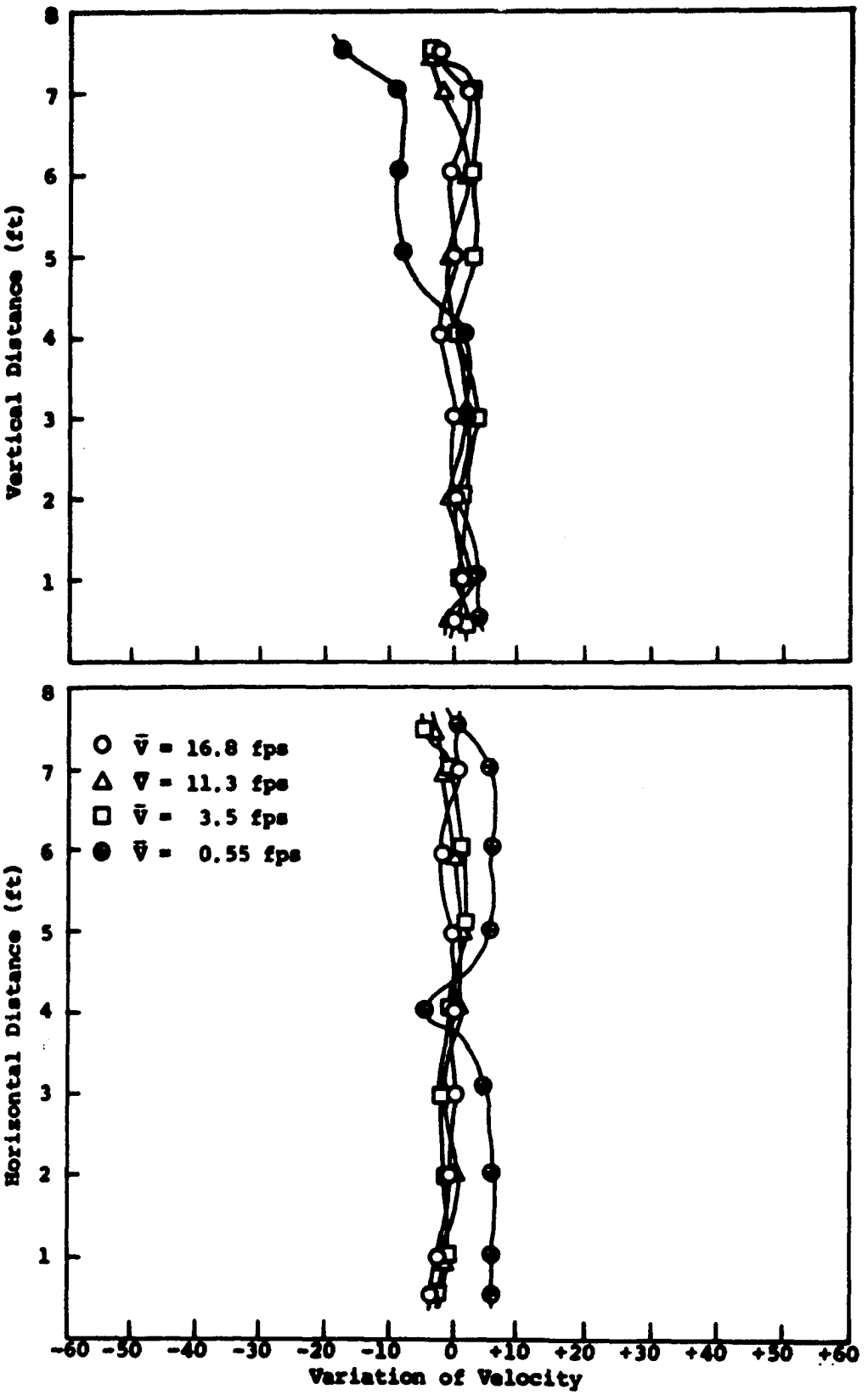

Figure 5. Wind Tunnel Velocity Profiles

c) Tunnel Section

The dynamic test section measures 8 feet by 8 feet in cross section and 20 feet in length. The floor and ceiling are made of sheet metal and the walls are constructed of concrete blocks. The floor of the test section is located about 2 feet above the ground level. The original design was modified to provide removable floor sections about 2 feet wide. The space beneath the floor is needed to provide room for the fuel delivery and weight loss measuring equipment needed to burn solid fuels. Two access doors are provided for this space.

The original design was modified to allow for a larger number of viewing windows so as to be able to observe multiple fires in the section. Four observation windows, made of 3/8 inch thick tempered plate glass for heat resistance and structural strength, were placed in the wall between the test section and observation and instrumentation room. Their location is shown in Figure 7. A clock, stop clock and counting device are located on another window directly across the farthest upstream observation window. These units are controlled from the observation and instrumentation room.

d) Static Test Room

The static test room measures 20 feet by 20 feet by 16 feet high. It serves the dual purpose of providing a large space for tests under calm conditions, and as a surge chamber during tests in the dynamic section. For the purpose

Figure 6. Thirty-Seconds Time Exposure Showing Strings Steady Flow

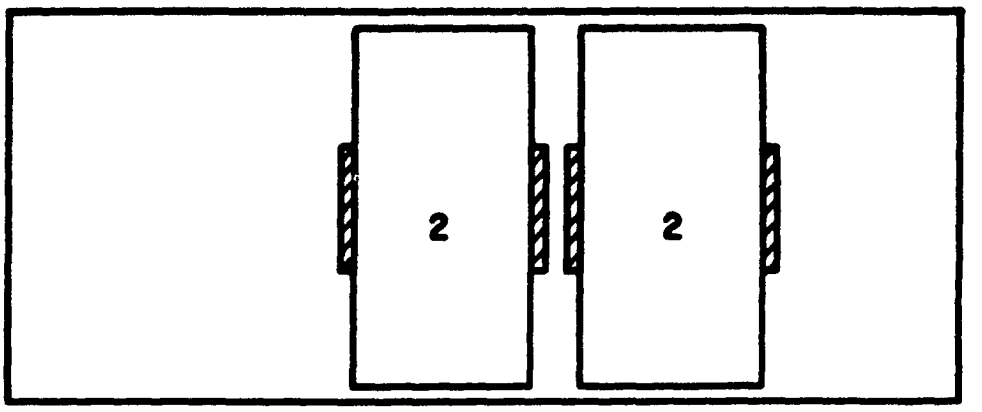

PLAN VIEW

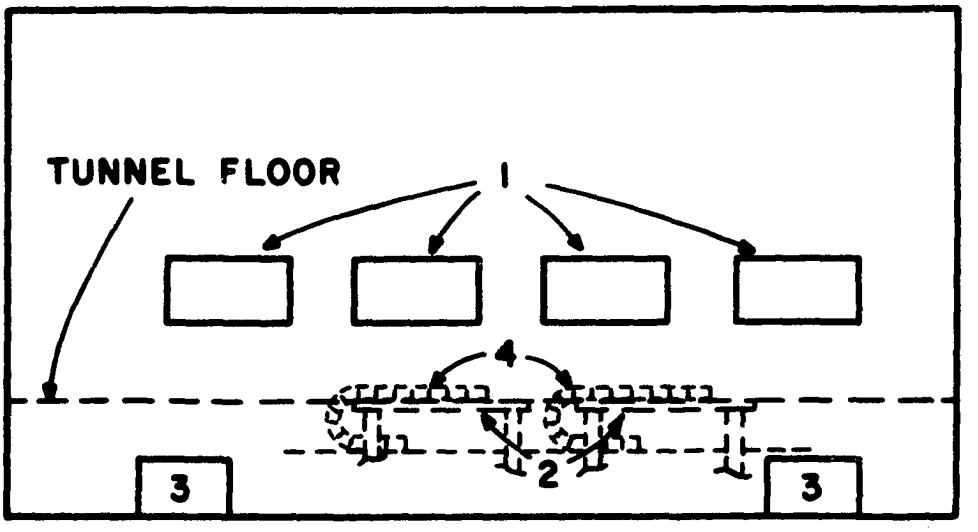

ELEVATION VIEW

KEY

1...WINDOWS
2...COMBUSTION TABLES
3...ACCESS DOORS
4...FUEL BEDS

Figure 7. Schematic Drawing of the Test Section

of collecting smoke and soot during static tests, a hood, measuring about 12 feet by 12 feet by 5 feet high, is suspended from the ceiling. The products of combustion are exhausted through a vent in the roof. Spring loaded shutters are provided in a hood covering the vent. Although the shutters allow combustion products to pass out, they are closed by prevailing outside wind. A 1/2 HP constant speed fan is located at the west side of the hood to aid in the exhausting process.

e) Observation and Instrumentation Room

The observation and instrumentation room measures 12 feet by 20 feet by about 10 feet high. The glass windows in the wall between the dynamic test section and observation room serve for visual and photographic observations of the flames. The controls for the blower, fuel feeding devices, static test room fan, etc. are located in this room. It also houses the recorders and photographic equipment. The features of the photographic equipment will be discussed later under the Instrumentation heading.

Fuel Delivery Equipment and Weight Loss Measuring System

The equipment necessary to burn the cribs and which substituted for the removed floor sections had to be designed and tested.

The following characteristics were established as desirable for the fuel delivery system:

a) capability of feeding the solid fuel so as to maintain a stationary fire,

b) capability of measuring the rate of weight loss continuously and accurately.

To satisfy the first requirement it was soon apparent that the fuel crib would have to come from beneath the floor and feed into the fire, since the minimum desired separation of the fires could not be obtained otherwise with the length of fuel bed utilized.

To satisfy the second requirement it was apparent that the weight of both fuel and ashes present at a given instant would have to be obtained simultaneously since in this way the measure of the rate of material volatilized would be obtained best.

A system satisfying the above requirements was designed and built. The location of the combustion tables in the test section is shown in Figure 7.

Due to the type of recording instrumentation available at the time when the design and construction of the table was begun, the measurement of the weight loss was initially carried out in a different manner for each of the two combustion tables. The differences will be pointed out as the discussion proceeds. The rest of the discussion applies to both devices.

One of the combustion tables is shown in Figure 8; the second was similar in most respects. Their frames were

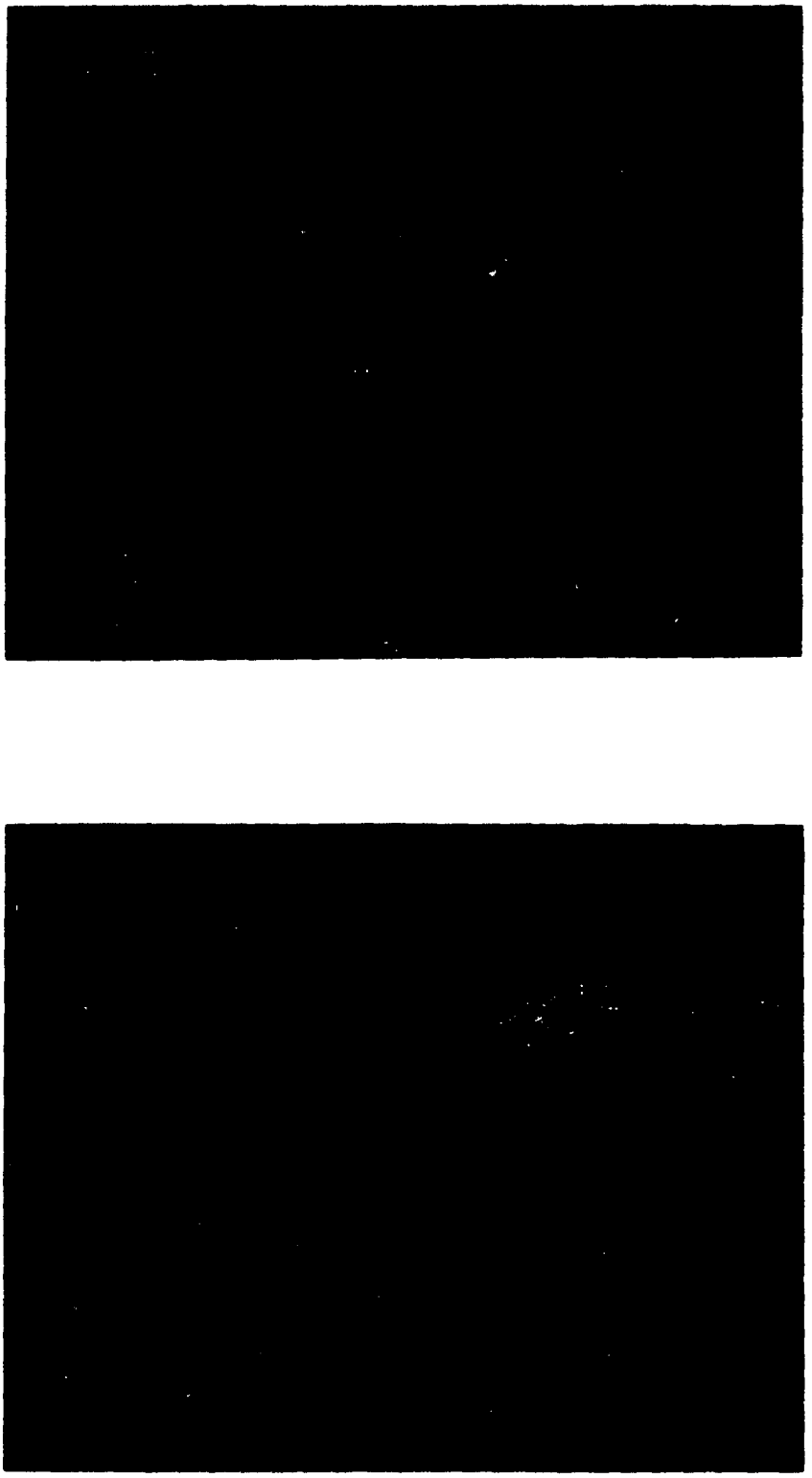

Figure 8. Views of One of the Combustion Tables (Top Assembly)

made of slotted steel angle. The tops measure about 4-1/2 feet by 8 feet. Several materials (steel sheets, fiberglass insulation, gypsum board, Transite board, Fiberfrax GH board) were tested to determine the best one to use for the table tops. Except for the Fiberfrax boards, all the others showed a great deal of deterioration, twisting, and buckling after supporting a crib under burning conditions. Figure 9 shows, as an example, what occurred during the tests with the gypsum board. The center portion of the board where a fire had been burning broke into pieces leaving a hole in it. The Fiberfrax boards (manufactured by Carborundum Co., Niagara Falls, New York) however, retained their structural integrity even after burning several fires on them. A slight softening was noticed when the board was hot, but with proper support (a 24 gage steel sheet underneath), this effect caused no problem. Due to the cost, Fiberfrax boards were used only in the center portion of the table top where the combustion took place. This section consisted of 4 pairs of boards 1 foot by 3 feet in size. Each pair consisted of two 1/4 inch thick boards joined together with a high temperature cement (Sauereisen cement No. 63, manufactured by Sauereisen Cements Co., Pittsburgh, Pennsylvania) to form a board 1 foot by 3 feet by about 11/16 inch thick.

The fuel feeding mechanism of each table consisted of a 6 feet long steel shaft supported between the two legs of the table by means of pillow-block bearings.

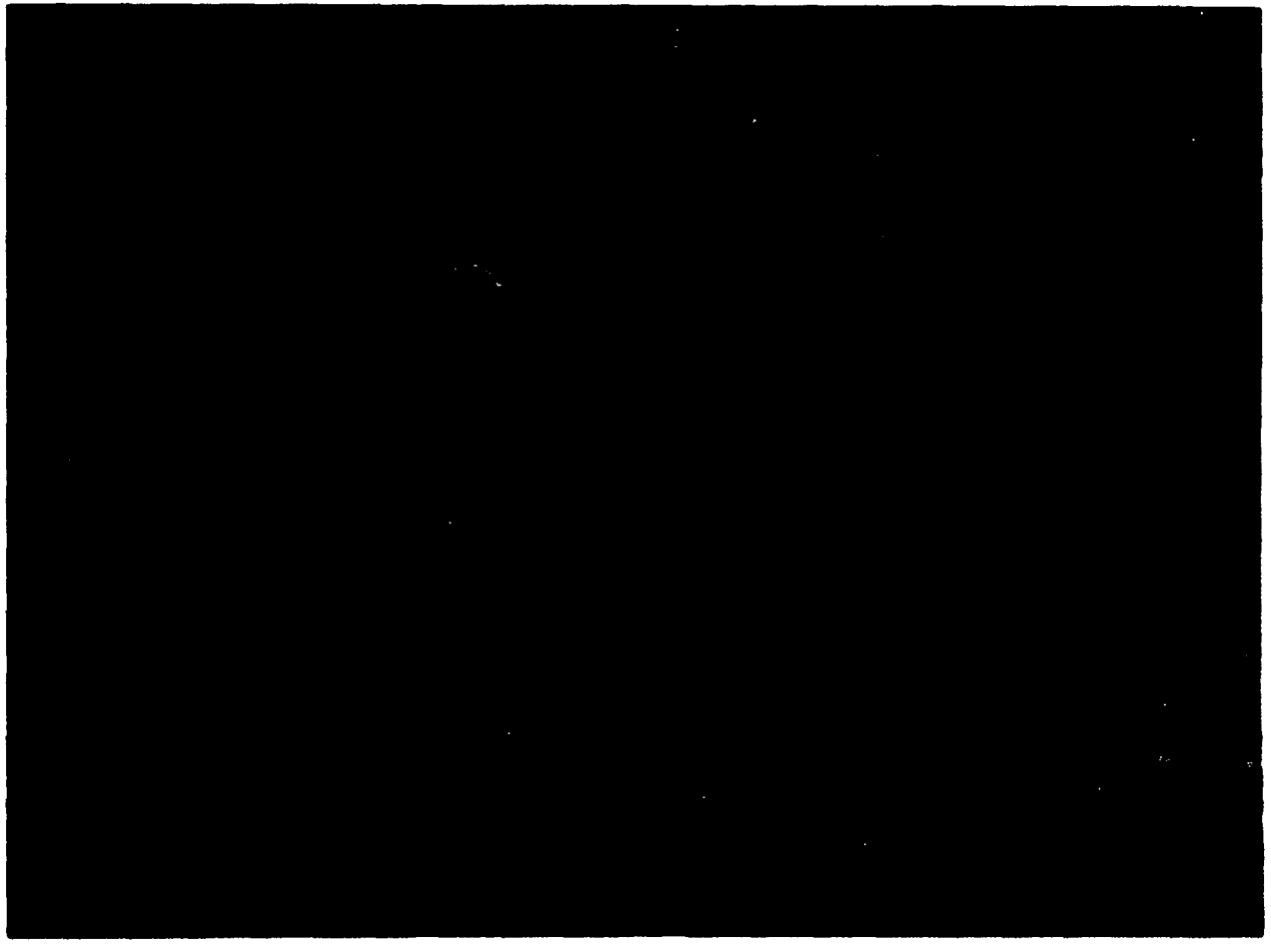

Figure 9. Underside of a Gypsum Board Showing the Deterioration Caused by a Fire Burning on Its Surface

The shaft was driven by a 1/15-HP electric motor coupled to a 1787:1 ratio gear reducer. The power supply to the electric motor was controlled by means of a variable autotransformer, in this way providing accurate adjustment of the speed of the shaft and, consequently, the feeding rate of the crib into the fire. Figure 10 shows a top view of the motor and part of the shaft. The steel airplane wires stapled to the cribs were attached to the shaft which turned and pulled the crib from under the floor level onto the table top and into the fire zone. As the crib burned, the ashes remained on the asbestos cloth, but, since the cloth also wrapped around the shaft and moved at the same rate as the advancing fire, the ashes did not collect in a particular spot on the table top.

An ash can made of 24 gage steel sheet and measuring 6 feet by 1 foot by 1 foot was located underneath the shaft. As the asbestos cloth wrapped around the shaft, the ashes lying on the cloth were dumped into the can. The can was supported by means of braces to the table frame so that the measurement of the load on the table included both the fuel and the ashes.

The fuel bed was fed onto the table top from a lower platform underneath the table top. The leading and trailing edges of the tables were provided with a rounded piece of steel sheet to provide a smooth motion of the fuel bed.

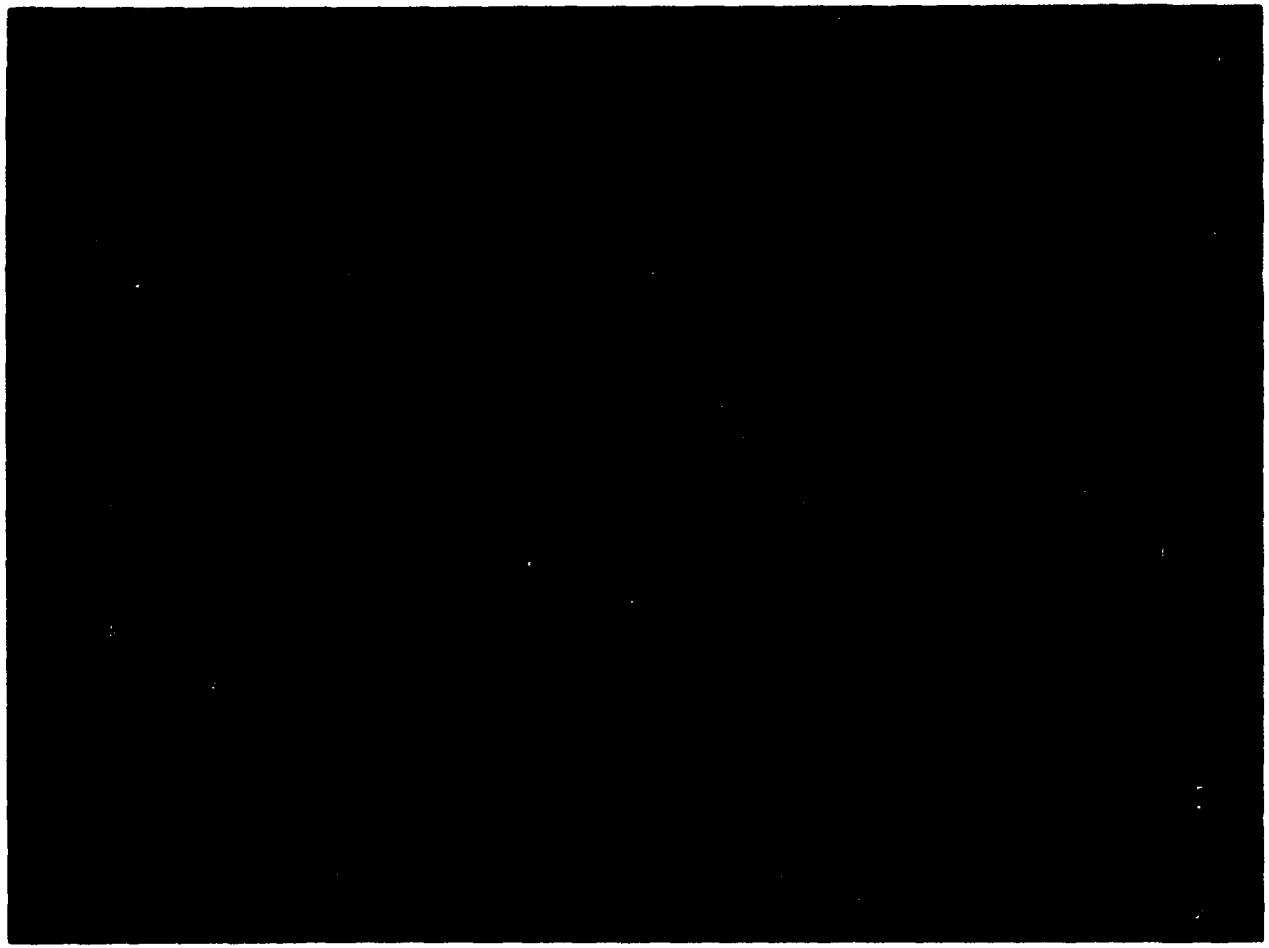

Figure 10. Top View of the Motor and Shaft Used to Feed the Fuel

One of the tables was initially mounted on top of four similar force-ring transducers, one under each leg of the table. Figure 11 shows a front and side view of one of the transducers. The strain produced by the force on the ring is transmitted to strain gages located at both the inner and outer sides of the ring. The net signal from all the strain gages was amplified and recorded. The four rings were wired so that their signals were additive, thus giving an indirect reading of the sum of the loads on the legs which must be equal, by static equilibrium considerations, to the distributed load on the table. Figure 12 shows the combustion table mounted on top of the transducers. A 5/8 inch thick piece of Fiberfrax insulation was put between the leg and the ring upper base to reduce the heat transfer by conduction through the leg. The transducers were covered with water jackets to avoid damage to the strain gages by the high temperature existing in the surroundings.

A different method of obtaining the weight loss was utilized with the second table due to the availability of a torque pickup and associated amplifier and recorder. The combustion table was suspended to a lower frame by means of four knife-edge links hanging from the legs. A view of the lower frame can be seen in Figure 13. The lower frame was made of slotted steel angle and had a pair of axles and pulleys mounted on it by means of pillow-block bearings. Figure 14 shows a schematic diagram of the

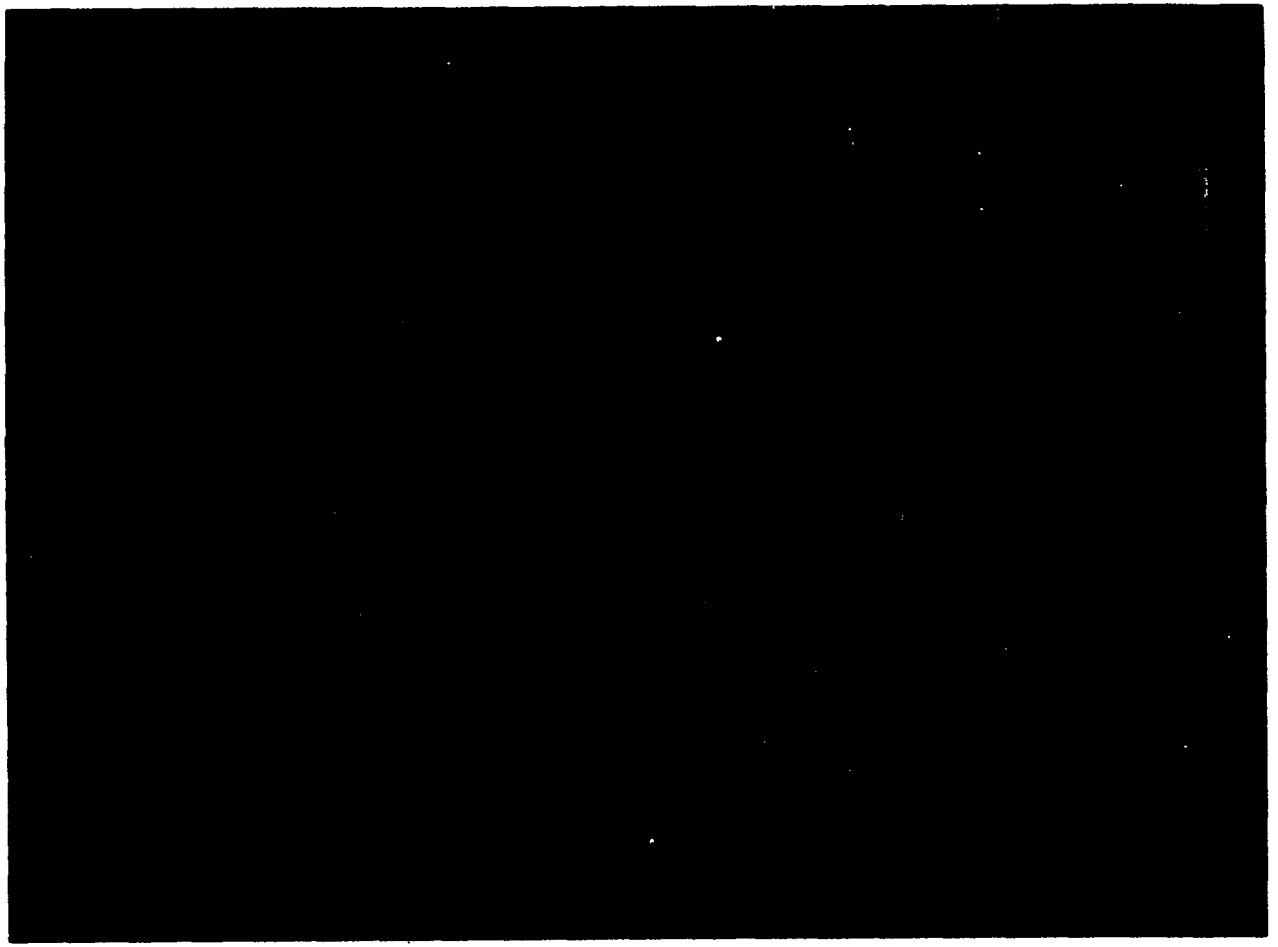

Figure 11. Force-Ring Transducer

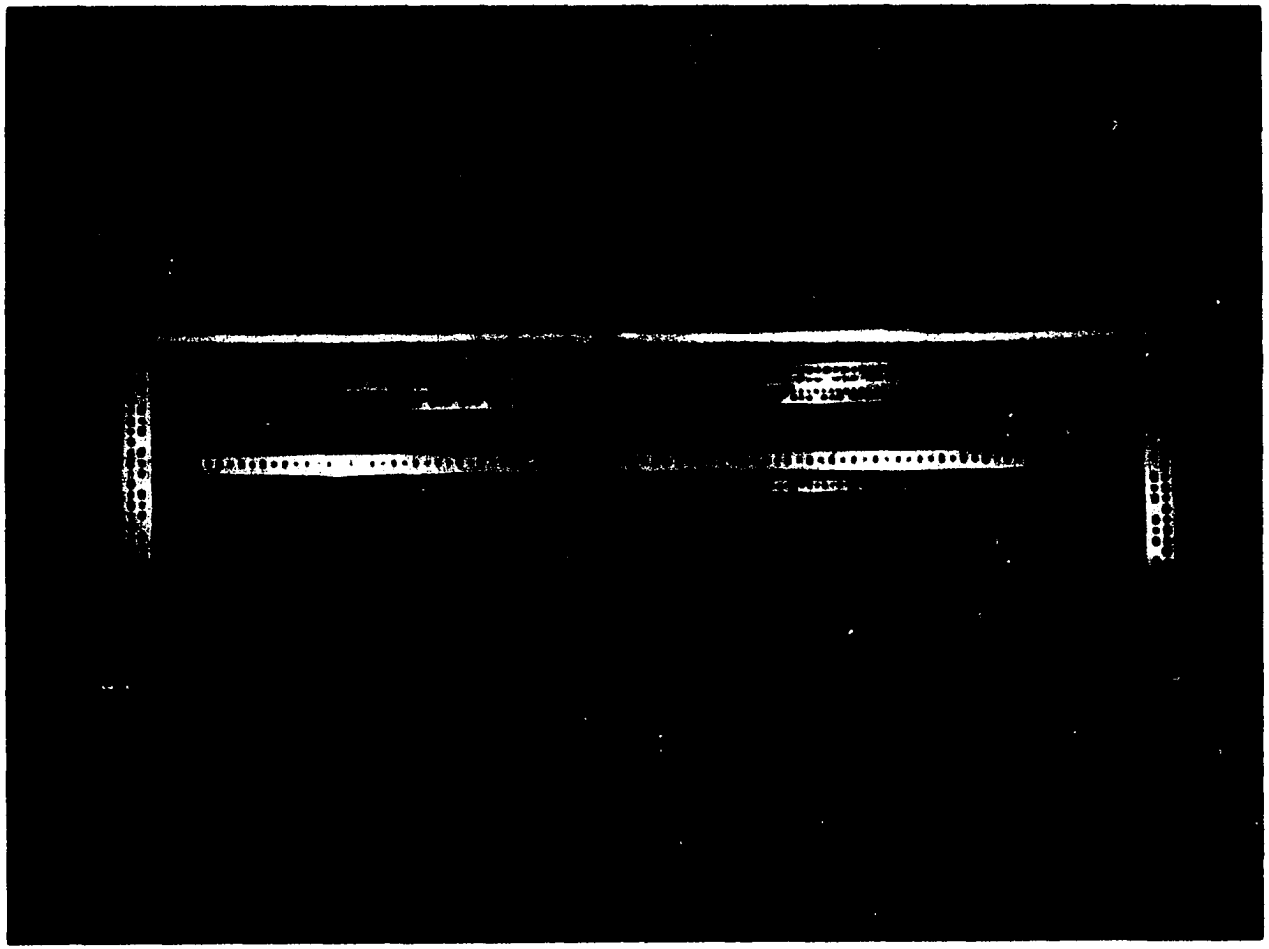

Figure 12. Combustion Table Mounted on Top of the Force-Ring Transducers

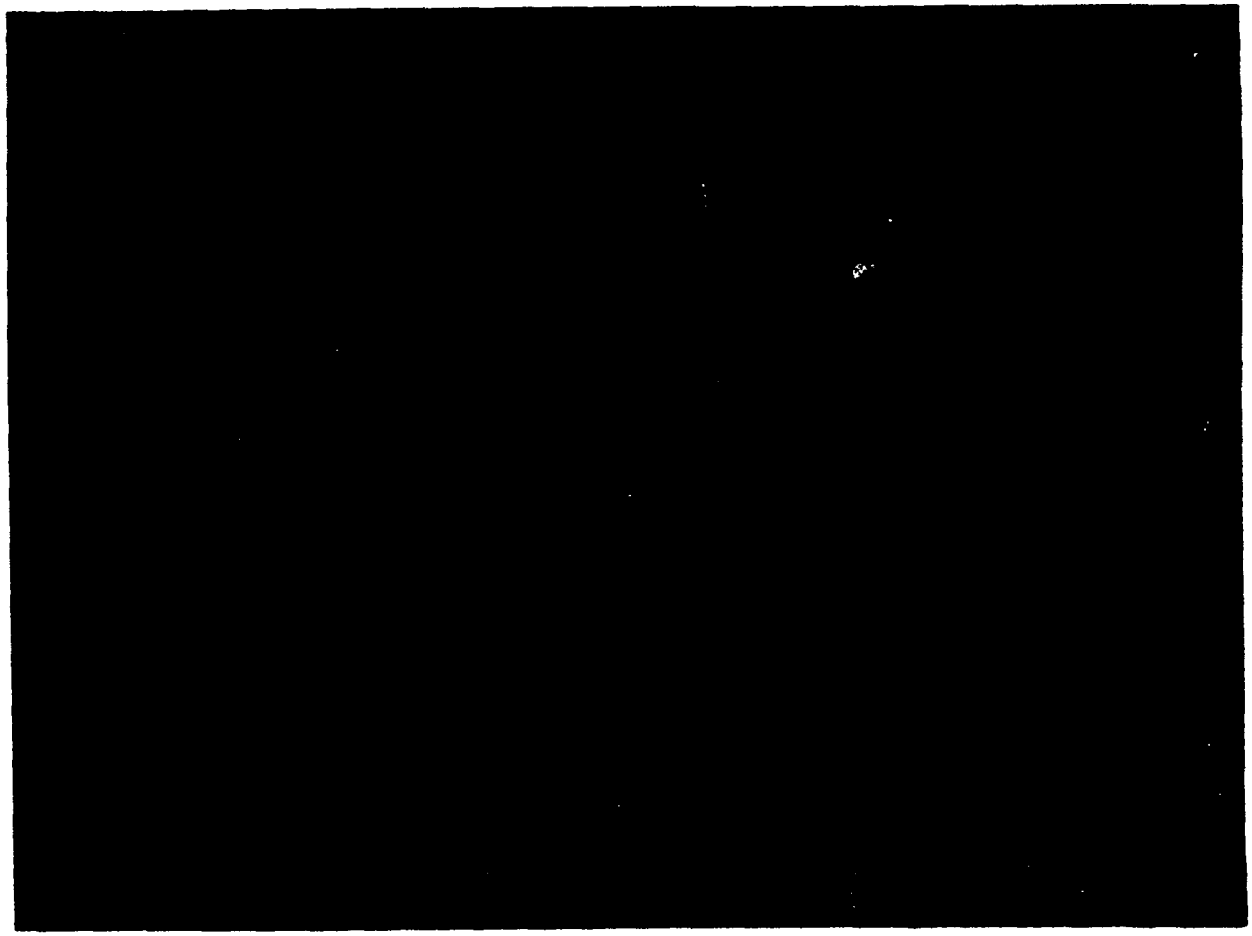

Figure 13. View of the Lower Frame

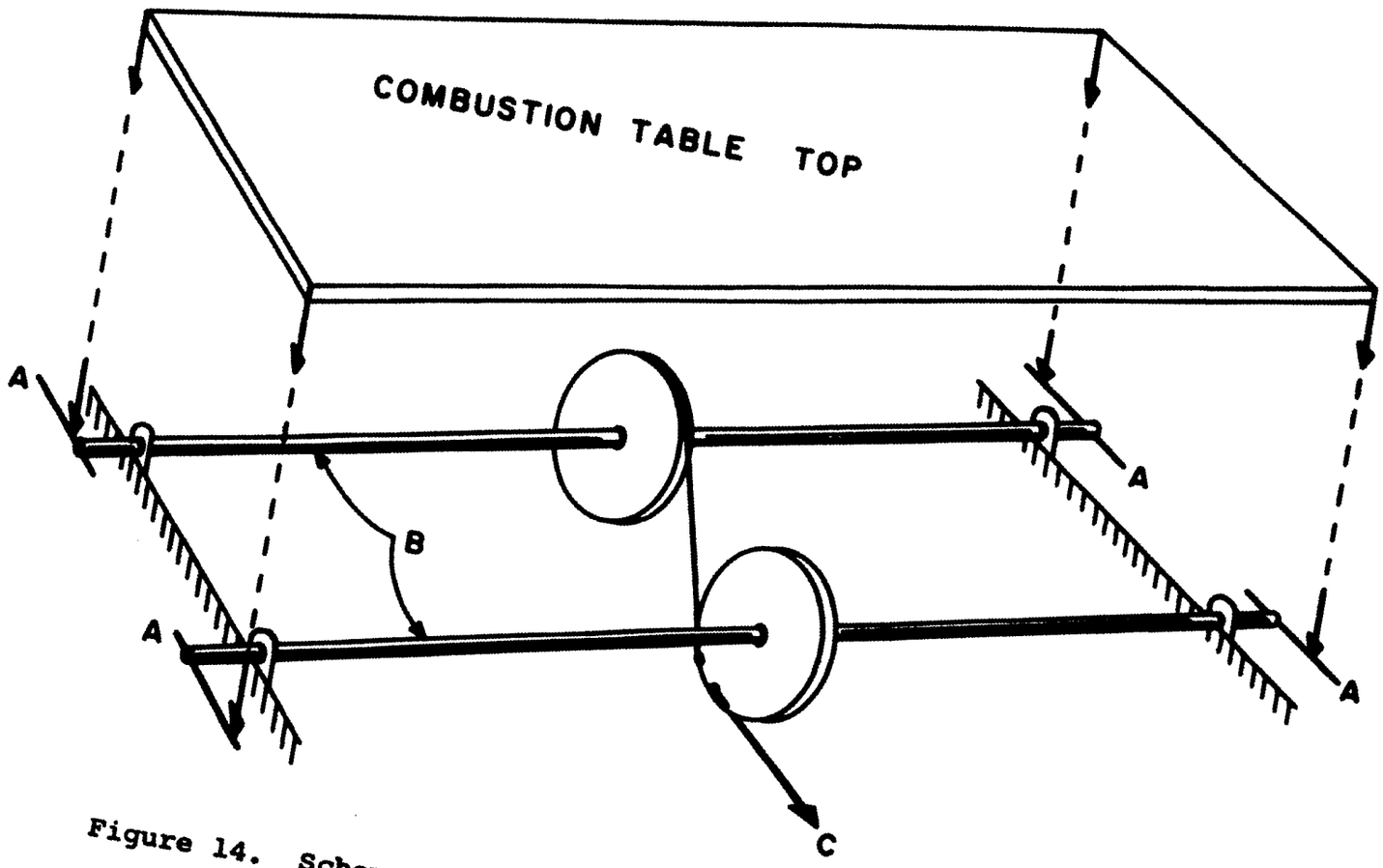

Figure 14. Schematic of the Load Transmission in the Lower Frame

load transmission. The load on the upper frame was transmitted by the knife-edge joints A to the end of the axles. This load tended to rotate the axles B. The arrangement of the shafts and pulleys was such that the rotation of the shafts was independent of uneven loading of the combustion table. The result was that the weight of the distributed material lying on the top was transmitted as a concentrated load by link C to a load pickup. The signal of the pickup was amplified and recorded continuously. A view of the combustion table mounted on the lower frame is shown in Figure 15.

The weighing devices were calibrated by placing 5-lb load increments on the table tops and noting the recorder output. Calibrations were made after proper warm-up and adjustment of the recorders. The readings of the recorders were linear for the range of loading used. The tables were loaded and unloaded several times in order to check for hysteresis and/or zero shift. These problems were not present.

Instrumentation

The wind speed was measured with an Alnor Type 8500 thermo-anemometer manufactured by the Alnor Instrument Company of Chicago, Illinois. The instrument consists of a probe and readout device. A 0.002 inch diameter wire is stretched between two supports at the tip of a 2 feet long probe. During operation of the instrument, electrical

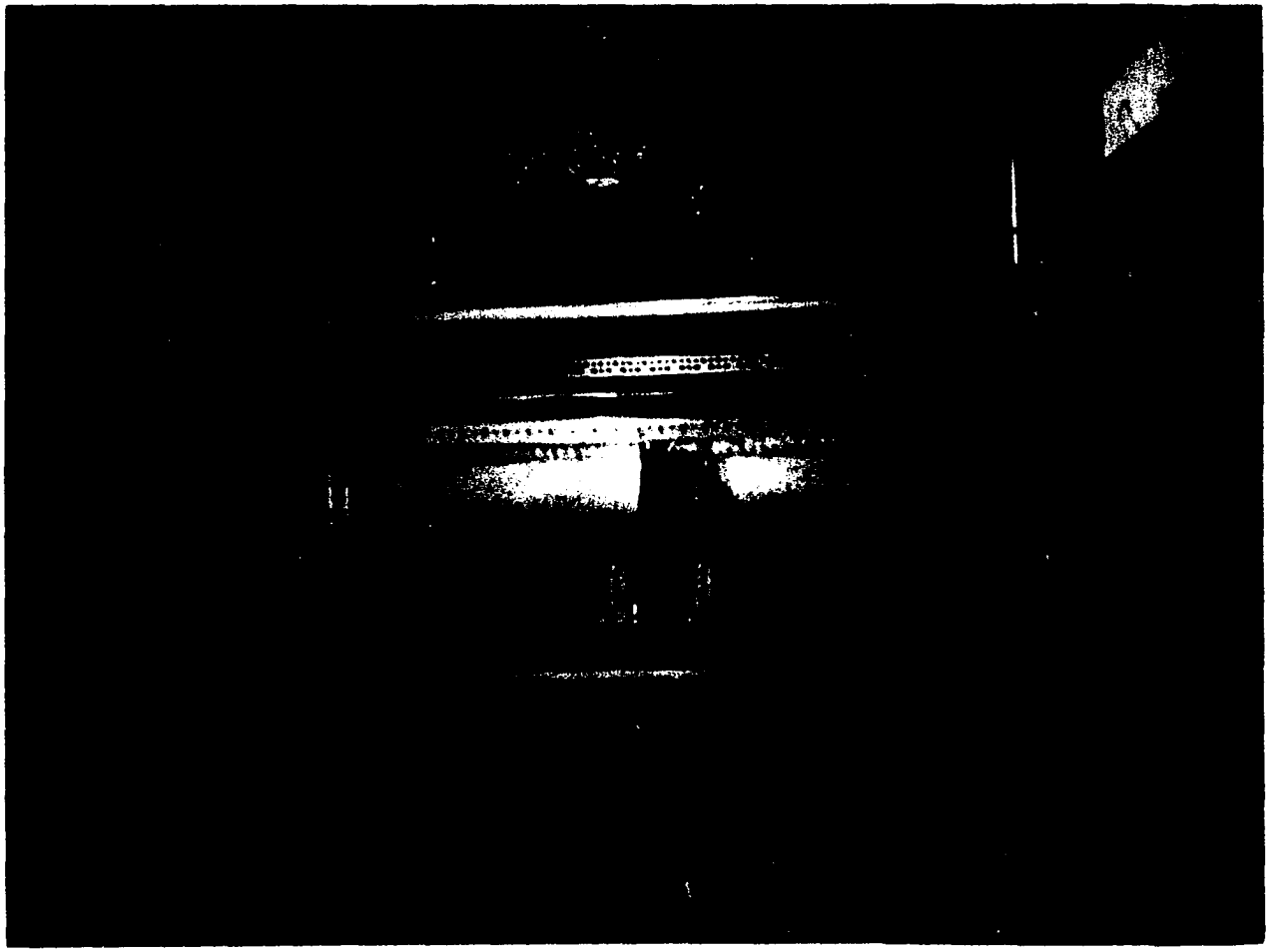

Figure 15. View of the Combustion Table Mounted on the Lower Frame

power is supplied to the wire. Thus, the temperature of the wire is raised to about 350°F in still air. The temperature is reduced when gas flows past the wire, due to convective cooling. A thermocouple made of fine wire (0.002 inch diameter) has its junction located at the center of the stretched wire. It measures the wire's temperature. The thermocouple has a built-in reference junction exposed also to the gas stream which compensates for differences in readings due to varying gas temperatures. The reading of the temperature of the wire is shown on a scale calibrated to read the gas speed in ft/min. The instrument range is from 10 to 2000 ft/min with two range scales. The accuracy is stated to be ± 2 ft/min or ± 3 per cent of the indicated value, whichever is larger.

For the measurement of the wind speed upwind of the fires, the probe was installed on a remotely controlled traversing device at a distance of about 2 feet from the edge of the upwind combustion table. A photograph of the traversing device is shown in Figure 16. Movement of the housing along the vertical direction is accomplished by means of the reversible DC electric motor located at the rear of the housing. Horizontal movement of the rail supporting the housing is accomplished by an arrangement of pulleys and wires. Both movements are controlled from inside the observation room and allow positioning of the probe at any desired location in the cross section except within 6 inches of the floor and ceiling. The readout

device is located inside the observation-and-instrumentation room and is connected to the probe by a 25 feet long cord. A pitot-static tube can also be seen protruding forward from the anemometer housing in Figure 16. It was not used for the tests due to its inaccuracy at low wind speeds.

An optical pyrometer was used to determine the optical flame temperature. Although possessing certain disadvantages due to the corrections necessary to obtain the true flame temperature, this device was considered sufficiently accurate for the intended purpose.

Mercury-in-glass thermometers with the stem graduated in increments of 1 degree Fahrenheit and with a range from -30° to 120°F were used to measure the dry- and wet-bulb temperatures.

Flame length and flame bending angles were determined photographically. Flame photography is a useful technique in visualizing and making measurements of the size and appearance of the flames, especially when dealing with turbulent flames where an exposure of short duration serves to average the irregular flame fluctuations. However, there are certain peculiarities associated with the technique which deserve mentioning. Generally, what the eye sees is different from what the film records. The appearance of the flames in the pictures varies also depending upon the type of film (black- and-white, color, infrared, visible sensitive) and exposure used. A certain amount of distortion in depth is also present in the picture since the flames do not lie in

a single focal plane. In these studies two special cameras were used to take still shots of the fires. One of the cameras consisted essentially of a wooden box with one of its faces built to retain a Polaroid film holder which used 4 x 5 film packets. A metallic disk with a circular hole in its center was fitted into the face of the box opposite the film. A piece of aluminum foil was cemented to cover the hole in the disk and a pinhole was then made on the foil by piercing it with a very fine wire. Since the focusing is done through the pinhole, objects at various distances in front of the camera appear always in focus on the picture. The camera was also built to have a very wide angle of approximately 100 degrees. The other camera was also of the pinhole type but its body was made of sheet metal. The wooden box camera had a manually operated shutter located in front of the pinhole. The sheet metal box camera had an internal shutter operated remotely by means of a solenoid located inside the camera. Two types of Polaroid films were used with the cameras. A very fast speed film (ASA 3000) was used in the cameras for photographing the fires. Exposures of 1 to 4 seconds were used. A positive-negative film (ASA 50) was used to photograph a grid positioned vertically in the center of the wind tunnel test section. This grid served as a reference datum and was prepared by painting an 8 feet by 8 feet board black with white parallel stripes spaced every inch and running in both the vertical and horizontal directions. The negative was used

as a template over the pictures of the fires to measure the height and horizontal displacement of the flame tip. The angle of inclination of the flames was also measured directly from the pictures with a protractor.

The temperature of the wake gases downstream of the fires was measured by means of iron-constantan and chromel-alumel thermocouples. The thermocouples were positioned throughout the cross section of the tunnel as shown in Figure 17. The thermocouples were fastened to a rack consisting of a pair of vertical plates mounted one on each side of the tunnel between which several wires were stretched. Springs were used to connect the ends of the wires to hooks fastened to the vertical plates so as to keep the wires tensed. The plates were mounted, by means of a sliding device, on railings running along both sides of the tunnel. The sliding devices could be moved up- and down-stream of the tunnel simultaneously by means of a reversible AC motor and a system of cables and pulleys. A picture of the rack is shown in Figure 18. The hot junctions of the thermocouples were protected from flame radiation by means of shields. A sketch and picture of one of the shields is shown in Figure 19. The shield consisted of a thin walled, nickel plated brass tube with cone-shaped copper shields attached to the ends. The thermocouple junction was inserted through a side tube of smaller diameter soldered to the side of the shield. Contact between the tube and the thermocouple wires was avoided by means of a ceramic insulator. The signals from the thermo-

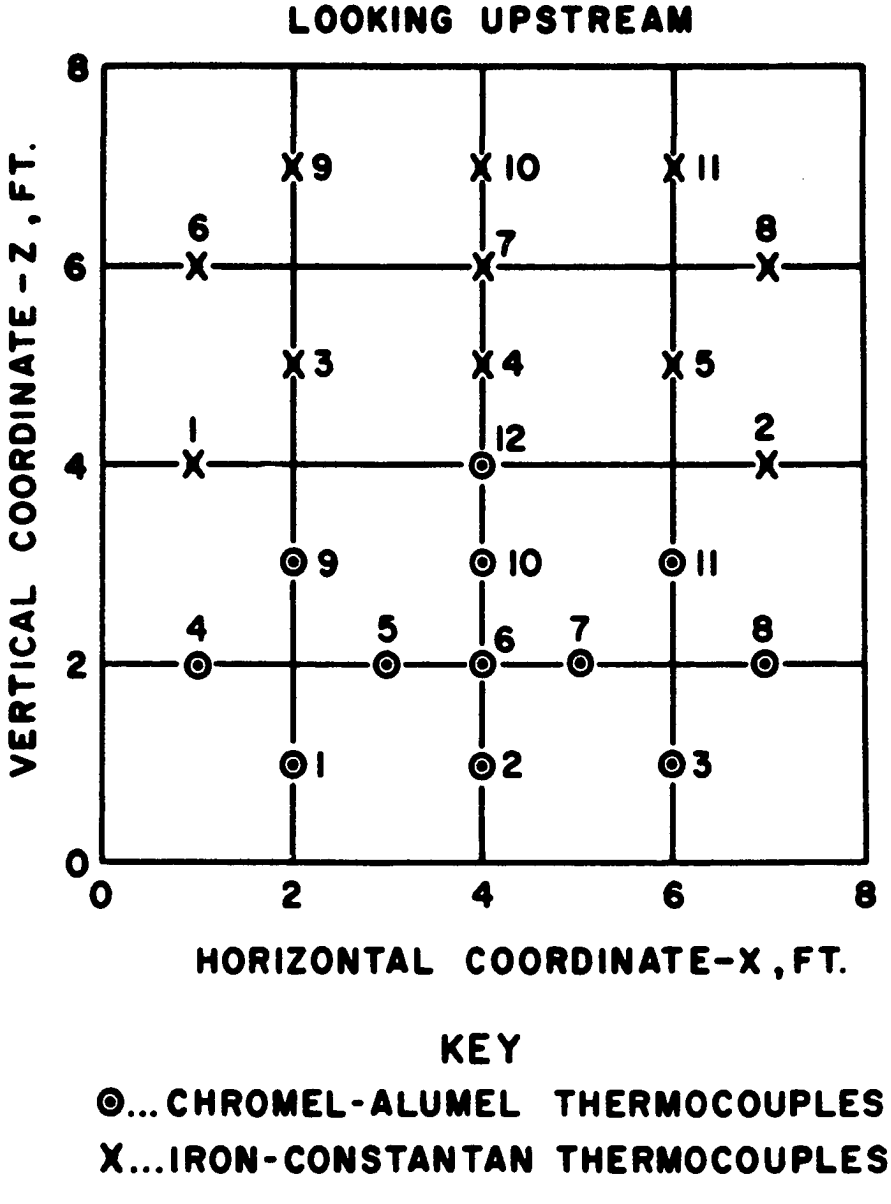

Figure 17. Location of the Thermocouples in the Cross Section of the Wind Tunnel

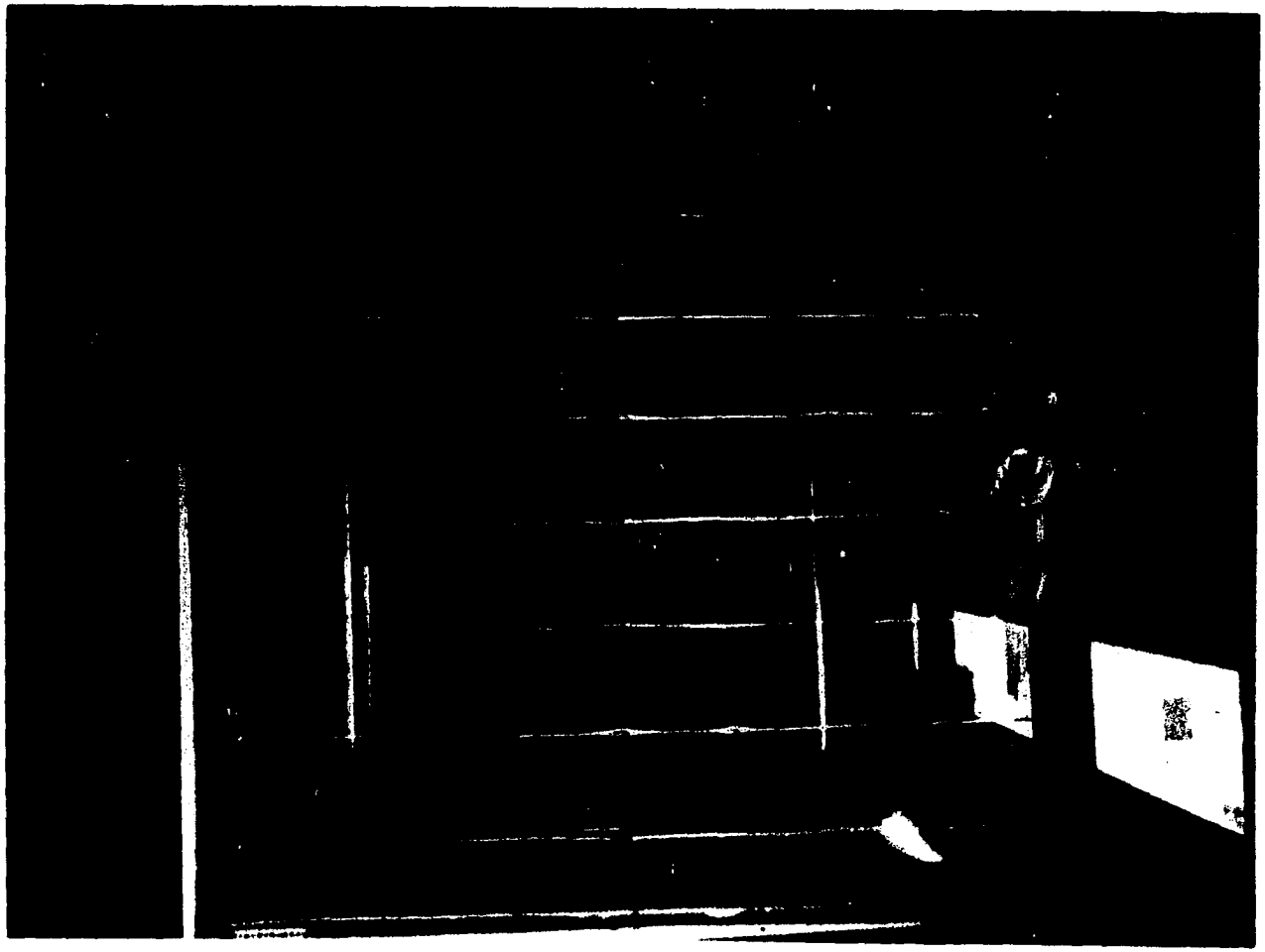

Figure 18. Thermocouple Rack

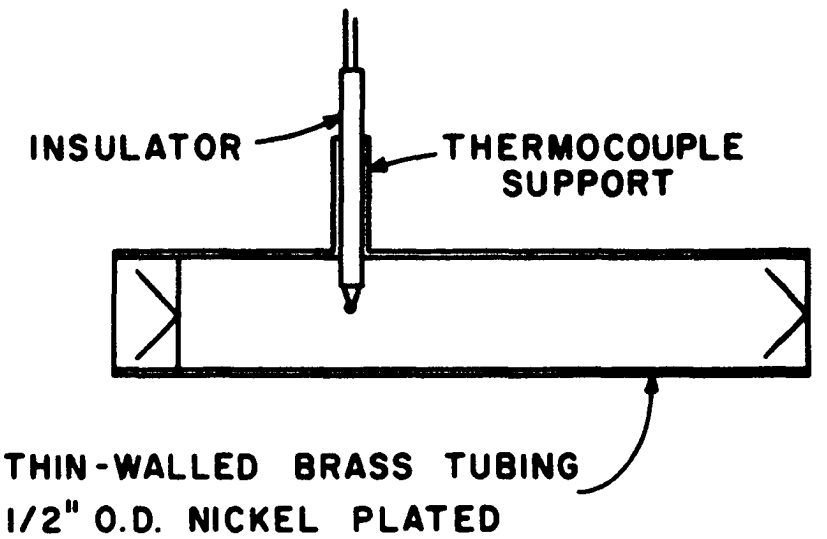

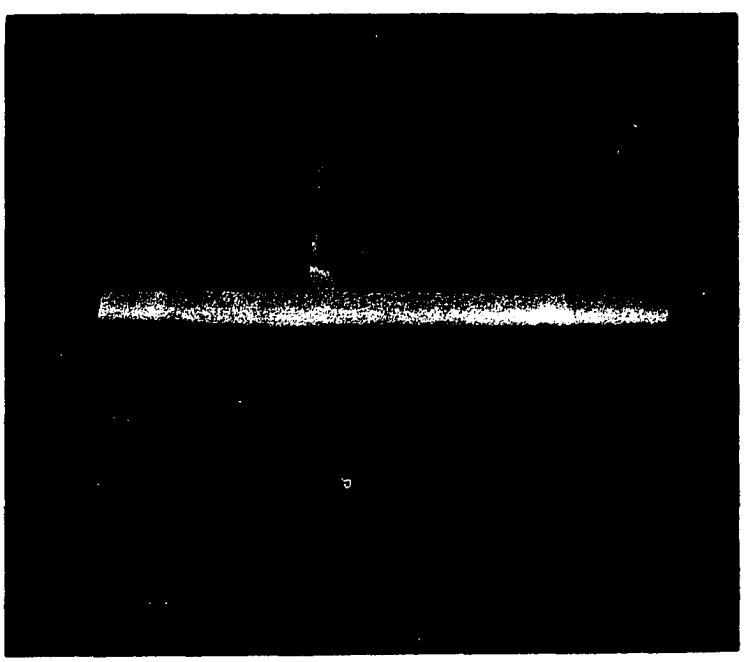

Figure 19. Thermocouple Shield

couples were recorded on two, 12-point recorders. One of the recorders was calibrated for use with chromel-alumel thermocouples and the other for use with iron-constantan thermocouples.

The flame radiation at a point downstream of the fires was measured with an asymptotic radiometer. The radiometer essentially consists of a copper body with a thin, blackened constantan foil suspended in a cavity. A fine copper wire is attached to the center of the foil and a differential thermocouple is made with the hot and cold junctions located at the center and periphery of the foil, respectively. A window protects the receiver from convective effects. The radiometer used had a range of 3 solar constants (about 3.6 Btu/ft^2-sec) with an output of 4.65 millivolts at 3.6 Btu/ft^2-sec indication. The radiometer was positioned at the centerline of the test section floor with the face of the receiver in a vertical plane facing the fires.

CHAPTER IV

EXPERIMENTAL PROCEDURE

A brief explanation of the experimental procedure is presented in this chapter. To the author's knowledge, the technique used in this study for the investigation of the characteristics of propagating fires has not been employed before. The technique differed from the others, basically in that (1) the position of the flames was fixed with respect to the stationary coordinates of the wind tunnel test section and (2) the weight loss of the cribs was continuously measured while the cribs burned at floor level. A discussion of various problems encountered is also included hoping that it can be of benefit for future users of the technique.

The preparations for the test usually started with the removal of the cribs from the polyethylene bags in which they were packed to maintain a constant moisture content. The samples of wood and of asbestos cloth included in each bag were kept in the bags for a later determination of their moisture content. The sticks on the side facing the observation windows were numbered using a marker. Next, the recorders of the weight-loss signal

were zeroed and a calibration curve was obtained on their chart paper by placing loads in five pound increments on the combustion table. The cribs were then loaded on the tables. In the case of the downstream combustion table (from hereon denoted as table B) the crib was placed on the tunnel floor with the leading portion of the crib resting on the combustion table. The pulling wires were then passed through the slot used to dump the ashes and were connected to the driving shaft. The connections were secured by placing a strip of tape on each one. The crib was then moved by hand so as to remove the slack from the wires. Subsequently, it was moved to the proper position on the combustion table by means of the feeding mechanism. The trailing portion was then bent downward and into the storage shelve under the top of the table. Next, the sections of the floor were moved into position. Fiberglass insulation boards, 3/4 inch x 3 feet x 4 feet covered with asbestos cloth, were utilized to insulate the sheet metal floor.

The loading of the upstream table (from hereon denoted as table A) was accomplished in a different manner due to the impossibility of reaching the table from the end of the test section exiting into the static test room. Thus, the crib was carried into the test section through the side door located after the last screen of the straightening section. A pair of wires was connected to the trailing

portion of the crib. These were routed on top of the combustion table, through the feeding slot, under the table and finally connected to the driving shaft. The crib was then fed in the reverse direction through the feeding slot and into the storage shelf under the top of the table, until the leading portion of the crib was in position. The next step consisted of removing the provisional pair of wires attached to the trailing portion of the crib and of connecting the wires from the leading portion to the driving shaft. The connections were secured with a piece of tape to avoid having any of the wires breaking loose during the test. A piece of sheet metal was then screwed to the floor of the test section. It served the dual purpose of covering the ash can, leaving just sufficient opening for the ashes to fall, and of providing support to the insulation. The floor section from the last screen to the upstream edge of combustion table A was subsequently covered with fiberglass insulation boards. Figure 20 shows the cribs positioned on the tables and the floor section covered with the insulation.

The next step consisted of placing the radiometer in the proper location. Its associated recorder was zeroed and calibrated. The thermocouple rack was then moved away from the location where the cribs were to be ignited.

A rectangular burner measuring 1 inch x 35 inches and 1/2 inch deep and filled with approximately 200 ml of

Figure 20. View of the Cribs Positioned on the Combustion Tables and the Surrounding Floor Covered With Insulation

acetone was used to initiate the combustion of the cribs loaded on table A. Initially, this same procedure was used to ignite the cribs at table B, but the burner was difficult to reach due to its location between the two cribs. This procedure usually resulted in spillage of the fuel while being filled. The liquid fuel would soak the asbestos cloth, and when ignited, it tended to burn over a much larger area and for a longer time resulting in an initial uneven ignition across the width of the crib. To avoid these difficulties, a gas burner was built and used for the rest of the tests to ignite the cribs on table B. The gas burner consisted essentially of a rigid copper tube 5/8 in. OD and about 4 feet long having several small holes of approximately 5/64 inch in diameter spaced at 1.5 inch intervals along a line on the side of the tube. The length of the row of holes was 3 feet. One end of the tube was sealed while the other end was connected to a mixing head (similar to the ones used in gas heaters) where the gas was discharged through an orifice and mixed with air to provide a premixed fuel mixture. The burner was connected to a rigid copper tube, 5/8 in. OD, and at 90 degrees to it. This copper tube served as the supply line for the burner while at the same time being long enough to facilitate the positioning and removal of the burner. The gas burner was connected by means of a flexible hose to a main gas line. This device worked satisfactorily; however, due to the smaller amount of energy provided by the very short

flames from the burner, it took a much longer time to establish a self-substaining combustion in the crib than the time required when using the liquid burner. This condition resulted in no problems, only requiring that the ignition of the crib at table B (downstream) be carried out prior to the ignition of the crib at table A (upstream).

The last stages of the preparation period consisted of filling the liquid fuel burner, of placing the gas burner on the test section and of turning on the chart paper feed of the various recorders. In addition the dry-bulb and wet-bulb thermometers were placed on the outside of the building and the barometric pressure was read.

A representative testing period started with the ignition of the cribs; the fire on table B being started about 4 to 8 minutes earlier than the one on table A. After self-substaining combustion was achieved the starting burners were removed and the blower was started after being certain that the variable vanes at the inlet of the blower were fully closed. The hot wire anemometer was then turned on and the wind velocity was adjusted to a value below the desired one. This procedure was necessary since it was found that with the growth of the fire from the moment of ignition to the instant where a steady burning rate was achieved, an increasing additional draft was created which aided the blower action. The vanes had to be adjusted by steps so as to avoid attaining a wind velocity of a higher value than desired. From there on, the

fires were monitored so as to maintain the proper spacing between the centers of the flames. The position of the fires in the test section had been preselected. The grid painted on the wall opposite the observation windows was used to position the flames visually in their respective locations. The fires were maintained at these positions by feeding the cribs in a semi-continuous manner at the proper rate. (Continuous feeding of the crib presented difficulties since as the weight of the crib decreased, the feeding rate accelerated.)

The weight loss, thermocouples, and radiometer readings were then observed and when a steady value of weight loss rate and thermocouple readings was reached, the run was started. This instant was marked on the several recording charts with the number of the run. Sufficient time was allowed for each run to record enough information on the charts (i.e. several inches on the graphs to determine the proper slope of the weight loss curve and several cycles of thermocouple readings to determine a proper average of the temperature). In the meantime, the other data were gathered. The optical temperature of each flame was obtained with the optical pyrometer. The observer stood on the floor of the test-section at the point where it discharges into the static test room while taking the measurements with the pyrometer. The dry-bulb and wet-bulb thermometers were read. The wind speed was noted and the

depth of the burning zone was determined visually. On occasions when the wind speed was high enough that the flame enveloped the crib on the downwind side, it was not possible to read the depth of the flaming zone. In this case the wind velocity was reduced to zero after all other readings had been taken. Because the flame returns to a vertical position at no wind it was possible to determine quickly the depth of the flaming zone. Each flame was photographed and each picture was marked with the run number to avoid confusion. Figure 21 is representative of the shape and bending of the wind-blown proximate flames. The wind speed blowing on the flames shown in the picture was 1.99 ft/sec and the spacing between the fires was 4 feet. The time at which each of the sticks of the top layer ignited as well as the number of the particular stick was noted. These readings were used to obtain the flame propagation rate averaged over the period of the run. When the flame bending was such that an exact determination of the stick catching fire was impossible, the flame propagation rate was measured indirectly by measuring the feeding rate. These two parameters are numerically equal. The feeding rate was determined by using a reference mark downstream of the position of the fire and noting the time and the stick number aligned with the mark every time the feeding device was turned off after feeding additional sticks to the fire zone.

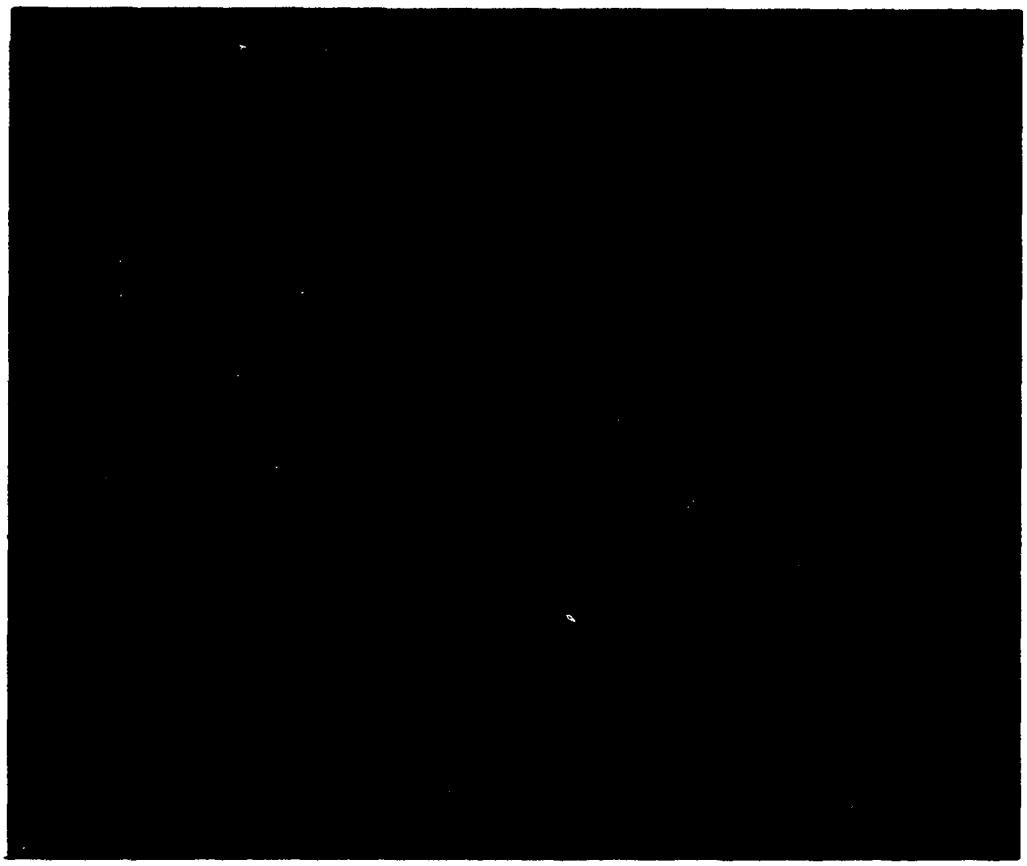

Figure 21. Representative Shape and Bending of Wind-Blown Proximate Fires

After completion of a run, if there was still sufficient unburned crib left on the tables, the conditions would be changed, enough time would be allowed to reach a new steady state and readings for the new run would proceed. The change in the experimental conditions consisted of a change in the separation of the centers of the fires, change in the position of the thermocouple rack and/or change in the wind speed. The radiometer was maintained at a distance of 12 feet from the center of the flame at table B for all the runs.

After the runs, the final stages of the test proceeded as follows: the chart paper feed of the recorders was turned off, (however, the amplifier section was left on, so as to insure proper warmup for the next test; they were only turned off when testing had to be stopped for any reason for more than three days). The anemometer readout was turned off and the protective cap was replaced on the probe. The dry-bulb and wet-bulb thermometers were taken back into the observation room and the pyrometer was put into its protective carrying case. The remaining portions of the cribs were watched until extinction occurred to insure that no accidental fires could occur from the glowing embers. The blower was left on with the vanes slightly opened during the above step to provide a cooling stream of air. Usually, this period lasted for about 20 minutes after which the blower was turned off. After

the test section had cooled, the radiometer was set aside and the fiberglass insulations were removed from the floor. The sheet metal floor sections were then slid away from combustion table B. The asbestos cloth, which had been wrapped around the feeding shaft, was removed by reversing the direction of rotation of the shaft to unwrap the cloth and, while the shaft was turning the cloth was pulled out through the feeding slot. The sheet metal covering the ash can of table A was then removed and the asbestos cloth was removed in a similar manner. The ashes from the cans were then removed and thrown in the dump can after being sure that they were completely extinguished. The combustion tables were then cleaned and checked for any damage before proceeding to the next test. The thermocouple shields were cleaned occasionally by blowing air through them. After the fire test, the wood samples were tested for moisture content following ASTM Method D #2016-62T (ref. 72). The values of moisture content obtained for each one of the cribs is summarized in Appendix C, Table 1, together with the density of the wood in the cribs.

At this point, it is advisable to recall several other experimental problems. One of the difficulties was connecting the wires of the crib to the driving shaft of combustion table B. To reach the shaft, it was necessary to crawl under the combustion table, which was difficult

because of the limited space under the table. For the same reason, it was difficult to remove the ashes from the can of table B.

On a few occasions the steel bars on top of the table on which the cribs slid were pushed forward by the moving crib. The bar then tended to break through the cloth locking the crib from further movement; in which case, the offending bar was immediately removed, and the test was continued without further interference. The burning rate determination was not affected by this problem; the removal of the bar only took a fraction of a minute. Following the first few occurrences, this problem was solved in a very simple way. The solution consisted of cutting a slot in the asbestos cloth covering the insulation of the table about 3 inches from the ends of the bars. The bars were then inserted through the slot in such a way that the tips were under the cloth. This procedure eliminated the contact between the crib and the ends of the bar which was the cause of the problem.

As mentioned before, the wind speed was increased gradually to about the desired level. A particular value of wind speed was difficult to achieve. The quasi-steady value obtained was determined, especially at low speeds, by the added induced draft produced by the flame as well as by the vane setting. It was also noticed that after having attained a relatively high wind speed, an attempt

to reduce it by slightly closing the vanes usually resulted in an instability in the flow and combustion processes. It usually took a long period to restore the flame behavior and appearance to its original conditions after resetting the vanes to their original position.

The tarpaulins used to cover partially the inlets to the blower housing reduced considerably the problem of outdoor wind gustiness. Fluctuations in the anemometer readings were observed at low wind speeds but these were due mainly to the pulsations of the flame.

An occasional difficulty encountered with the metallic pin-hole camera was due to the heating of the body of the camera by the radiant energy emanating from the fires. The heating caused an expansion of the frame holding the film holder and the holder became loose on several occasions. To eliminate this problem, the holder was taped securely to the camera. The heating also was the cause of failures of the solenoid operating the shutter.

In general, no problems were encountered with the feeding mechanism of the tables. The deterioration of the insulation used on the combustion table tops was slight.

Failure of the recording equipment associated with combustion table A after burning about 2/3 of the total number of fires forced a change in the method of weight loss measurement for that table. The base of the table was rebuilt in the same manner as for table B and the

concentrated load was applied to a cantilever beam type of strain-gauge pickup since a recorder suitable for the pickup was available.

CHAPTER V

EXPERIMENTAL RESULTS AND DATA ANALYSIS

The purpose of this study was to explore the behavior and characteristics of proximate fires under the action of wind. The examination of the burning rate behavior, rate of spread and flame bending was given primary attention. The first part of this chapter consists of a qualitative description of the behavior of the fires observed during the tests. The second part considers the aspects of data reduction and analysis.

Qualitative Observations

After ignition, the fires tended to grow until a steady burning rate was attained. The growth period was dependent upon the wind speed. In the case of low wind speed (less than 2 ft/sec) this period lasted about 7 to 10 minutes and increased with increasing wind speed. With no wind blowing through the test section, the proximate fires both burned at about the same rate and with flames of about similar dimensions. The flames also tended to burn slightly inwardly toward each other. However, in almost every case, when the very slightest movement of wind was imposed the upstream fire burned with a flame

tilted in the direction of the wind while the downstream fire burned either vertically or with a slight inclination from the vertical. As the wind speed increased, the interactions were such that, for the highest speeds, both flames tended to burn at about the same rate. The flame angles of the downstream fires also increased with increasing wind speeds although to a lesser degree than those of the upstream fires. The depths of the flaming zone of the downstream fires increased with increasing wind speed but to a lesser degree than those of the upstream fires. The variations in the heights of the flames with wind were not significant even when tilted. The heights* of the flames for cribs (see page 65 for description) are shown in Figure 22 for the range of wind speeds used in this study; the spacing between fires was varied from 2 to 5 feet. Although the length* of the flames increased with increasing wind speed, the flame heights attained were about the same as those of fires in still air. The length of each flame increased mainly because of the increase in the depth of the respective flaming zone with increasing wind speeds.

Some vortices were noticed on the lee side of the upstream flame for the smallest separation between the fires used. The downstream flame tended to undulate and its envelope tended to break considerably while at this position due to the highly disturbed flow existing on the lee of the upstream flame.

---

*See page 41 for definition of flame height and length.

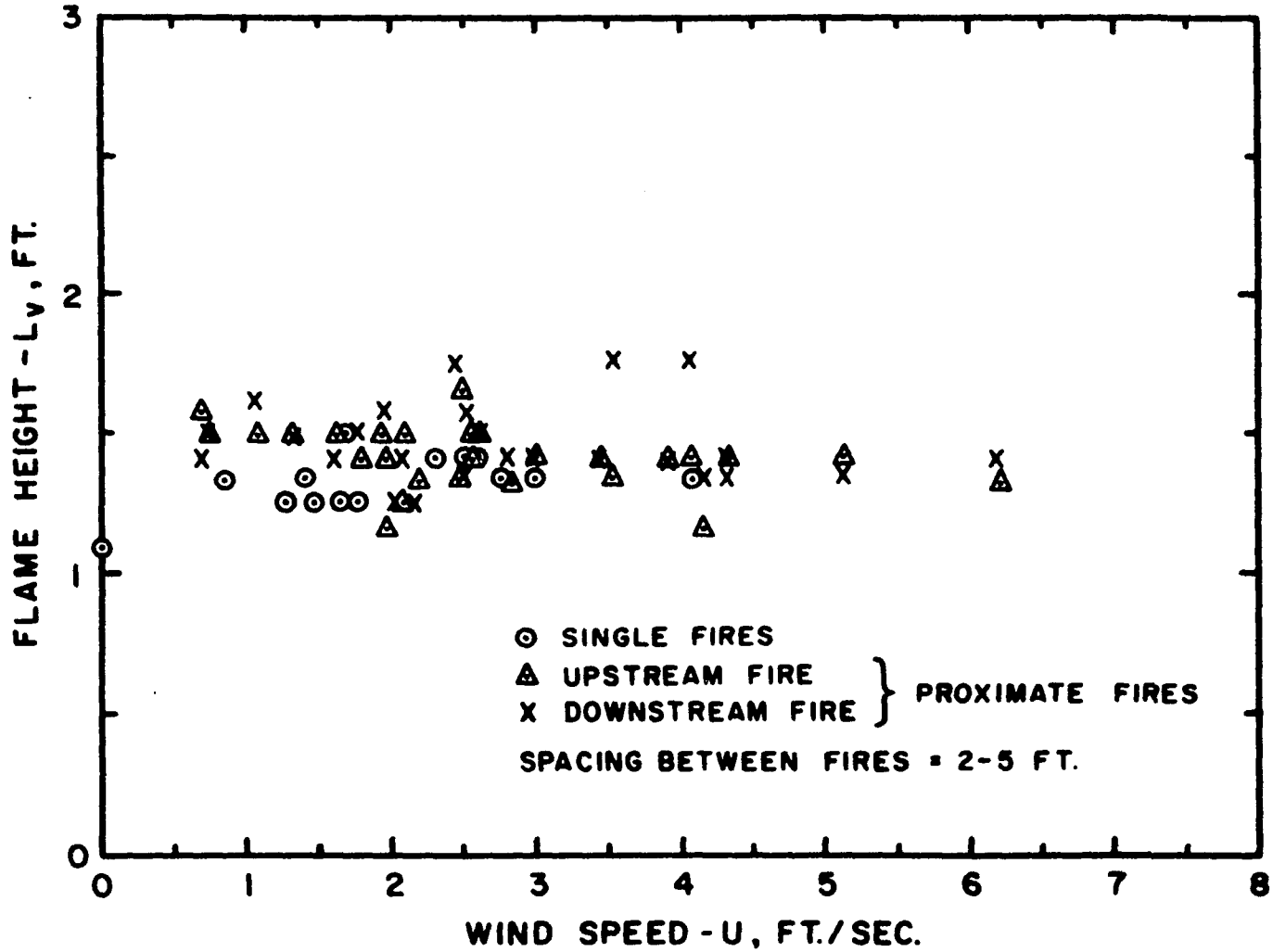

Figure 22. Flame Heights for the Range of Wind Speeds Used

The temperatures sensed by the various thermocouple stations downstream of the fires were more uniform for the low (below 3 ft/sec) wind speeds. Slight variations in the temperatures recorded occurred between printing cycles of the recorders at the low speeds, but in the majority of the cases, the variations increased in magnitude with increasing wind speeds. The temperature data obtained are found in Tables 2 and 3 and in Tables 4 and 5 of Appendix C for the single fires and the proximate fires, respectively. Temperature profiles for the vertical centerline readings of the thermocouples were drawn for the various tests. An analysis of the profiles revealed that the constraints imposed by the tunnel walls, and especially that of the ceiling in many instances, caused a disturbance in the temperature profiles and a significant deviation from what would be expected to occur if the fires were burned in the open. Two such profiles are shown in Figure 23, for the case of the single fires. They correspond to wind speeds of 1.43 and 2.98 ft/sec and are representative of the profiles obtained. It is observed that, in the case of the higher wind speeds, a peak in the temperature profile occurs within the lower half of the height of the test section. This peak corresponds to the temperature of the hottest gases in the wake of the flame. However, near the roof of the test section, the temperature increases again. This temperature increase is due to a convective heating of the air by the roof of the test section. At low wind speeds, most of the

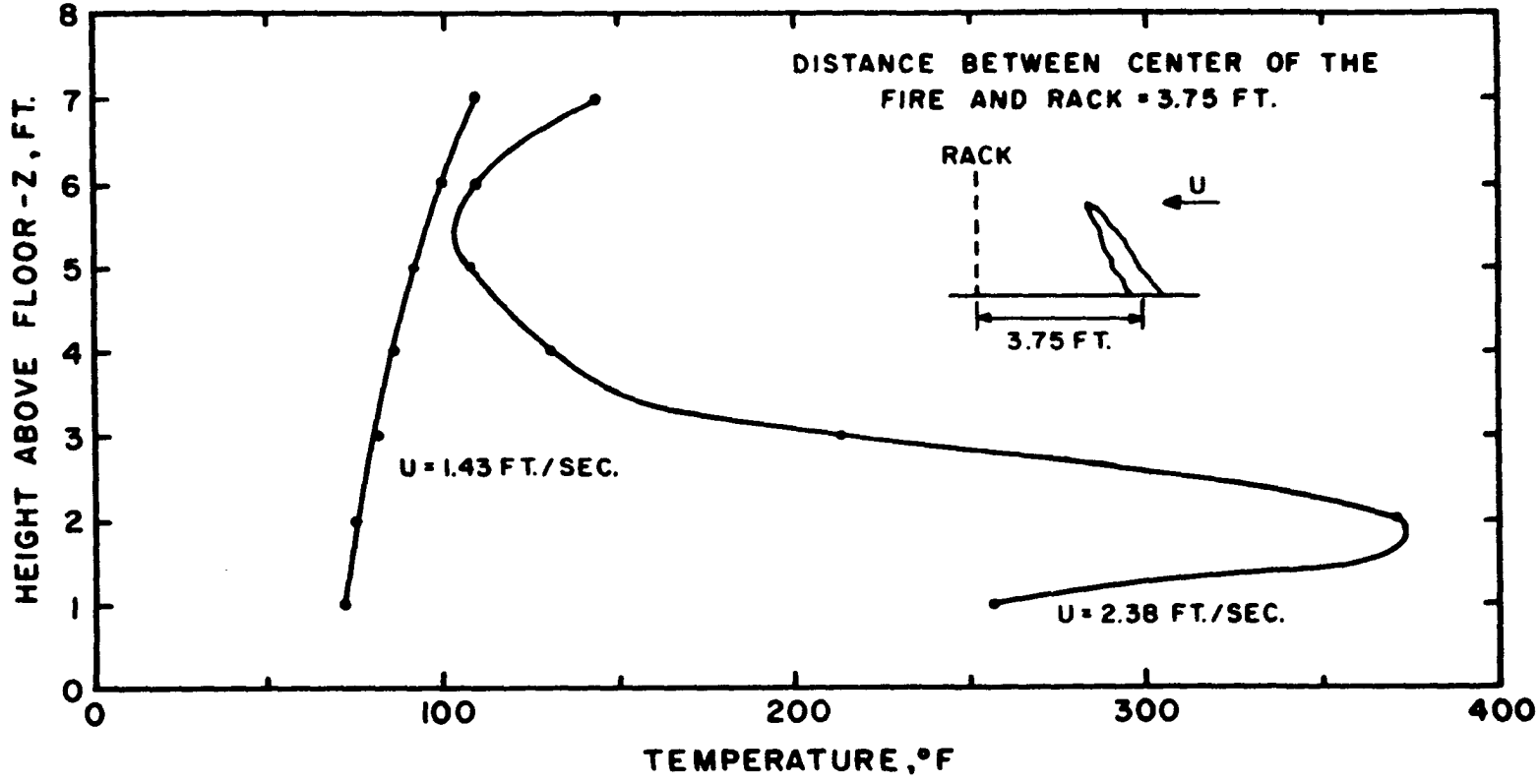

Figure 23. Wake Gas Temperature Profiles: Single Fire

gases flow near the roof of the test section. Figure 24 shows similar representative temperature profiles for the case of the proximate fires. They correspond to wind speeds of 1.79, 3.91 and 4.15 ft/sec. The ratio x/s is equal to 0.9 for all three curves, where x is the distance from the centerline between the two fires to the position of the thermocouple rack and s is the spacing between the centers of the fires.

The speed of the wind in the tunnel, as indicated by the anemometer probe, was uniform for wind speeds above 1.7 ft/sec but was affected by the gustiness of the prevailing outside winds at the lower speeds. However, the main source of disturbance at low speeds seems to be due to the flame pulsations themself.

The radiometer readings indicated that, in most instances, the radiation sensed was still increasing during the time of the run. It was observed that the burning rate (weight loss in cribs) was the first variable to reach steady state, and was followed in turn by the temperatures in the wake gases and the rate of fire spread. However, the attainment of a steady state condition for the radiometer readings required burning for a longer period than was practical due to the limited fuel supply. In most cases, the run was terminated before the radiation reading reached equilibrium. This same condition was observed by McCarter and Broido (47). Such a phenomenon may be of importance in

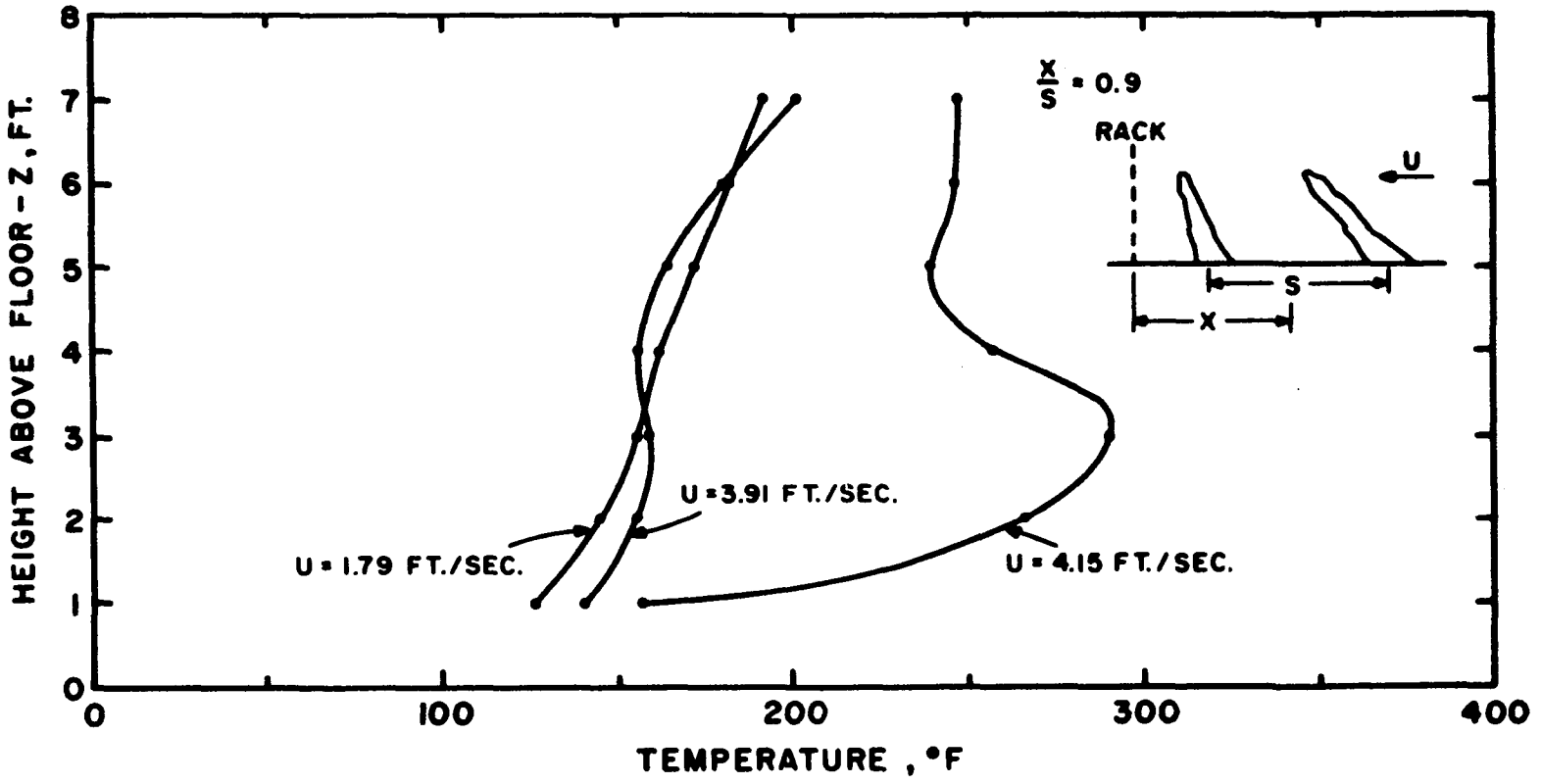

Figure 24. Wake Gas Temperature Profiles: Proximate Fires

selecting fuels for initial investigations aimed primarily at the study of radiation from large flames. Usually, solid fuels are more expensive than liquid or gaseous ones.

In all, a total of 40 cribs were burned, of which 7 were consumed in single fires; 31 were burned in dual fires and 2 were used in the preliminary tests. The wind velocity was varied between 0.7 ft/sec and 6.2 ft/sec. The spacing between the centers of the fires was varied between 2 feet to 5 feet. The temperature field was monitored at various distances (roughly 1 to 8 feet downwind from the downstream fire).

Analysis of the Data

In correlating the data obtained experimentally, the approach consisted of initially correlating the various factors of interest for the case of the proximate fires in terms of previous successful correlations by other experimenters. Thus, the data obtained from the single fire tests have been utilized to test whether or not they agree with previous correlations. The behavior of the proximate fires has been compared with that of the single fires. An attempt has been made to explain and/or relate the differences in terms of the imposed physical differences.

Burning Rate Correlations

The burning rate per unit area was analyzed following the approach of Byram, et al. (10) and Fons(25) in terms

of the dimensionless groups $\dot{m}''D/\mu_a$ and gD^3/ν_a^2, where $\dot{m}''$ represents the burning rate per unit area, μ_a and ν_a are the dynamic and kinematic viscosity of air, respectively, g is the gravitational acceleration and D represents the depth of the flaming zone.

The experimental burning rate per unit area, $\dot{m}''$, was calculated by dividing the burning rate, $\dot{m}$, determined from the slope of the rate of weight-loss record by the product of the width of the crib, W, and the depth of the flaming zone, D, i.e.

$$\dot{m}'' = \frac{\dot{m}}{DW} \tag{38}$$

The data of the single fire of this study are compared with data on solid fuels from Byram (10) and on liquid fuels from Fons (25) and Welker (81) in Figure 25. Byram's data were obtained burning square wood cribs in still air. The size of stick used was 0.252 inch with a spacing between sticks of 0.75 inch. The size of Byram's square cribs, represented by D on the plot, was varied from 0.19 foot* to 1.28 feet on the side while the height was constant and equal to 3.1 inches. The cribs were ignited simultaneously throughout. Referring to Figure 25, one notices that the slopes of the curves for the wood cribs are nearly the same. Using Welker's data on liquid fuels (cyclohexane, normal-hexane, benzene, methanol, and acetone), the dimensionless groups

---

*Consists only of 3 sticks.

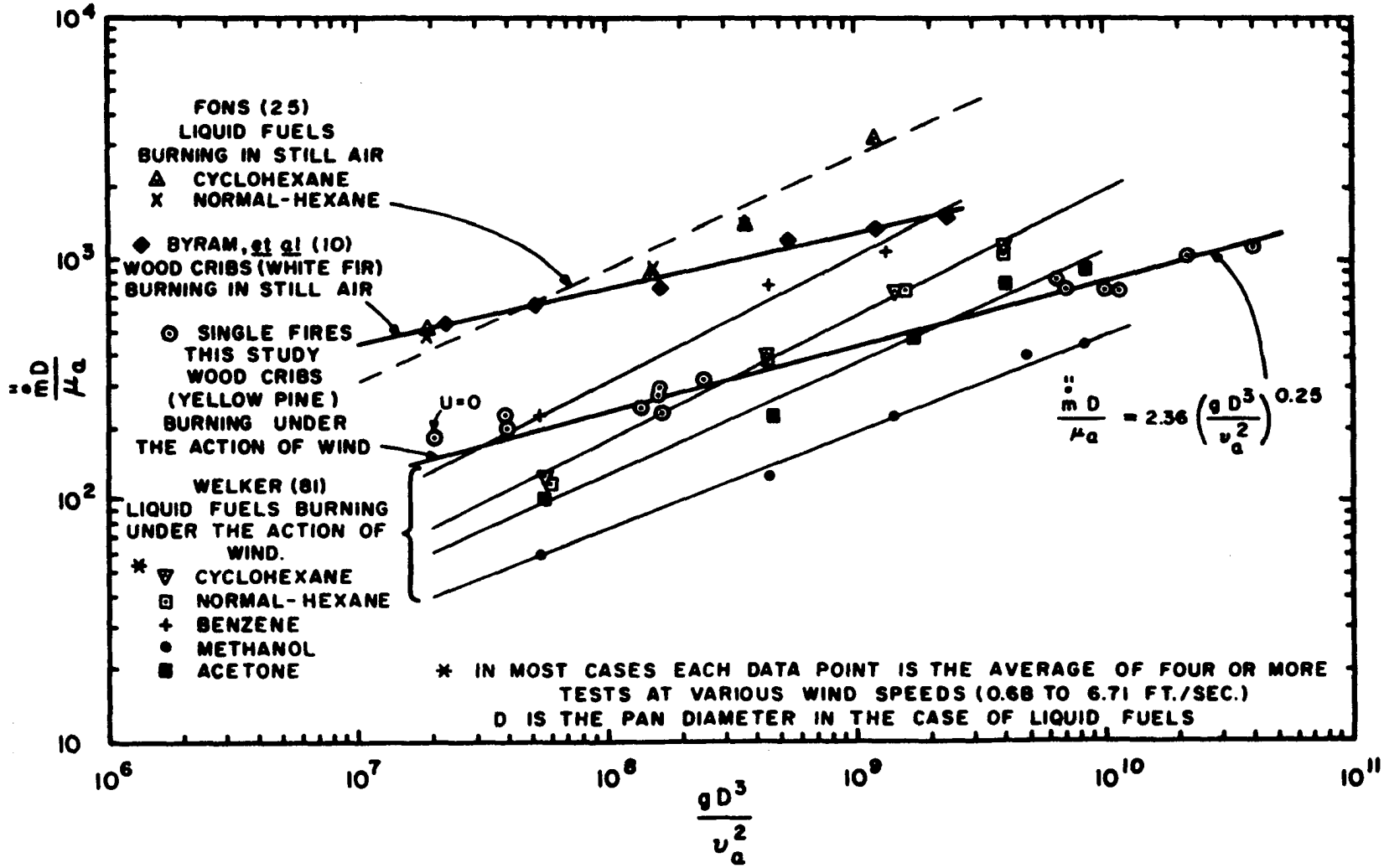

Figure 25. Burning Rate Per Unit Area Correlation

were also evaluated. In the case of liquid fuels, D, represents the pool diameter. Each point shown for Welker's data is the average of four or more tests at various wind speeds (0.68 to 6.71 ft/sec). The curves for the various liquid fuels show a higher slope than for the wood cribs.

A comparison of Fons' and Welker's data of cyclohexane and normal-hexane indicated that, while the burning rates obtained by Fons were about four times those obtained by Welker for comparable pan diameters, the magnitude of the dimensionless group $\dot{m}''D/\mu_a$ reported by Fons was smaller than obtained from Welker's data. A re-evaluation of the dimensionless groups using the liquid burning velocity of cyclohexane reported by Fons indicated that the values of $\dot{m}''D/\mu_a$ calculated by Fons were in error by about a factor of ten. The corrected values are included in Figure 25. The cause of the discrepancy in the magnitudes of the burning rates for comparable pool sizes, obtained by the two studies, has not been established.

A least squares correlation of the single fire data of this study resulted in the relationship

$$\frac{\dot{m}''D}{\mu_a} = 2.36\left(\frac{gD^3}{\nu_a^2}\right)^{0.25} \qquad (39)$$

where

$\dot{m}''$ = burning rate per unit top surface area

μ_a = viscosity of the surrounding air

g = gravitational acceleration

D = characteristic size of the flame: (depth of the flaming zone in the direction of the wind)

ν_a = kinematic viscosity of the surrounding air

In the above relationship, the effect of the wind is present through the increase in the depth of flaming zone which it causes.

For a given characteristic size of fire, the variations in the magnitude of $\ddot{m}D/\mu_a$ are due mainly to differences in the burning rate. These differences seem to be attributable to the physical properties and configuration of the fuel. Two configuration parameters have been considered in comparing the magnitude of the burning rate of the wood cribs. They are the initially exposed area of the fuel in the cribs and the mass of fuel in the crib per unit top surface area of the crib. It is known that as the exposed area of the fuel increases, the burning rate also increases within a certain range. Also, as the amount of fuel contained in a unit volume increases, the burning rate tends to diminish due to the much higher amount of energy required to cause ignition.

The initially exposed surface area of the fuel per unit of the top surface of the crib, $\ddot{A}_e$, was determined by the relationship

$$\ddot{A}_e = [(m+\alpha)^2 d^2][2N+1]+[(m+\alpha)(m-1+\beta)sd][4N-1] \qquad (40)$$

and the mass of wood beneath a unit area of the top surface of the crib--hereafter denoted as fuel loading, $\ddot{M}$,--by the relationship

$$\ddot{M} = \rho_w N[m+\alpha][(m+\alpha)d+(m-1+\beta)s]d^2 \qquad (41)$$

Derivations of these equations are presented in Appendix A.

The burning rate per unit area, $\ddot{m}$, was assumed proportional to the exposed area of the fuel, $\ddot{A}_e$:

$$\frac{\ddot{m}}{(\ddot{m})_{ref}} = \frac{\ddot{A}_e}{(\ddot{A}_e)_{ref}} \equiv A_R \qquad (42)$$

where A_R represents the initially exposed surface area ratio of the cribs. The data of Byram were reduced accordingly, using the data of this study as the reference. It can be seen that the introduction of the factor, A_R, into the ordinate of Figure 26 improves the agreement between Byram and this study over that shown in Figure 25.

In a similar way, the burning rate per unit area was assumed inversely proportional to the fuel loading of the crib:

$$\frac{\ddot{m}}{(\ddot{m})_{ref}} = \frac{(\ddot{M})_{ref}}{\ddot{M}} \equiv FL_R \qquad (43)$$

where FL_R represents a fuel loading ratio. Using the data obtained in this study as the reference condition, Byram's data are processed accordingly with the additional factor, FL_R, introduced in the ordinate of Figure 27. Again it can be seen that there is further improvement in agreement over Figure 26.

The fact that a significant improvement in correlation was achieved by introducing two configuration parameters--compare Figure 25 with Figure 27--lends support to

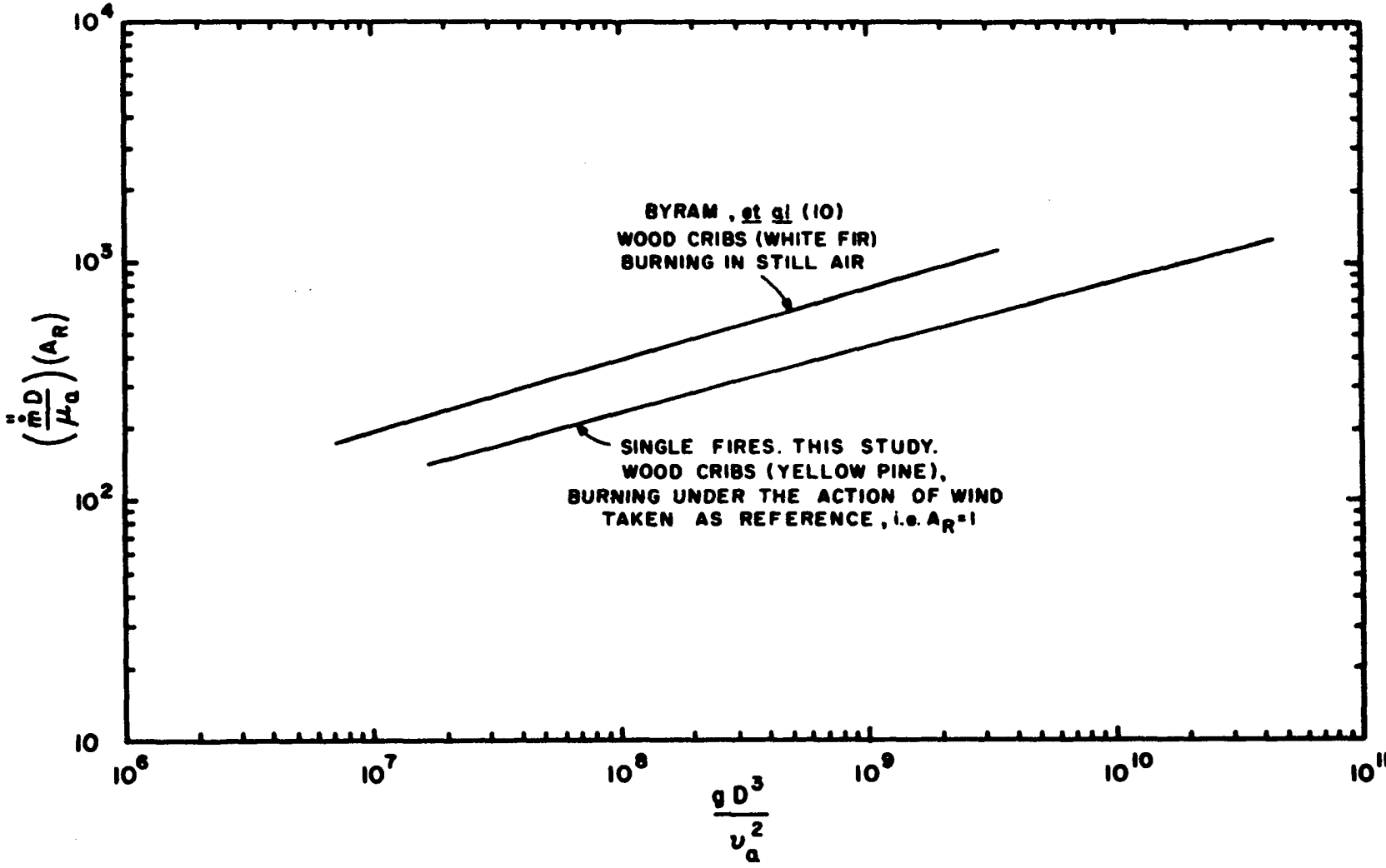

Figure 26. Burning Rate Per Unit Area Correlation Corrected for the Initially Exposed Surface Area

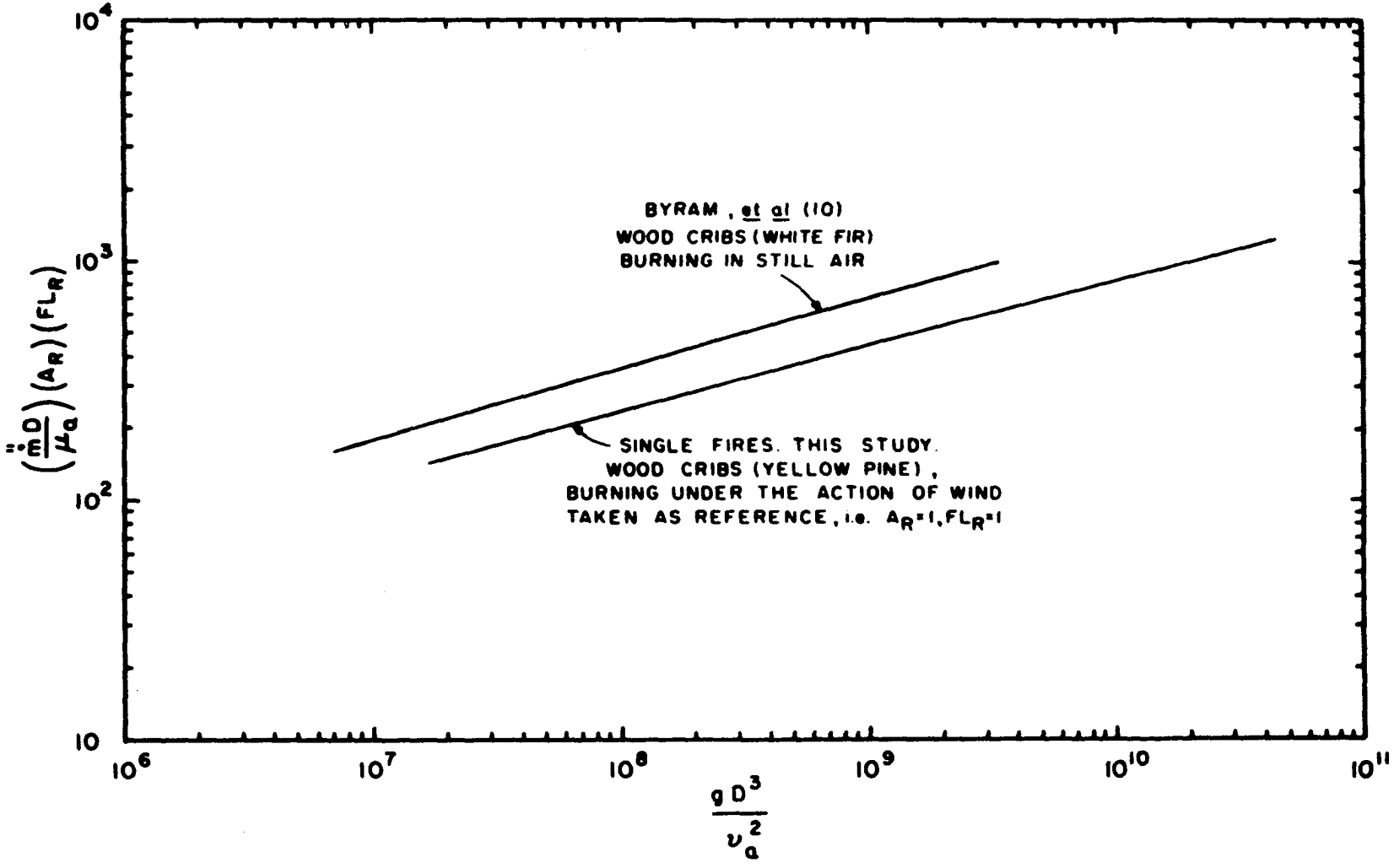

Figure 27. Burning Rate Per Unit Area Correlation Corrected for the Initially Exposed Surface Area and Fuel Loading

the speculation that further improvement could be realized by including properties of wood which affect its burning rate, such as volatile content, heat of combustion, specific heat, thermal conductivity, moisture content and density. However, a detailed study of the significance of each of these variables would be required before the appropriate factor, which would reduce the data from a variety of wood cribs to a single curve, could be established.

The data obtained in this study for single fires and proximate fires are compared in Figure 28 in terms of the dimensionless groups gD^3/ν_a^2 and $\dot{m}''D/\mu_a$. (Note that the configuration factors A_R and FL_R are both equal to 1 since only data from this study are presented.) Most of the data seems to lie along a straight line although a deviation from linearity is noticed for values of $gD^3/\nu_a^2 < 0.8 \times 10^8$. The data points, excluding those for which gD^3/ν_a^2 was less than 0.8×10^8, were fitted by a straight line. The equation of the line is given approximately by

$$\frac{\dot{m}''D}{\mu_a} = 1.16 \left(\frac{gD^3}{\nu_a^2} \right)^{0.28} \tag{44}$$

Since the variation of μ_a and ν_a is small, one can disregard their contribution, and in this case, the above relation becomes

$$\dot{m}''D \sim (D^3)^b \tag{45}$$

or

$$\dot{m}'' \sim D^c \tag{46}$$

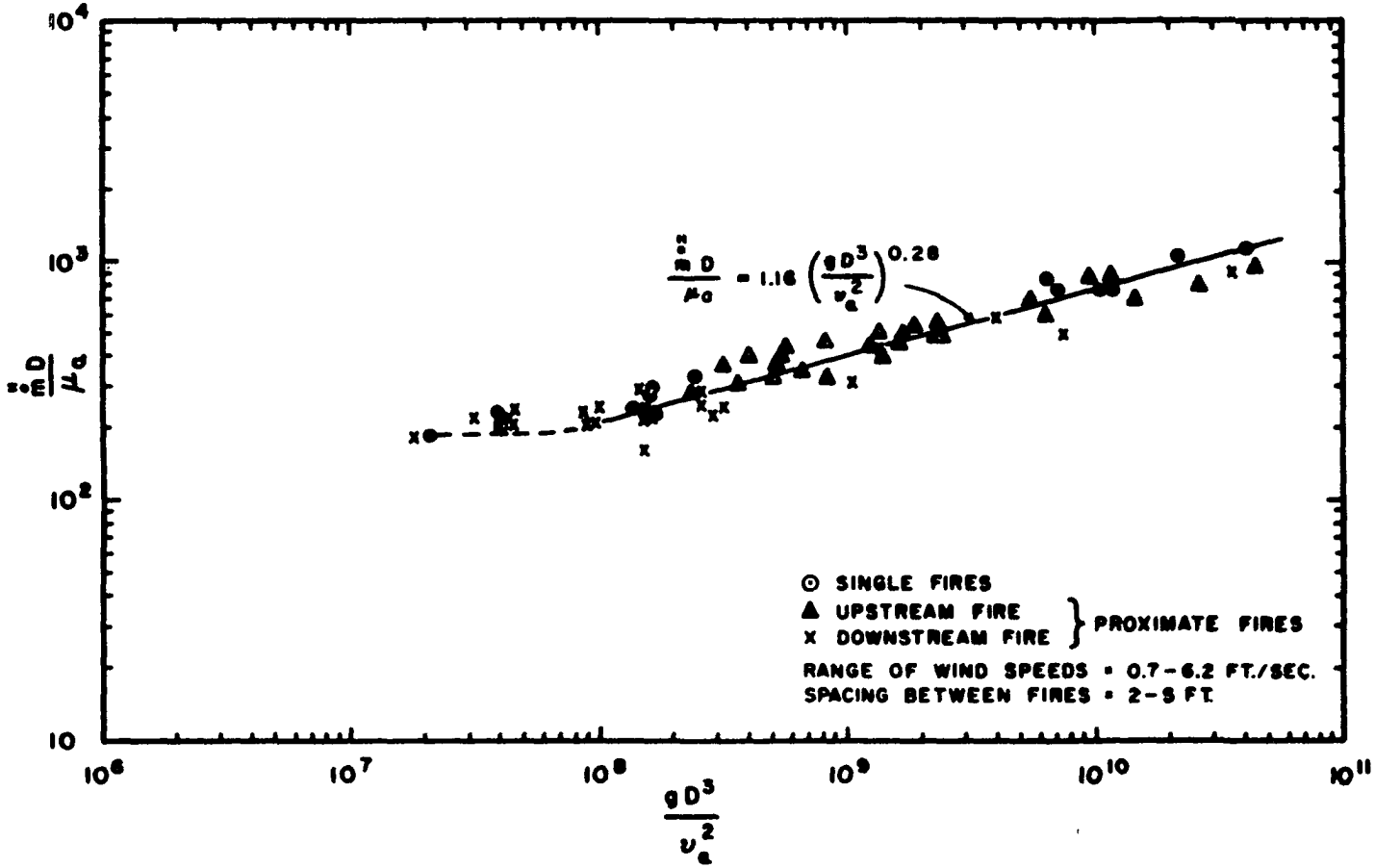

Figure 28. Burning Rate Per Unit Area Correlation--Single and Proximate Fires

where b and c are constant exponents. A plot of $\dot{m}''$ against D is shown in Figure 29. A least-squares fit of the data resulted in the expression

$$\dot{m}'' = 0.0052\ D^{-0.29} \qquad (47)$$

where D is expressed in ft and $\dot{m}''$ in lb/ft^2-sec. Note that in the case of proximate fires, D is evaluated for each fire. The fact that the data for single and proximate fires can be expressed in terms of a single correlation indicates that in so far as burning rates are concerned there is little, if any, interaction whether exposed to calm or windy environment.

A decrease in the magnitude of the burning rate per unit area as the depth of the flaming zone increases is shown in Figure 29. This decrease is probably due to a reduction in the residence time of the flame, i. e., the time taken by the flame front to traverse a reference point in the fuel bed (see also page 136). It was observed visually that for low values of wind speeds, which result in small values of the depth of flaming zone and a longer residence time, the ashes tended to be more powdery, showing a more complete burning of the fuel. For the high values of wind speed, the residue tended to be of a more rigid nature indicating less complete consumption.

From Equation (38) and the relationship (47), one can establish that

$$\dot{m} = W(D)\,(0.0052)\,(D)^{-0.29} \qquad (48)$$

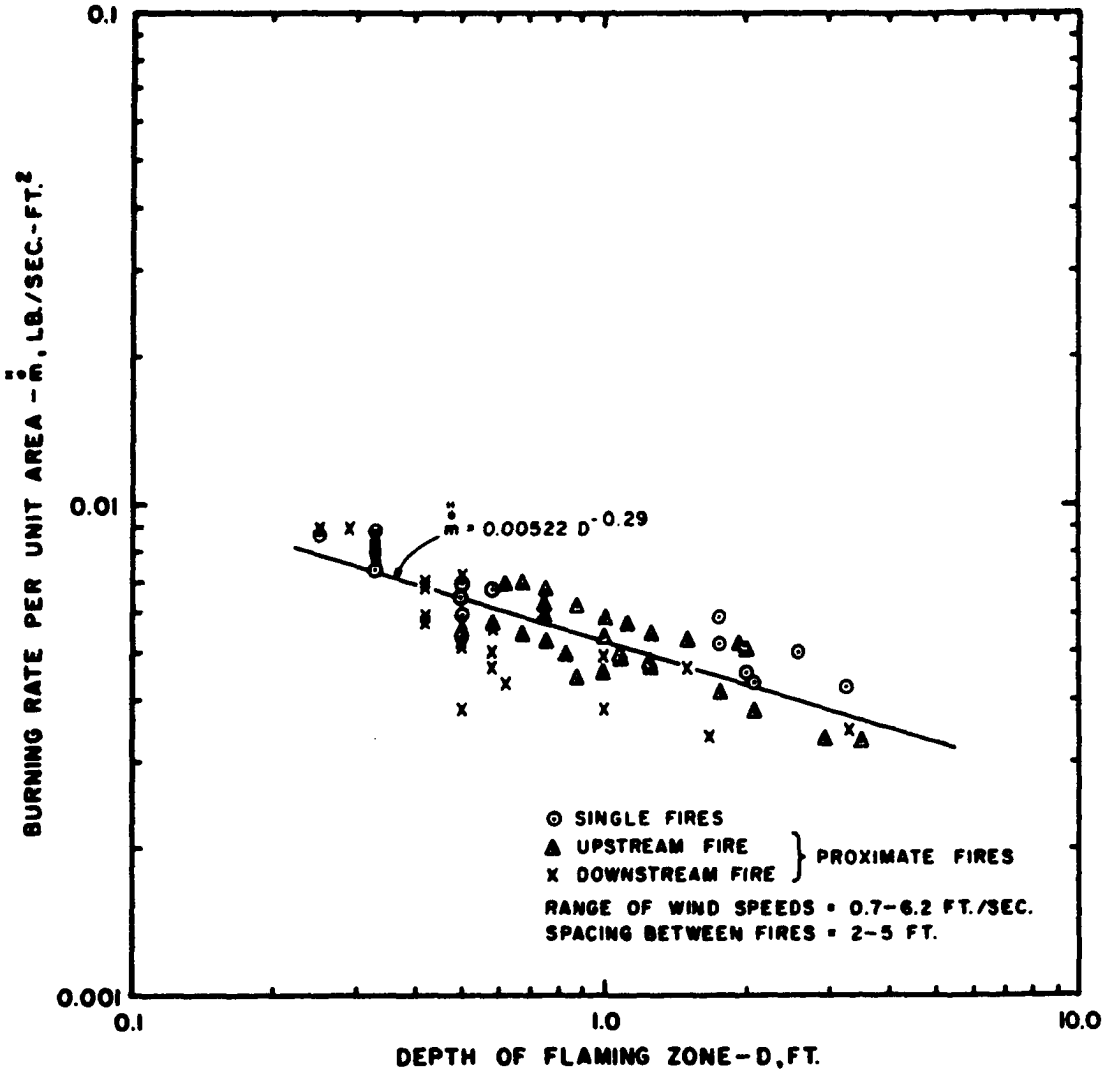

Figure 29. Correlation of Burning Rate Per Unit Area and Depth of Flaming Zone

Since W was constant in this study,

$$\dot{m} \sim D^{q} \tag{49}$$

where q is a constant exponent. A plot of the burning rate data in terms of the depth of the flaming zone is shown in Figure 30*. In this instance, a least-squares fit of the data yielded the correlation expression

$$\dot{m} = 0.015\ D^{0.72} \tag{50}$$

where $\dot{m}$ is expressed in lb/sec and D is in ft.

Flame Length Correlations

The data on the length of the flame obtained photographically were correlated in terms of the dimensionless groups L/D and $\dot{m}''/\rho_a\sqrt{gD}$. A plot of the experimental data in terms of these dimensionless groups is shown in Figure 31. The data of both the single fire and the proximate fires tended to lie along a straight line on the log-log plot. In this case, a least-squares fit resulted in the relation

$$\frac{L}{D} = 51.6 \left(\frac{\dot{m}''}{\rho_a\sqrt{gD}}\right)^{0.74} \tag{51}$$

Equation (15) of Thomas is shown also in Figure 31. It was obtained from the data of Thomas and Fons (74) of wood cribs burning in still air.

Since ρ_a is nearly constant, the above expression (51) can be written in terms of the depth of flaming zone.

---

*Note that the ordinate in Figure 30 is the total burning rate, $\dot{m}$, whereas in Figure 29 the ordinate is given in terms of the burning rate per unit area, $\dot{m}''$.

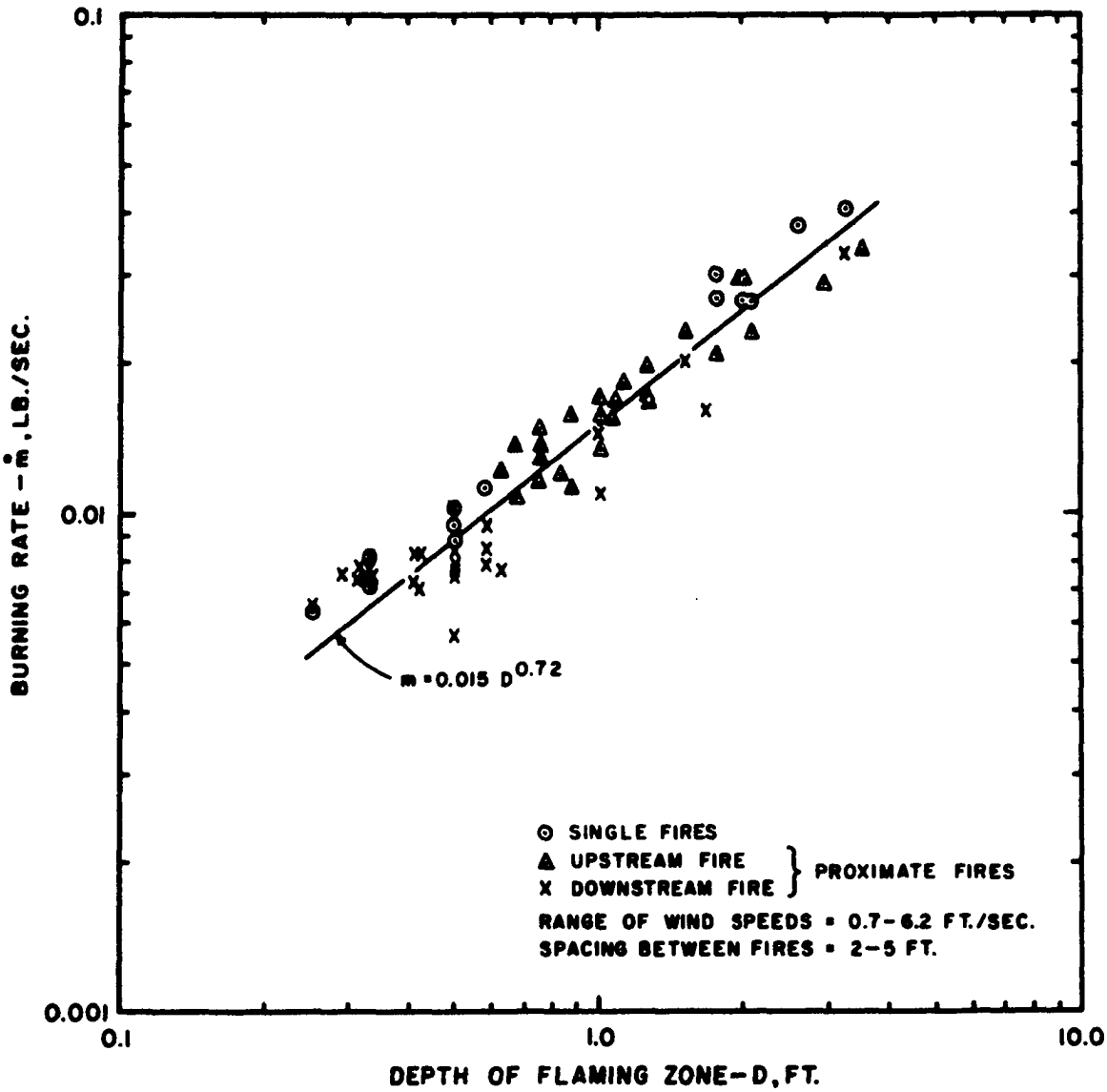

Figure 30. Correlation of Total Burning Rate and Depth of Flaming Zone

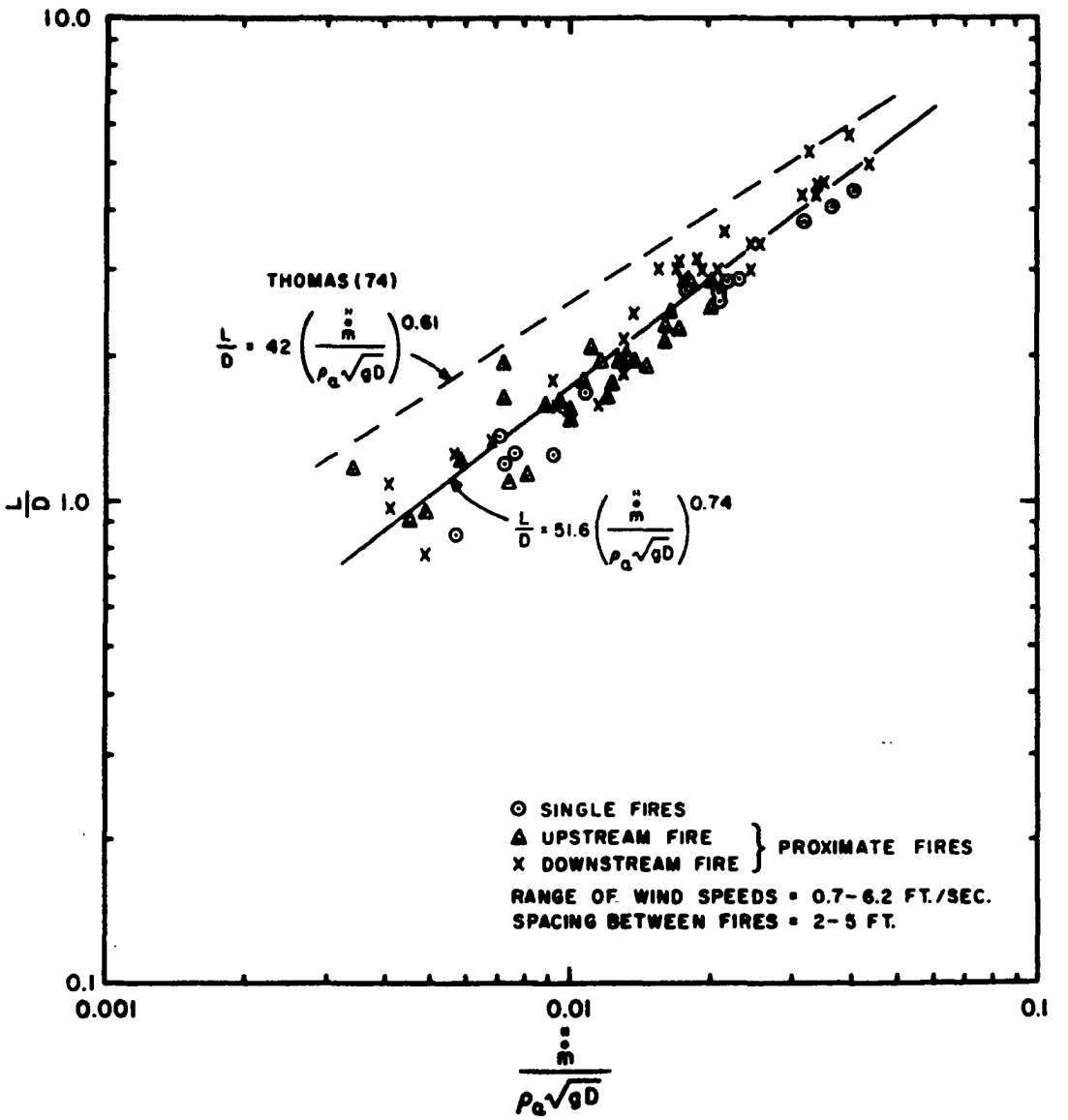

Figure 31. Correlation of Flame Length Data

Substituting Equation (46) in Equation (51),

$$\frac{L}{D} \sim \left(\frac{D^c}{D^{\frac{1}{2}}}\right)^f \tag{52}$$

or

$$L \sim D^j \tag{53}$$

where c, f, and j are constant exponents.

The data on the length of the flame for the various tests were plotted in terms of the depth of flaming zone in Figure 32. The data show a linear trend on the log-log plot. A least-squares correlation of the data resulted in the expression

$$L = 1.91\ D^{0.36} \tag{54}$$

where L and D are expressed in ft. The plot indicates an increase in the length of the flame occurs as the depth of the flaming zone increases.

Propagation Rate Correlation

The propagation rate of the fire through the crib was determined experimentally by noting the time it took the fire to propagate from stick to stick along the upper layer of the crib and in some cases in terms of the rate fuel was being fed into the fire, as was explained in the section on experimental procedure. Since the propagation rate is related to the burning rate, the possibility of relating the propagation rate to the depth of the flaming zone was investigated. The experimentally determined values of propagation rate, $\dot{p}$, were plotted on log-log coordinates in terms of the

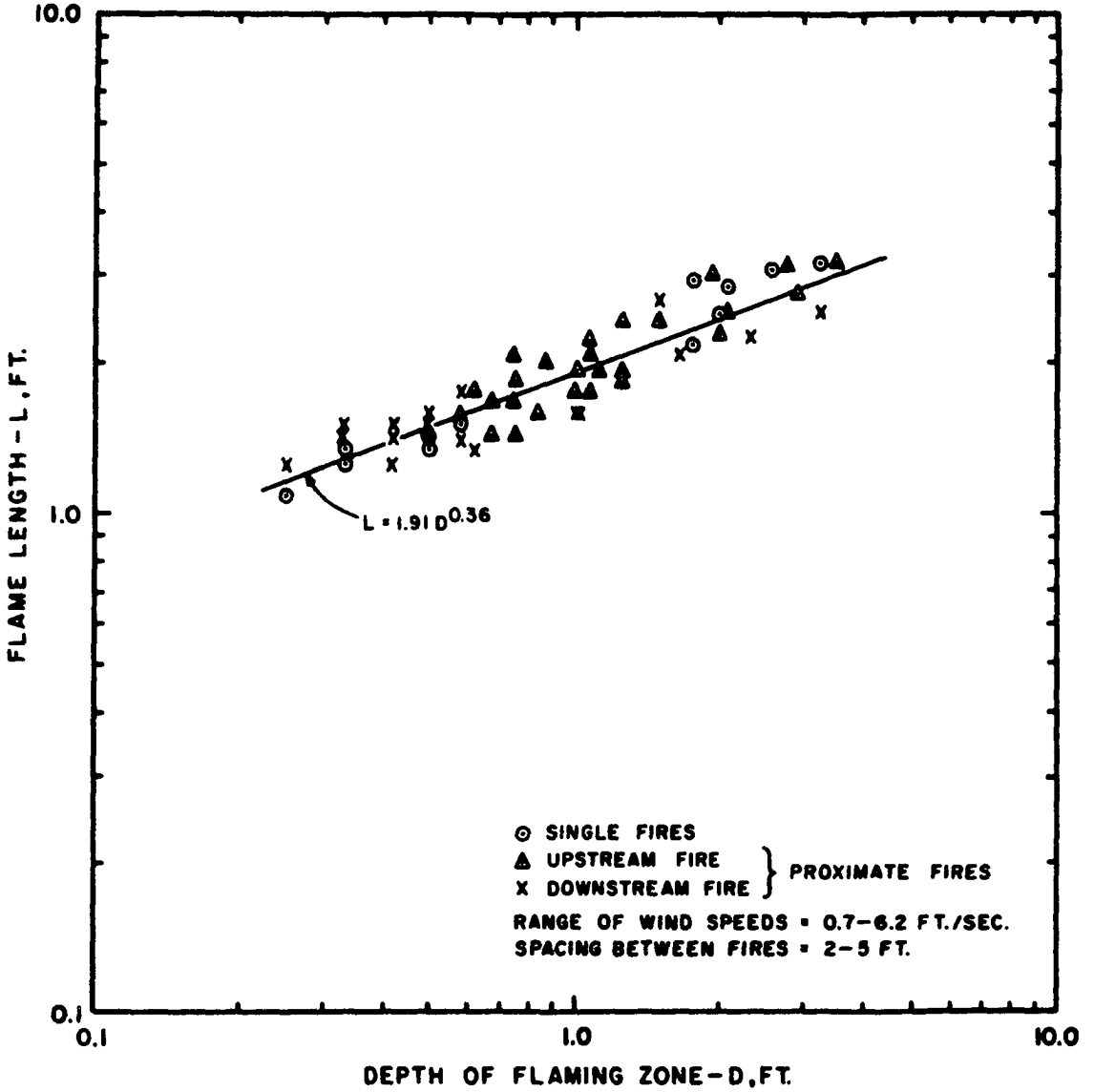

Figure 32. Correlation of Flame Length and Depth of Flaming Zone

depth of flaming zone, D, in Figure 33. The data show a higher degree of scatter than the preceding correlations based on burning rate. However, the scatter is due primarily to the inaccuracy of the visual measurements involved in the propagation rate. A least-squares fit of the data resulted in the expression

$$\dot{p} = 0.00194\ D^{0.67} \qquad (55)$$

where the propagation rate, $\dot{p}$, is expressed in ft/sec and the depth of the flaming zone, D, is in ft.

The flame propagation rates were also determined from the experimental burning rate data. Consider a flame of depth D in the direction of propagation, as shown in the diagram below, and propagating at a rate $\dot{p}$. The time taken

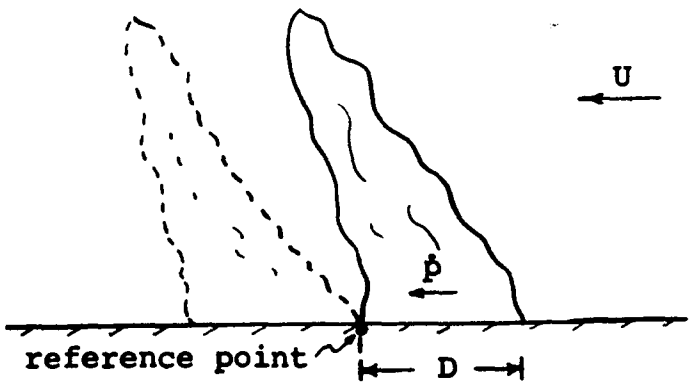

—— position of the flame at time τ_1

----- position of the flame at time τ_2

residence time = $\Delta\tau = \tau_2 - \tau_1$

for the flame to traverse the position of a reference point in the fuel bed is the residence time mentioned before. The residence time $\Delta\tau$ is related to the depth of flaming zone and the propagation velocity through the relation

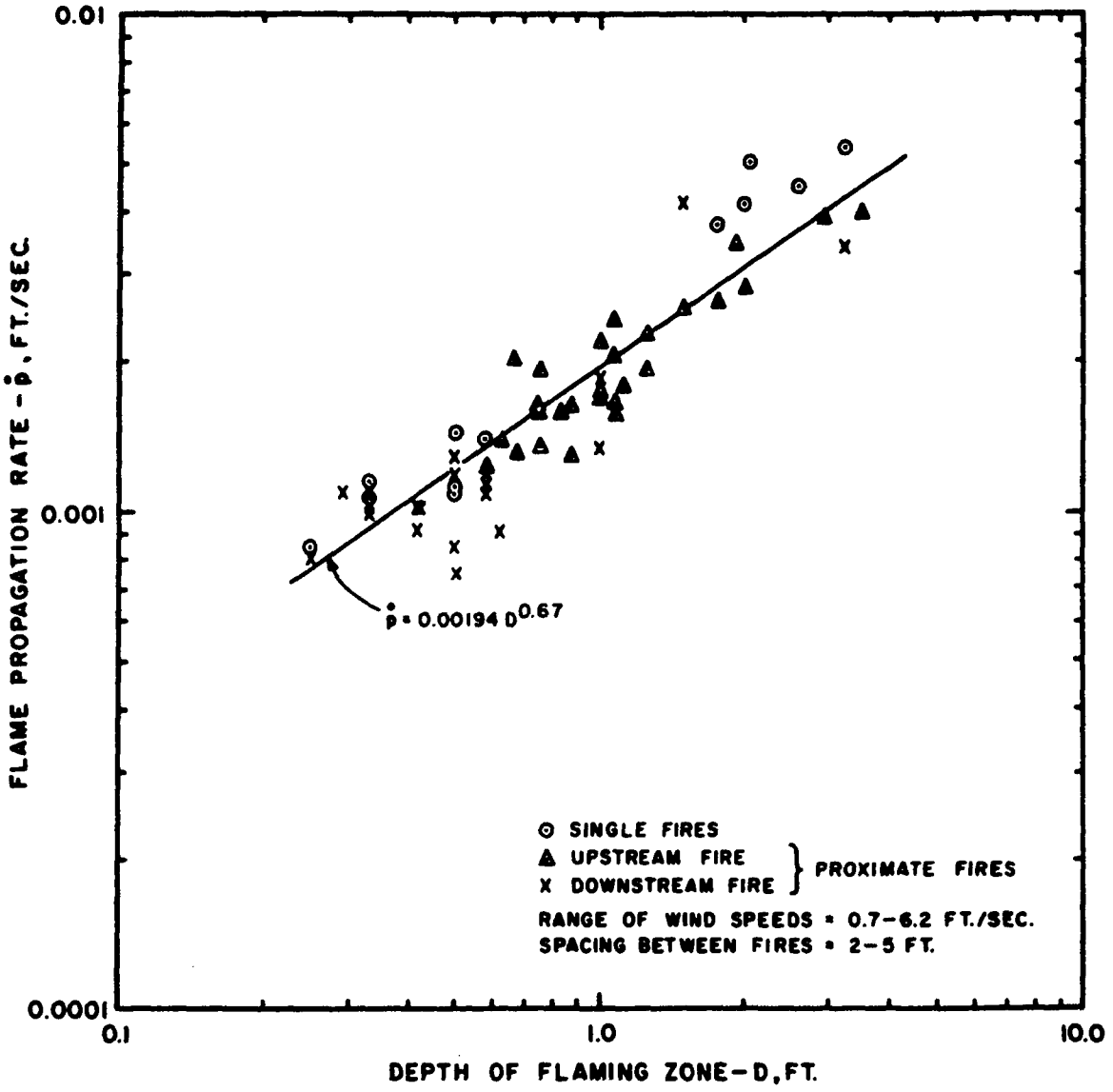

Figure 33. Correlation of Flame Propagation Rate and Depth of Flaming Zone

$$\Delta\tau = \frac{D}{\dot{p}} \tag{56}$$

However, the residence time can also be expressed in terms of the burning rate and the fuel loading as

$$\Delta\tau = \frac{\ddot{M}}{\ddot{m}} \tag{57}$$

where $\ddot{M}$ is the fuel loading as defined in Equation (41) and $\ddot{m}$ is the burning rate per unit area of the top crib surface as defined in Equation (38). Equating the above two relations yields

$$\frac{D}{\dot{p}} = \frac{\ddot{M}}{\ddot{m}} \tag{58}$$

or

$$\dot{p} = \frac{\ddot{m}D}{\ddot{M}} \tag{59}$$

The values calculated by means of the above relation from the burning rate per unit area and depth of the flaming zone data are compared against the values determined experimentally, for the data of this study, in Figure 34. The calculated values are, for the majority of the tests, of higher magnitude than those obtained experimentally. The difference is probably partly due to the fact that at high propagation or spread rates, the burning is less complete and the actual percentage of fuel loading which is burned is therefore less. In addition, the inability to make an accurate visual measurement of the depth of the flaming zone also accounts in part for the difference between calculated and experimental rates of spread. This last condition was also

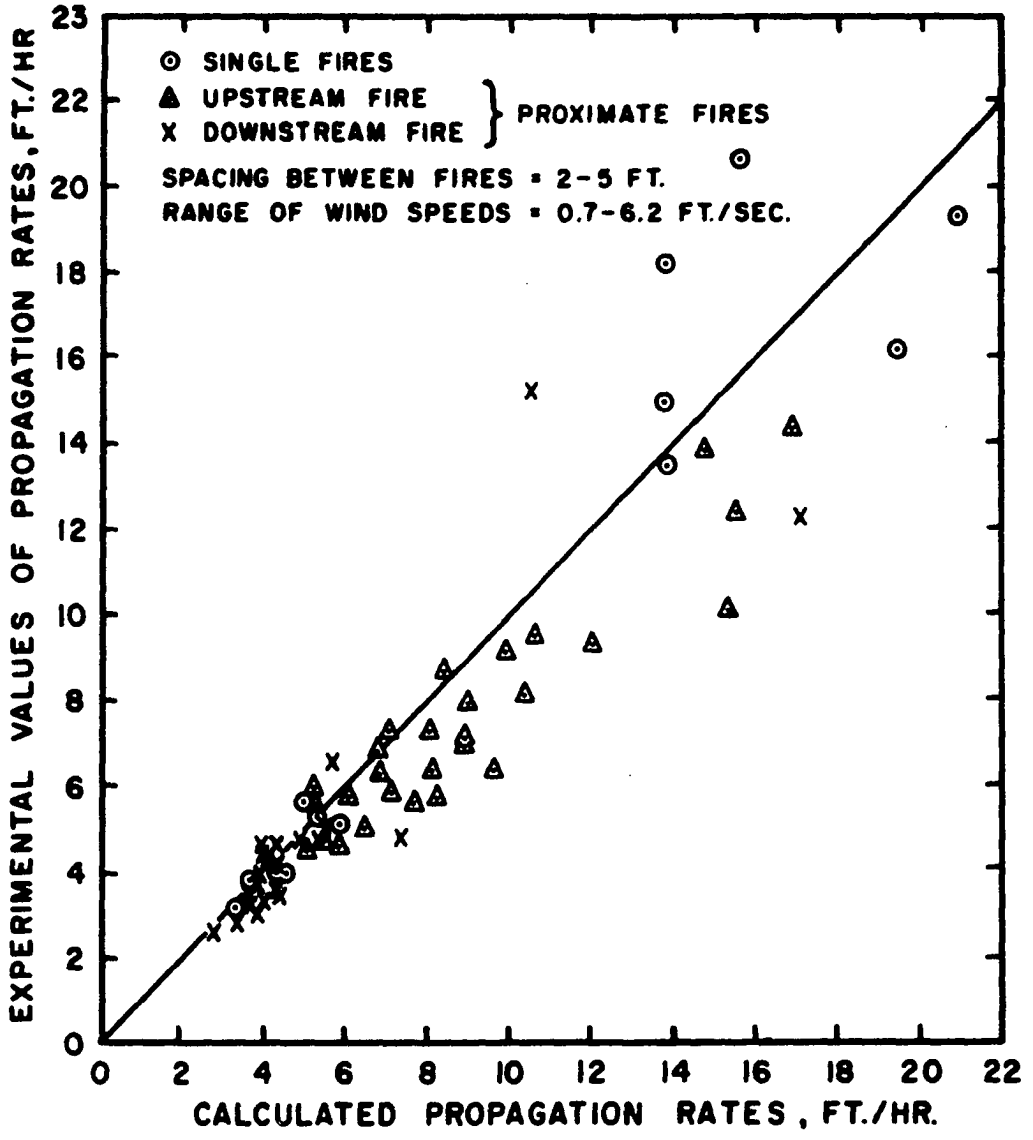

Figure 34. Comparison Between Experimental and Calculated Propagation Rates

reported by Anderson (1) who made visual measurements of the flaming zone as well as determinations of the flaming zone from thermocouple data. The thermocouples were imbedded in the surface of mat-type fuels. He noted that apparently the human eye sees a wider reaction zone than is measured by the thermocouples.

Effect of Wind on Depth of Flaming Zone

From the preceding discussions it is apparent that the burning rate per unit area, the burning rate, the length of the flame and the rate of flame propagation can be determined for the single fire as well as for proximate fires under windy conditions in terms of the depth of flaming zone. The next step was to investigate how the depth of flaming zone was affected by the existing wind. Figure 35 shows a plot of the depth of flaming zone data against the wind speed. Although there is a large amount of scatter, the trends are apparent. They indicate that a much higher wind speed is required for proximate fires to attain a depth of flaming zone comparable to that of single fires. In comparing the depth of the flaming zone of the proximate fires one observes that the depth of flaming zone is larger for the upstream fire than for the downstream fire. The depth of flaming zone of the downstream fire tends to approximate that of the single fire for wind speeds below 1 ft/sec. However, at these low speeds, the depth of flaming zone of the upstream fire remains larger than that of the single fire.

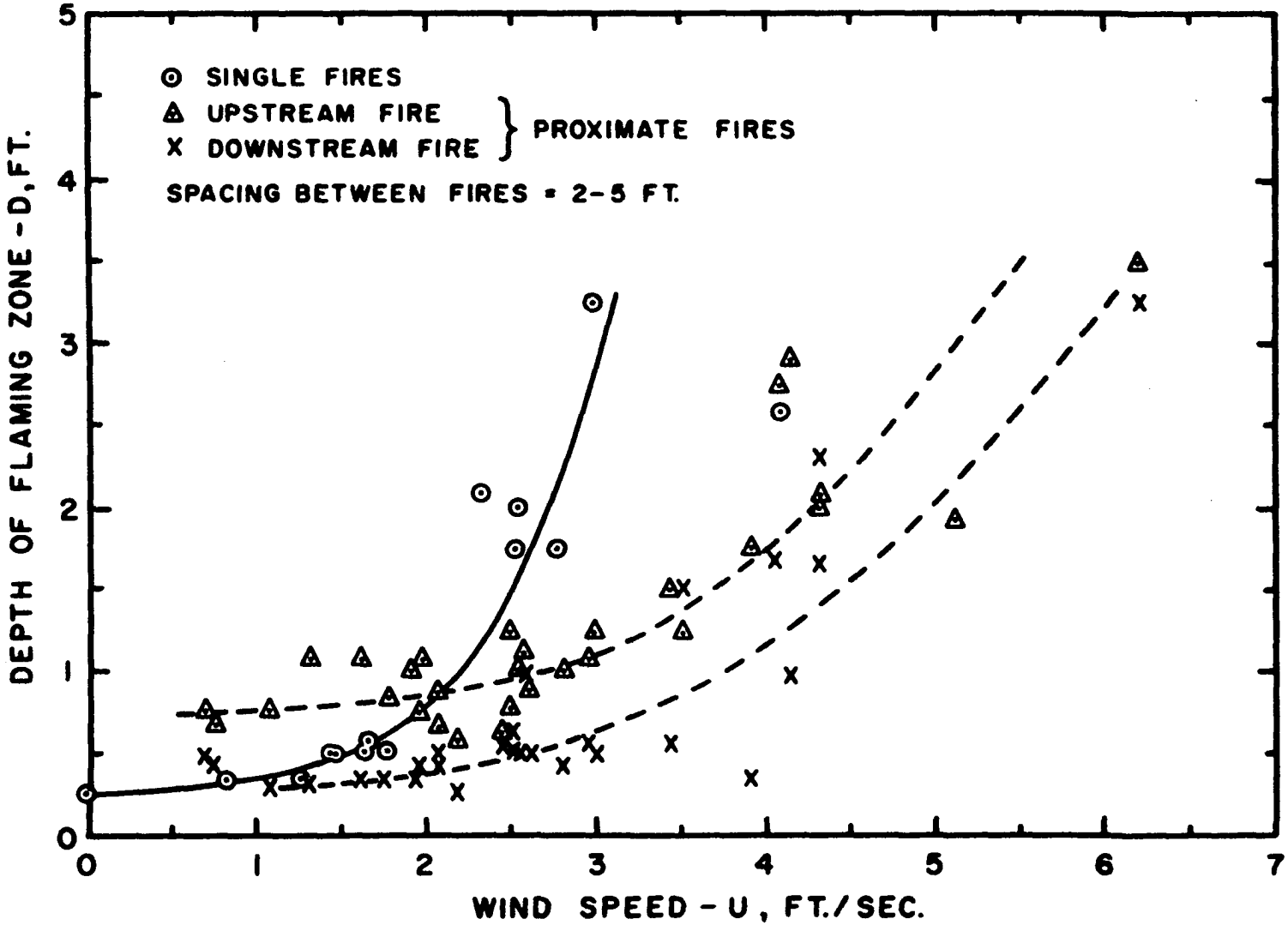

Figure 35. Relationship Between Depth of Flaming Zone and Wind Speed

An attempt to correlate the effect of the spacing between the two fires on the depth of flaming zone proved unsuccessful.

Flame Bending

A mathematical model for the bending of flames by wind is presented in Appendix B. Two pertinent equations result:

Single flame:

$$\frac{\tan \theta}{\cos \theta} = C_f \left(\frac{U^2}{Dg}\right) \left(\frac{T_f}{T_f - T_a}\right) \tag{60}$$

Upstream flame of the proximate fires:

$$\frac{\tan \theta}{\cos \theta} = (C_f - C_\ell) \left(\frac{U^2}{Dg}\right) \left(\frac{T_f}{T_f - T_a}\right) \tag{61}$$

The coefficients to be used with Equations (60) and (61) to determine the flame bending angles for the case of single fires and the upstream flame of the proximate fires respectively were calculated using the experimental data. The equations were rearranged so as to express the coefficients in terms of the other measurable parameters. Tables 12 and 13 in Appendix C contain the data and results obtained. The correlation of the coefficients in terms of the parameter (ReFr), as used by Welker (81), was investigated. A plot of the data is shown in Figure 36. In the case of the single fires from liquid fuels investigated by Welker, the data clustered about a straight line of slightly negative slope. However, in the case of the fires propagating through a crib

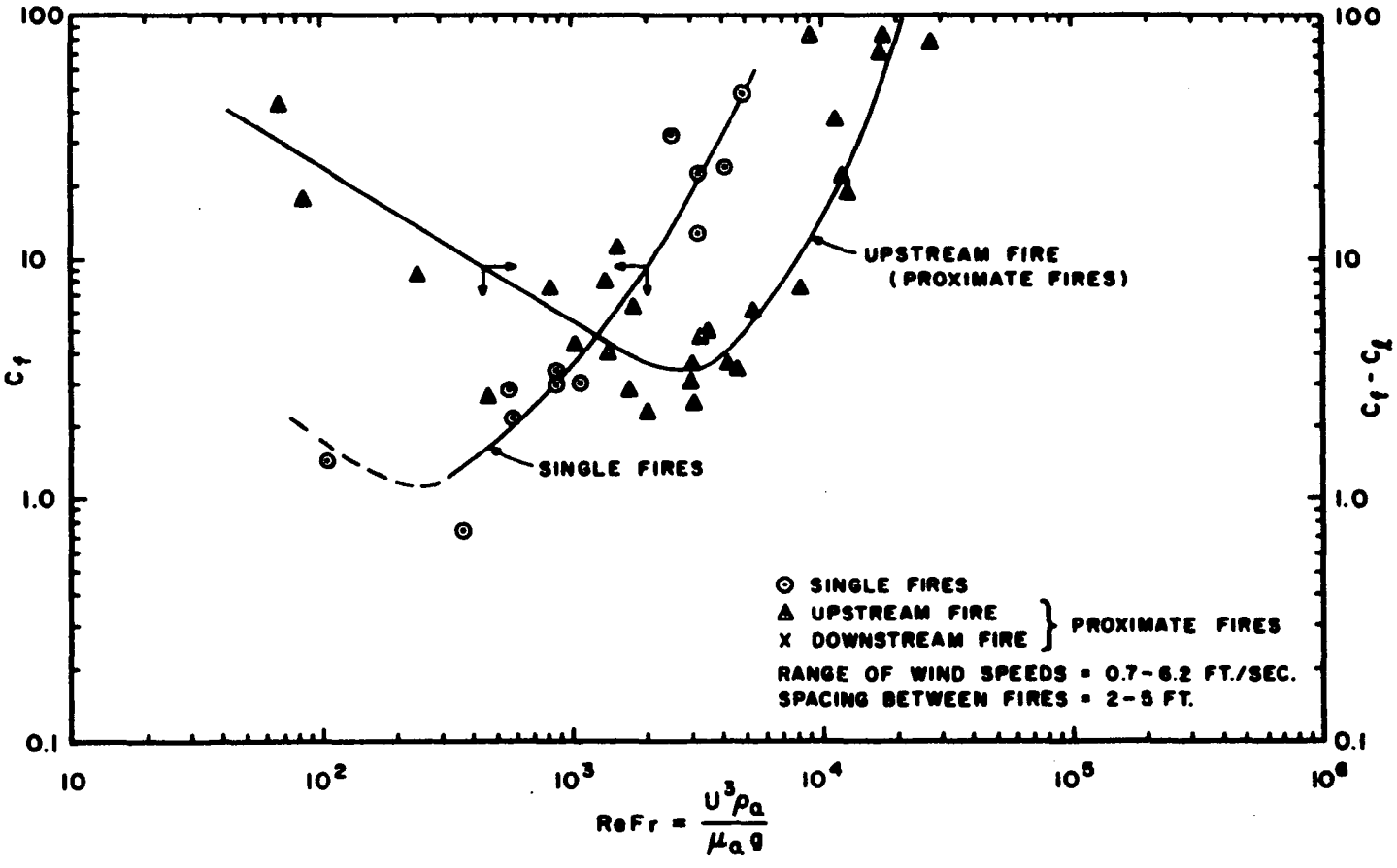

Figure 36. Coefficients for the Flame Bending Models

in this study, the coefficients reach a minimum and start increasing in magnitude again as the wind speed increases. One possible explanation for the appearance of a minimum in the case of wood cribs is the variation in the depth of the flaming zone, which in the case of liquid fires is a constant equal to the pool diameter. It can be noted in Equation (60) $C_f \sim D$.

The curve for the single fire data in Figure 36 shows the same trend as for the upstream fire data. However, due to the inability to obtain sufficiently low wind speeds in the wind tunnel, the condition of a minimum for the single fire data is not completely established. Nevertheless, the curves appear similar, with just a relative displacement in the plot. The flame bending model presented in Appendix B is, however, difficult to apply to the downstream fire since the flow of air is completely altered by the encounter of the airstream with the upstream fire.

The ratio of the flame bending angle of the downstream flame to the upstream flame (θ_{dn}/θ_{up}) is shown in Figure 37 in terms of the spacing Froude number U^2/sg. U is the undisturbed wind velocity and s is the spacing between the centers of the flames, as shown in the diagram on page 146. Referring to Figure 37 it can be seen that as U^2/sg approaches zero--either as a result of low wind speeds or large spacing, or both--the ratio of the bending angle of the downstream flame to the bending angle of the upstream

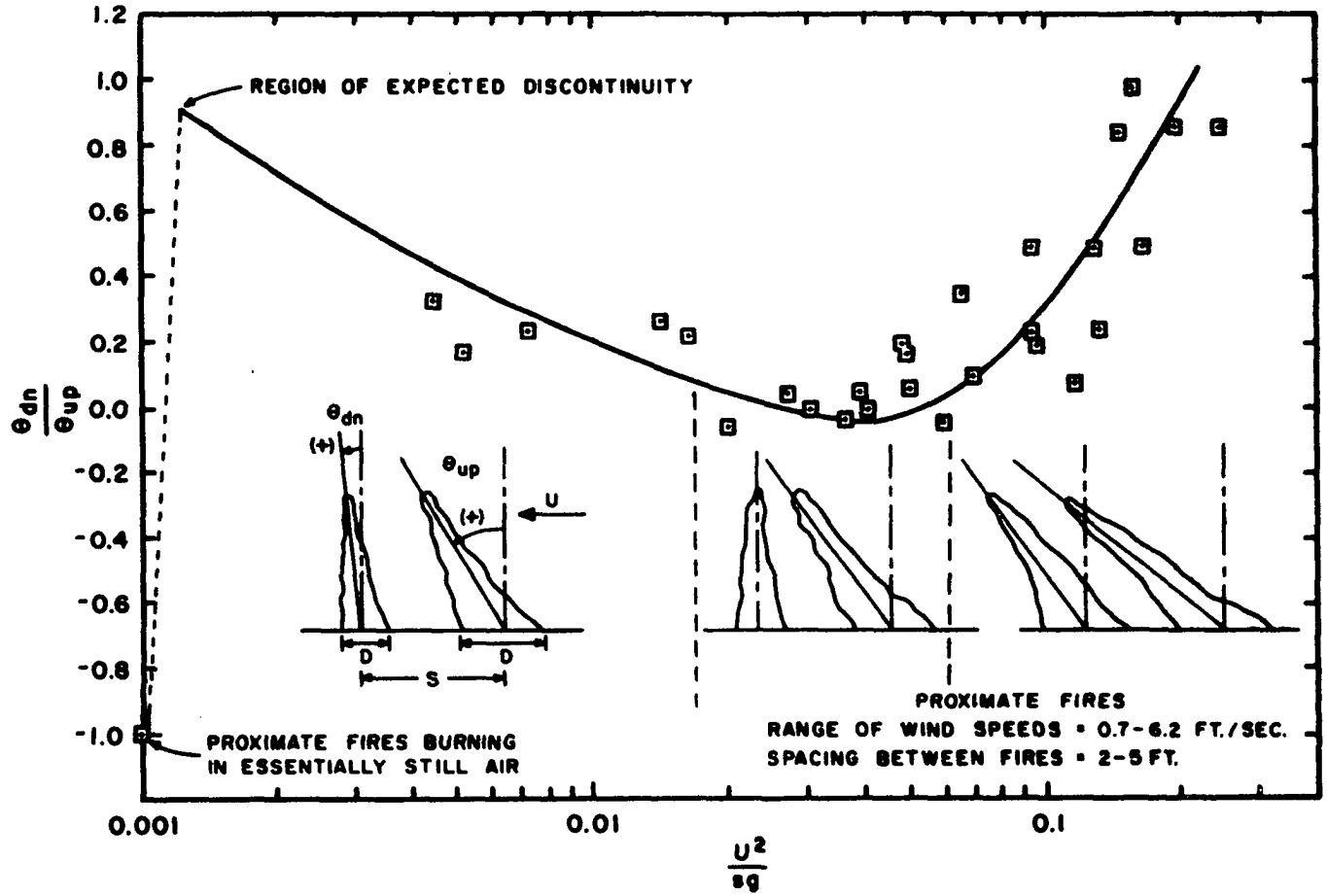

Figure 37. Relationship Between θ_{dn}/θ_{up} and Spacing Froude Number U^2/sg

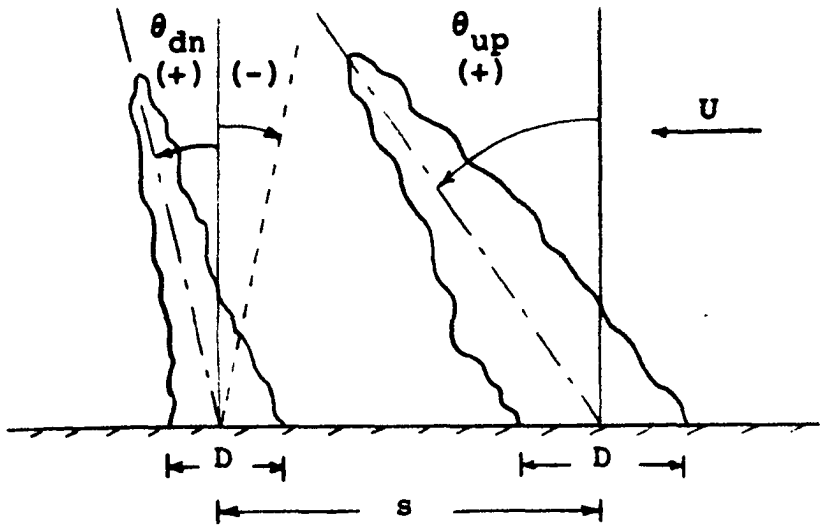

flame, θ_{dn}/θ_{up}, approaches 1, in which case the bending angles are equal. Conversely, at high values of U^2/sg, the ratio θ_{dn}/θ_{up} again passes through 1 and conceivably continues to increase although no data were obtained in the range beyond. At intermediate values of U^2/sg, between 0.02 and 0.05, a minimum value for θ_{dn}/θ_{up} occurs which is very nearly equal to zero or, as indicated by the data of Figure 37, even less than zero. A zero value for this ratio implies that the downwind flame is standing vertical, whereas for negative values of this ratio the downwind flame is tilted toward the upwind flame.

Visual observations of two flames which are separated a great distance indicate that the flames burn vertically in still air. As the flames are brought closer together, they tend to bend toward each other in still air and to merge with further decrease in distance of separation. At

a characteristic distance just short of incipient merging (76) it has been observed that the bending angles become numerically equal but opposite in sign, for which case θ_{dn} is negative and θ_{up} is positive. Since at this point the separation distance, s, is still finite but the wind velocity, U, is zero (still air) so that U^2/sg is zero, it follows that a discontinuity occurs in the curve of Figure 37 (shown by the dashed vertical line) where the value of θ_{dn}/θ_{up} drops suddenly from +1.0 to -1.0.

CHAPTER VI

CONCLUSIONS

1. The burning rates per unit area of the single fire as well as for each flame of two proximate fires can be correlated in terms of the depth of the flaming zone only, and are independent of the wind velocity or spacing between the fires. In reality the effect of wind is present indirectly through its influence on the depth of the flaming zone.

2. Total burning rates, length of flames and propagation rates for single fires or each flame of proximate fires can also be correlated in terms of the depth of the flaming zone, irrespective of wind velocity and spacing.

3. The rate of propagation can be predicted satisfactorily from burning rate and depth of flaming zone data for either single or proximate fires.

4. The burning rate correlation obtained in this study is in reasonable agreement with results presented by Byram for wood cribs burning in still air after correcting for differences in the initially exposed area and fuel loading between these two studies.

5. The burning rate per unit area correlation for wood cribs is approximately the same as for liquid fires, reported by others, except that the latter has a larger exponent.

6. The equation for flame bending due to wind, which had been previously proposed for liquid and gas fires, can be applied to single fires from wood cribs by using the drag coefficient derived empirically in this study. For the upstream flame of proximate fires a further modification in the basic equation, which introduces a lift coefficient in addition to the drag coefficient, is required.

7. The data obtained on temperatures in the wake of the gases from the fires clearly indicated that the wind tunnel (8 x 8 ft in cross-section) was too small, or conversely that the fires were too large (3 feet in width with depth of flaming zone varying from 0.29 to 3.5 feet), to simulate temperature profiles that would be obtained for fires burning in the open. In these tests the walls, and particularly the ceiling, exerted a pronounced effect on the temperature profiles.

8. The data indicated that steady state was never achieved with respect to radiation, even after steady state was reached in burning rate, temperature of the wake gases and rate of fire spread in that order.

REFERENCES

1. Anderson, H. E., "Mechanisms of Fire Spread: Research Progress Report No. 1," U. S. Forest Service Research Paper INT-8, 1964.

2. Anderson, H. E., and R. C. Rothermel, "Influence of Moisture and Wind Upon the Characteristics of Free Burning Fires," Tenth Symposium (International) on Combustion, 1009-1018, The Combustion Institute, Pittsburg, Pennsylvania (1965).

3. Ball, F. K., "Some Observations of Bent Plumes," Quart. Jour. Royal Met. Soc., 84, 61 (1958).

4. Blinov, V. I., and G. N. Khudyakov, "Certain Laws Governing Diffusive Burning of Liquids," Academiia Nauk, SSSR Doklady, 113, 1094-1098 (1957).

5. Bosanquet, C. H., W. F. Carey, and E. M. Halton, "Dust Deposition from Chimney Stacks," Proc. Inst. Mech. Engrs. No. 1-4, 355 (1950).

6. Broido, A., and A. W. McMasters, "Effects of Fires on Personnel in Shelters," Pacific Southwest Forest and Range Experimental Station, Technical Paper No. 50, Berkeley, California (1960).

7. Brown, A. A., "Forest Fire Research in the Forest Service--USDA," Fire Research Abstracts and Reviews, 6, 216 (1964).

8. Burgess, D. S., J. Grumer, and H. G. Wolfhard, "Burning Rates of Liquid Fuels in Large and Small Open Trays," The Use of Models in Fire Research, National Academy of Sciences-National Research Council, Publication No. 786 (1961).

9. Burgoyne, J. H., and L. L. Katan, J. Inst. Petrol. 33, 158 (1947). Cited in reference (62).

10. Byram, G. M., H. B. Clements, E. R. Elliot, and P. M. George, "An Experimental Study of Model Fires," Technical Report No. 3 for OCD and NBS, Forest Service, Southeastern Forest Experiment Station, Macon, Georgia (June 29, 1964).

11. Combustion and Flame, Quarterly Journal of the Combustion Institute, Butterworths, London.

12. Countryman, C. M., "Mass Fires and Fire Behavior," First Interim Report for Office of Civil Defense, Office of the Secretary of the Army, Pacific Southwest Forest and Range Experiment Station (1964).

13. Curry, J. R., and W. L. Fons, "Rate of Spread of Surface Fires in the Ponderosa Pine Type of California," J. Agricultural Research, 57, No. 4, 239-267 (1938).

14. Directory of Fire Research in the United States, National Academy of Sciences--National Research Council Publication 1189 (1964).

15. Directory of Forest Fire Research Projects, Forest Fire Research Institute, Ottawa, Canada, Dept. of Forestry Publication No. 1129 (1965).

16. Eggleston, L. A., J. E. Ambrose, W. W. Bradshaw, and C. H. Yuill, "The Development of Models for Use in the Investigation of Fire Spread," Southwest Research Institute, Department of Structural Research, Fire Research Section (Nov. 2, 1964).

17. Emmons, H. W., "Some Observations on Pool Burning," The Use of Models in Fire Research, National Academy of Sciences--National Research Council, Publication No. 786, 50-66 (1961).

18. Étienne, Ct., "Rapport de Mission--Incineration de la Land de Trensacq," Ministere de l Interieur, Paris, France (April 13, 1955).

19. Faure, J., "Study of Convection Currents Created by Fires of Large Area," The Use of Models in Fire Research, National Academy of Sciences--National Research Council, Publication No. 786 (1961).

20. Fenimore, C. P., Chemistry in Premixed Flames, Macmillan Co. (1964).

21. Fire Research Abstracts and Reviews, published by the Committee on Fire Research, Division of Engineering and Industrial Research, National Academy of Sciences--National Research Council, since 1958.

22. Fons, W. L., "Analysis of Fire Spread in Light Forest Fuels," Journal of Agricultural Research, 72, No. 3, 93-121 (1946).

23. Fons, W. L., "An Eiffel Type Wind Tunnel for Forest Research," Jour. Forestry, 38, 881-884 (1940).

24. Fons, W. L., et al., "Project Fire Model," Summary Progress Report No. 1, 1 Nov. 1958, 30 April 1960, U. S. Dept. of Agriculture, Forest Service, Pacific Southwest Forest and Range Experiment Station, Berkeley, California (1960).

25. Fons, W. L., "Rate of Combustion from Free Surfaces of Liquid Hydrocarbons," Combustion and Flame, 5, 283 (1961).

26. Fons, W. L., H. D. Bruce, and W. Y. Pong, "A Steady-State Technique for Studying the Properties of Free-Burning Wood Fires," The Use of Models in Fire Research, National Academy of Sciences--National Research Council, Publication No. 786 (1961).

27. Fons, W. L., H. B. Clements, and P. M. George, "Scale Effects on Propagation Rate of Laboratory Crib Fires," Ninth Symposium (International) on Combustion, Academic Press, Inc., New York (1963).

28. Fristrom, R. M., and A. A. Westenberg, Flame Structure, McGraw Hill, Inc. (1965).

29. Fuel, A Quarterly Journal of Fuel Science, Butterworths, London.

30. Gay-Lussac, J. L., Ann. Chem. Phys. 18, 221 (1821). Cited in reference (69).

31. Gaydon, A. G., The Spectroscopy of Flames, Chapman and Hall, Ltd., London (1957).

32. Gaydon, A. G., and H. G. Wolfhard, Flames: Their Structure, Radiation, and Temperature, Chapman and Hall, Ltd., London (1957).

33. Gross, D., "Experiments on the Burning of Cross Piles of Wood," Journal of Research of the National Bureau of Standards - C. Engineering and Instrumentation, 66C, No. 2, 99-105 (April-June, 1962).

34. Hamada, M., "A Study of Flame Inclination Due to Wind," Bulletin of Fire Protection Society of Japan, 1 No. 2, 41-43 (1952).

35. Hirst, R., and D. Sutton, "The Effect of Reduced Pressure and Airflow on Liquid Surface Diffusion Flames," Combustion and Flame, 5, 319 (1961).

36. Hottel, H. C. Review of Reference, (4), Fire Research Abstracts and Reviews, 1, 41-44 (1959).

37. Hottel, H. C., G. C. Williams, and F. R. Stewart, "The Modeling of Fire Spread Through a Fuel Bed," Tenth Symposium (International) on Combustion, 997-1007, The Combustion Institute, Pittsburgh, Pennsylvania (1965).

38. Huffman, K., Personal Communication, December, 1965.

39. International Symposia on Combustion, A series of ten (currently) volumes, published by various companies, containing papers presented at the Combustion Institute meetings over the years.

40. Katan, L. L., "On the Combustion of Liquids Burning at a Free Surface," Department of Scientific and Industrial Research and Fire Offices' Committee, Joint Fire Research Organization, F. C. Note No. 12 (1949). Cited in reference (62).

41. Khudyakov, G. N., Bull. Acad. Sci. U.R.S.S., No. 10-11, 1115 (1945). Cited in reference (62).

42. Khudyakov, G. N., Bull. Acad. Sci. U.R.S.S., No. 7, 1015 (1951). Cited in reference (62).

43. Kinbara, T., "A Survey of Fire Research in Japan," Fire Research Abstracts and Reviews, 3, 1 (1961).

44. Lawson, D. I., "Fire Research in the United Kingdom," Fire Research Abstracts and Reviews, 1, 149 (1959).

45. Lewis, B., and G. von Elbe, Combustion, Flames, and Explosions of Gases, Academic Press, New York (1961).

46. Magnus, G., "Test on Combustion Velocity of Liquid Fuels and Temperature Distribution in Flames and Beneath Surface of the Burning Liquid," The Use of Models in Fire Research, National Academy of Sciences--National Research Council, Publication No. 786 (1961).

47. McCarter, R. J., and A. Broido, "Radiative and Convective Energy from Wood Crib Fires," 1964 Spring Meeting, Western States Section, The Combustion Institute, Stanford University (April, 1964).

48. Morton, B. R., "Buoyant Plumes in a Moist Atmosphere," Journal of Fluid Mechanics, 2, 127-144 (1957).

49. Morton, B. R., "The Ascent of Turbulent Forced Plumes in a Calm Atmosphere," International Journal of Air Pollution, 1, 184-197 (1959).

50. Morton, B. R., "Forced Plumes," J. Fluid Mech., 5, 151 (1959).

51. Morton, B. R., "Modeling Fire Plumes," Tenth Symposium (International) on Combustion, 973-981, The Combustion Institute, Pittsburgh, Pennsylvania (1965).

52. Morton, B. R., G. I. Taylor, and J. S. Turner, "Turbulent Gravitational Convection From Maintained and Instantaneous Sources," Proc. Roy. Soc. (London), A234, 1 (1956).

53. Murgai, M. P., and H. W. Emmons, "Natural Convection Above Fire," Journal of Fluid Mechanics, 8, 611-624 (1960).

54. Nielsen, H. J., and L. N. Tao, "The Fire Plume Above a Large Free-Burning Fire," Tenth Symposium (International) on Combustion, 965-971, The Combustion Institute, Pittsburgh, Pennsylvania (1965).

55. Pipkin, O. A., and C. M. Sliepcevich, "Effect of Wind on Buoyant Diffusion Flames," I. and E. C. Fundamentals, 3, 147 (1964).

56. Priestley, C. H. B., "A Working Theory of the Bent-Over Plume of Hot Gas," Quart. J. Royal Met. Soc., 82, 165 (1956).

57. Putnam, A. A., "A Model Study of Wind-Blown Free-Burning Fires," Tenth Symposium (International) on Combustion, 1039-1045, The Combustion Institute, Pittsburgh, Pennsylvania (1965).

58. Putnam, A. A., and C. F. Speich, "A Model Study of the Interacting Effects of Mass Fires," Battelle Memorial Institute Summary Report No. 1 (Nov. 9, 1961).

59. Putnam, A. A., and C. F. Speich, " A Model Study of the Interacting Effects of Mass Fires," Battelle Memorial Institute Summary Report No. 2 (March 27, 1963).

60. Putnam, A. A., and C. F. Speich, "A Model Study of the Interaction of Multiple Turbulent Diffusion Flames," Ninth Symposium (International) on Combustion, 867-875, Academic Press, Inc., New York (1963).

61. Pyrodynamics, A journal of applied thermal processes, published by Gordon and Breach Science Publishers, New York.

62. Rasbash, D. J., E. W. Rogowski, and G. W. V. Stark, "Properties of Fires of Liquids," Fuel, 35, 94-107 (1956).

63. Robertson, A. F., "Fire Research at the National Bureau of Standards," Fire Research Abstracts and Reviews, 1, 159 (1959).

64. Rouse, H., C. S. Yih, and H. W. Humphreys, "Gravitational Convection from a Boundary Source," Tellus, 4, 201-210 (1952).

65. Schmidt, Wilhelm, "Turbulente Ausbreitung eines Stromes erhitzter Luft," Zeitschrift fur Angewandte Mathematik und Mechanik 21, 265-278 and 351-363 (1941).

66. Show, S. B., "Climate and Forest Fires in Northern California," Journal of Forestry, 17, 965-979 (1919).

67. Spalding, D. B., "The Combustion of Liquid Fuels," Fourth Symposium (International) on Combustion, 847-864, Williams and Wilkins Co., Baltimore (1953).

68. Strasser, A., and J. Grumer, "Air Flows into Uncontrolled Fires," Final Report No. 3909, Bureau of Mines (Jan. 8, 1964).

69. "A Study of Fire Problems," National Academy of Sciences, National Research Council Publication, No. 949 (1961).

70. Sutton, O. G., "The Dispersion of Hot Gases in the Atmosphere," Jour. of Met., 7, 307 (1950).

71. Taylor, G. I., U. S. Atomic Energy Commission, MDDC-919, LADC-276 (1945).

72. "Tentative Methods of Test for Moisture Content of Wood," ASTM Designation D2016-62T, American Society of Testing Materials (1962).

73. Thomas, P. H., "Buoyant Diffusion Flames," Combustion and Flame, 4, No. 4, 381-382 (1960).

74. Thomas, P. H., "The Size of Flames From Natural Fires," Ninth Symposium (International) on Combustion, 844-858, Academic Press, Inc., New York (1963).

75. Thomas, P. H., "Some Studies of Building Fires Using Models," The Use of Models in Fire Research, National Academy of Sciences--National Research Council, Publication No. 786 (1961).

76. Thomas, P. H., R. Baldwin, and A. J. M. Heselden, "Buoyant Diffusion Flames: Some Measurements of Air Entrainment, Heat Transfer and Flame Merging," Tenth Symposium (International) on Combustion, 983-996, The Combustion Institute, Pittsburgh, Pennsylvania (1965).

77. Thomas, P. H., and R. Scott, "Research on Forest Fires," Report on Forest Research for the Year Ended March 1962, 116-119 (1962).

78. Thomas, P. H., C. T. Webster, and M. M. Raftery, "Some Experiments on Buoyant Diffusion Flames," Combustion and Flames, 5, 359-367 (1961).

79. The Use of Models in Fire Research, National Academy of Sciences--National Research Council, Publication No. 786 (1961).

80. Waterman, T. E., W. G. Labes, F. Salzberg, J. E. Tamney, and F. J. Vodvarka, "Prediction of Fire Damage to Installations and Built-up Areas from Nuclear Weapons," Final Report -- Phase III, Experimental Studies -- Appendices A-G, IIT Research Institute Report for National Military Command System Support Center, Contract No. DCA-8, November, 1964.

81. Welker, J. R., "The Effect of Wind on Uncontrolled Buoyant Diffusion Flames From Burning Liquids," Ph.D. Dissertation, The University of Oklahoma (1965).

82. Welker, J. R., O. A. Pipkin, and C. M. Sliepcevich, "The Effect of Wind on Flames," Fire Technology 1, 122-129 (1965).

83. Williams, F. A., Combustion Theory, Addison-Wesley Co. (1965).

84. Williams-Leir, G., "The Rate of Burning of Liquids," Department of Scientific and Industrial Research and Fire Offices' Committee, Joint Fire Research Organization, F. P. E. Note No. 62 (1951). Cited in reference (62).

85. Yokoi, S., "Upward Convection Current from a Burning Wooden House," The Use of Models in Fire Research, National Academy of Sciences--National Research Council, Publication No. 786 (1961).

86. Yokoi, S., Report No. 24, Building Research Institute, Ministry of Construction, Japan (1964).

NOMENCLATURE*

$\ddot{A}_e$	=	Initially exposed surface area of the fuel per unit of top surface area of crib
A_R	=	Initially exposed surface area ratio
b	=	Exponent
c	=	Exponent
C_f	=	Flame drag coefficient
C_ℓ	=	Lift coefficient
d	=	Size of square cross section of stick
D	=	Depth of flaming zone in the direction of fire propagation
f	=	Exponent
F_f	=	Field force
FL_R	=	Fuel loading ratio
Fr	=	Froude number
g	=	Gravitational acceleration
g_c	=	Gravitational constant
j	=	Exponent
L	=	Flame length
m	=	Number of sticks in the crib in a unit length
$\dot{m}$	=	Total burning rate

*The nomenclature included in this section is the one used in this study only.

$\dot{m}''$ = Burning rate per unit area of the top surface of the crib

M'' = Mass of wood beneath a unit area of the top surface of the crib (fuel loading)

MV = Momentum

N = Number of layers of sticks forming a crib

$\dot{p}$ = Flame propagation rate

q = Exponent

Re = Reynolds number

s = Spacing between the centers of two proximate fires; spacing between sticks in the crib

T = Temperature

U = Undisturbed wind speed

V'' = Volume of wood beneath a unit area of top surface of crib

W = Width of crib

x = Distance from the center line between two proximate fires to the position of the thermocouple rack

Greek

α = Fraction of stick

β = Fraction of a space between sticks in crib

θ = Flame angle of tilt from vertical

μ = Dynamic viscosity

ν = Kinematic viscosity

ρ = Density

τ = Time

$\Delta\tau$ = Residence time; interval of time

Subscripts

a	=	Property of ambient air
dn	=	Downstream
f	=	Property of flame
g	=	Property of fuel vapor
I	=	Refers to quantities entering system
O	=	Refers to quantities leaving system
up	=	Upstream
w	=	Property of wood

APPENDIX A

DERIVATION OF THE FORMULA FOR THE INITIALLY EXPOSED SURFACE AREA OF THE STICKS IN THE CRIB AND FUEL LOADING

Initially Exposed Surface Area of the Sticks in the Crib per Unit Area of the Top Crib Surface

Consider a crib made of N identical layers of sticks arranged in a criss-cross pattern with the sticks lined up in alternate layers. Assume the sticks making up the crib are all of the same square cross section of side dimension d. Assume that the spacing between sticks is s. A section of such a crib is shown in Figure 38A. Consider now a unit square area of the top crib surface as indicated by the dark solid line in the figure. Position such a unit area so that one of its edges coincides with the outermost edge of one of the sticks as shown in Figure 38B. Consider now the number of sticks present in the unit length of the side of the unit square. Let the number of whole sticks be denoted by m and let α represent the fraction of stick included by the unit length as shown in Figure 38B. Therefore, the number of sticks is given by

$$m + \alpha \tag{62}$$

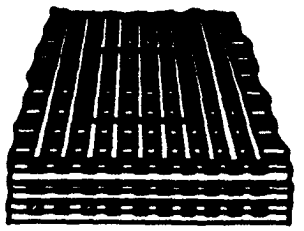

CRIB

A

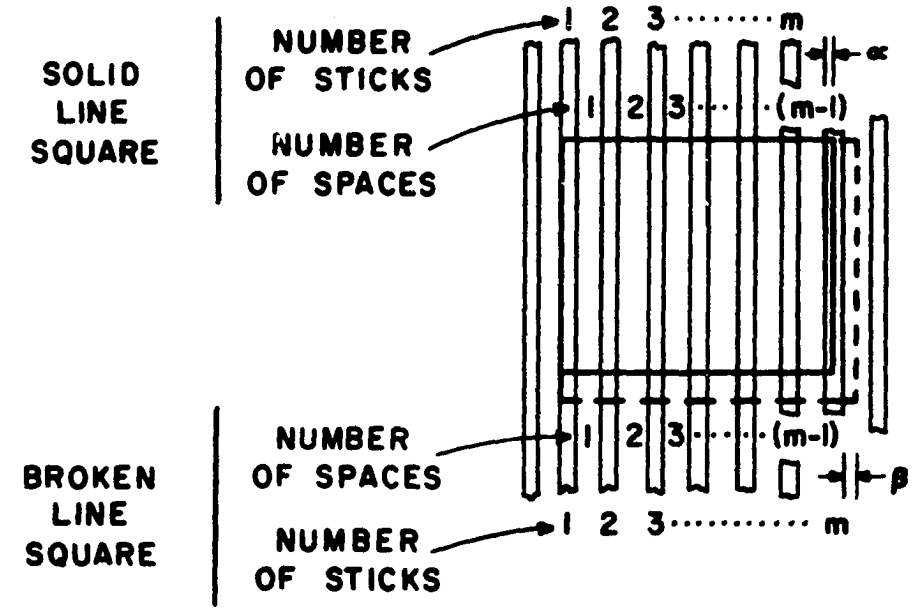

B

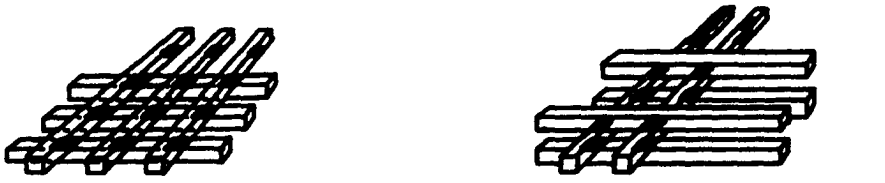

C D

Figure 38. A. Section of a Crib; B. Layer of Sticks; C. Exposed Surface Area of Top Layer in the Crib; D. Exposed Surface Area of Interior Layers in the Crib

The number of spaces between the sticks in the unit length equal m-1. In case the unit length does not include a fraction of a stick but a fraction of space, as shown by the dashed line in Figure 38B, let β represent the fraction of such a space. Therefore, the number of spaces in the unit length will be given by

$$(m-1) + \beta \tag{63}$$

The unit length in terms of the above parameters of the crib is then given by

$$(m+\alpha)d + [(m-1)+\beta]s \tag{64}$$

Since the layers have been assumed identical, the above expression also represents the length of the sticks within the unit surface area.

Now proceed to calculate the exposed surfaces of the material in the various layers. The top and bottom layers must be evaluated separately from the inner layers due to boundary conditions.

Consider first the top layer (see Figure 38C). One notices that for each stick, there are three completely exposed sides. Their area is given by

$$3[(m+\alpha)d + (m-1+\beta)s]d \tag{65}$$

On the fourth side (bottom one), part of the area is masked by the joints and therefore does not constitute an exposed surface. The area of the bottom side is then given by

$$[(m+\alpha)d + (m-1+\beta)s]d - [md^2+\alpha d^2] \tag{66}$$

The total exposed area of the top layer is then given by

$$[m+\alpha]\{4[(m+\alpha)d+(m-1+\beta)s]d-[md^2+\alpha d^2]\} \quad (67)$$

Consider now the interior layers (Figure 38D). In this case, the area of two sides is completely exposed and is given by

$$2[(m+\alpha)d+(m-1+\beta)s]d \quad (68)$$

The remaining two sides are affected by the joints and therefore their contribution is given by

$$2\{[(m+\alpha)d+(m-1+\beta)s]d-[md^2+\alpha d^2]\} \quad (69)$$

Thus, the total exposed area for one stick in these layers is

$$4[(m+\alpha)d+(m-1+\beta)s]d-2[md^2+\alpha d^2] \quad (70)$$

The total area for one interior layer is

$$[m+\alpha]\{4[m+\alpha)d+(m-1+\beta)s]d-2[md^2+\alpha d^2]\} \quad (71)$$

For the total of (N-2) interior layers, the total area is then,

$$[N-2]\{m+\alpha\}\{4[(m+\alpha)d+(m-1+\beta)s]d-2[md^2+\alpha d^2]\} \quad (72)$$

In the case of the bottom layer, each stick has two completely exposed sides whose area is given by

$$2[(m+\alpha)d+(m-1+\beta]s]d \quad (73)$$

and a top side whose area is reduced by the joints and therefore given by

$$[(m+\alpha)d+(m-1+\beta)s]d-[md^2+\alpha d^2] \quad (74)$$

The total exposed area of the stick in the crib per unit square area of the top surface of the crib is then given by the sum of the various exposed areas in the N layers, i.e.

$$\{(m+\alpha)\}\{4[(m+\alpha)d+(m-1+\beta)s]d-[m+\alpha]d^2\}+\{N-2\}\{m+\alpha\}$$
$$\{4[(m+\alpha)d+(m-1+\beta)s]d-2[m+\alpha]d^2\}+\{m+\alpha\}\{3[(m+\alpha)d+ \quad (75)$$
$$(m-1+\beta)s]d-[m+\alpha]d^2\}$$

In order to simplify the algebra, let

$$m + \alpha = p \tag{76}$$

$$m - 1 + \beta = q \tag{77}$$

The above expression reduces to

$$p\{4pd^2+4qsd-pd^2\}+\{N-2\}\{p\}\{4pd^2+4qsd-2pd^2\}+ \{p\}\{3pd^2+3qsd-pd^2\} \tag{78}$$

Letting A_e'' denote total exposed surface of the sticks in the crib per unit square area of the top surface of the crib, and further simplifying the above expression, then

$$A_e'' = 4p^2d^2+4pqsd-p^2d^2+(N-2)4p^2d^2+(N-2)4pqsd-(N-2)2p^2d^2+3p^2d^2+3pqsd-p^2d^2$$

$$A_e'' = p^2d^2[4-1+4(N-2)-2(N-2)+3-1]+pqsd[4+4(N-2)+3]$$

$$A_e'' = p^2d^2[4-1+4N-8-2N+4+3-1]+pqsd[4+4N-8+3]$$

$$A_e'' = p^2d^2[2N+1]+pqsd[4N-1]$$

Substituting the values of p and q

$$A_e'' = [(m+\alpha)^2d^2][2N+1]+[(m+\alpha)(m-1+\beta)sd][4N-1] \tag{40}$$

Mass of Wood Per Unit Area of the Top Crib Surface (Fuel Loading)

The volume of material per unit square area of the top surface of the crib can be determined as follows:

The volume of material in one stick within this unit per square area is

$$[(m+\alpha)d+(m-1+\beta)s]d^2 \tag{79}$$

The volume of m sticks is

$$m[(m+\alpha)d+(m-1+\beta)s]d^2 \tag{80}$$

and the volume of a fraction α of a stick is

$$[(m+\alpha)d+(m-1+\beta)s][d][\alpha d] \tag{81}$$

The volume of $(m + \alpha)$ sticks is, therefore,

$$[(m+\alpha)d+(m-1+\beta)s][m+\alpha]d^2 \tag{82}$$

The volume of N layers (denoted by $\overset{''}{V}$ is finally given by

$$\overset{''}{V} = N[m+\alpha][(m+\alpha)d+(m-1+\beta)s]d^2 \tag{83}$$

The mass of the material comprised in the above volume can be calculated by

$$\overset{''}{M} = \rho_w N[m+\alpha][(m+\alpha)d+(m-1+\beta)s]d^2 \tag{41}$$

where ρ_w is the average density of the material (in this case wood) and $\overset{''}{M}$ denotes mass of the crib per unit square area of top surface of the crib.

APPENDIX B

FLAME BENDING MODEL

Consider the flame shown in Figure 39A. A momentum balance applied to such a flame may be written, for an accounting period $\Delta\tau$, in difference form as

$$\Delta(MV)_\tau = \Sigma(MV)_I - \Sigma(MV)_O + g_c \Sigma \int_\tau^{\tau+\Delta\tau} (F_f+F_b)d\tau \qquad (84)$$

where

MV = momentum

F_f = field forces

F_b = body forces

g_c = gravitational constant

τ = time

Subscripts I and O denote in and out respectively. Considering only steady-state flames, the momentum change with respect to time is zero, and the above expression reduces to

$$\Sigma(MV)_I - \Sigma(MV)_O + g_c\Sigma(F_f+F_b)\Delta\tau = 0 \qquad (85)$$

Referring to Figure 39A, the momentum into the flame zone is due to the air entrained laterally and to the fuel

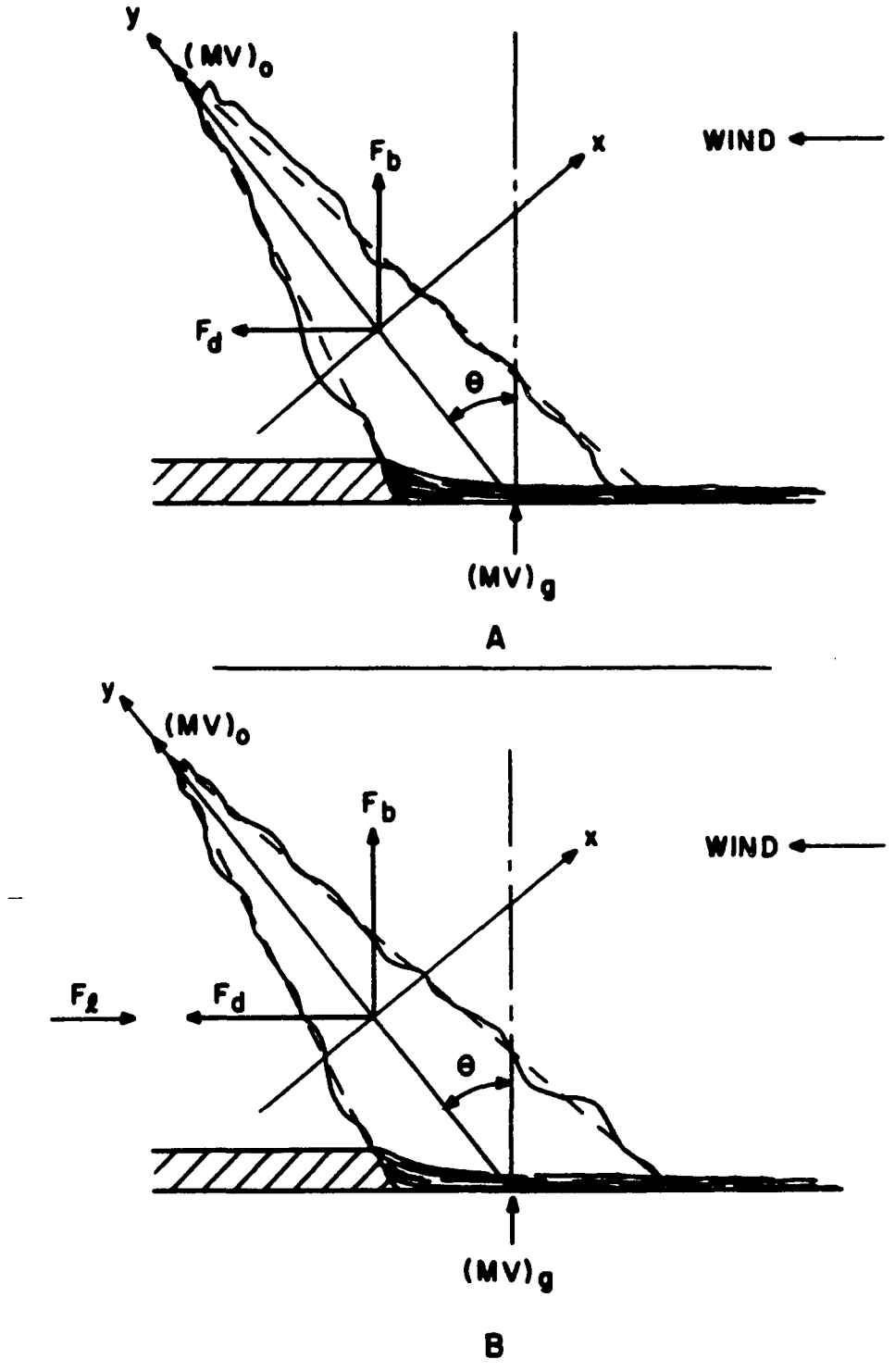

Figure 39. Mathematical Model of Wind-Blown Fires

gases rising from the fuel. The only body force acting on the flame is the drag force of the wind, and the field force is that due to buoyancy of the flame gases.

If one assumes approximately equal magnitudes of air entrainment on opposite sides of the flame, then there is no net momentum transfer into the flame due to the influx of air.

Consider now the components of the momentum balance along the x and y coordinates. The momentum balance along the x-axis can be written as

$$(MV)_g \sin\theta + g_c(F_b \sin\theta - F_d \cos\theta)\Delta\tau = 0 \qquad (86)$$

where $(MV)_g$ is the momentum contribution of the gases entering at the base of the flame. F_d denotes the drag force due to the wind and is given by

$$F_d = C_f \rho_a \frac{U^2}{2g_c} WL \cos\theta \qquad (87)$$

where

C_f = flame drag coefficient

ρ_a = density of the surrounding air

U = wind velocity

g_c = gravitational constant

W = width of flame zone in a direction perpendicular to the air flow

L = length of the flame

The term $\frac{\rho_a U^2}{2g_c}$ represents a dynamic pressure and WL cos θ is the projected area of the flame.

F_b denotes the field force due to buoyancy. It is given by

$$F_b = (\text{Flame Volume}) \frac{g}{g_c} \rho_f \frac{T_f - T_a}{T_a} \tag{88}$$

Assuming a triangular cross section of flame as shown in Figure 39A, the volume of flame is given by 1/2 DWL. Substituting in the above relation

$$F_b = \frac{DWL}{2} \frac{g}{g_c} \rho_f \frac{T_f - T_a}{T_a} \tag{89}$$

where

g = gravitational acceleration

ρ_f = density of the gases in the flame

T_f = temperature in the flame

T_a = temperature of the surrounding air

Substituting in Equation (86),

$$(MV)_g \sin\theta + g_c \left[\frac{DWL}{2} \frac{g}{g_c} \rho_f \frac{T_f - T_a}{T_a} \sin\theta - C_f \frac{\rho_a U^2}{2g_c} WL \cos^2\theta \right] \Delta\tau = 0 \tag{90}$$

The contribution of the gases entering the base of the flame has been found to be negligible, so that the term involving $(MV)_g$ can be neglected, which results in

$$\frac{DWL}{2} \; g\rho_f \; \frac{T_f - T_a}{T_a} \quad \sin\theta - C_f \frac{\rho_a U^2}{2} \quad WL \cos\theta \cos\theta = 0 \tag{91}$$

after dividing by $\Delta\tau$. Rearranging the above expression,

$$\tan\theta = \frac{C_f \frac{\rho_a U^2}{2} \, WL \cos\theta}{\frac{DWL}{2} \, g\rho_f \frac{T_f - T_a}{T_a}} \tag{92}$$

or

$$\frac{\tan\theta}{\cos\theta} = \frac{C_f U^2 \rho_a}{Dg\rho_f \frac{T_f - T_a}{T_a}} \tag{93}$$

From the perfect gas law, and assuming that the molecular weight of the gases in the flame zone is nearly the same as that of the surrounding air,

$$\frac{\rho_a}{\rho_f} = \frac{T_f}{T_a} \tag{94}$$

Substituting this relation in Equation (93), it becomes

$$\frac{\tan\theta}{\cos\theta} = C_f \frac{U^2}{Dg} \frac{T_f}{T_f - T_a} \tag{60}$$

This equation is similar to that of Welker (81) except that in his case the flame cross section was assumed as cylindrical for the flames from circular burners and in the shape of a parallelogram in the case of the rectangular burners.

The model described above, which applies to a single fire, can be extended to the upstream fire of the proximate flames. However, the disturbance in the air flow caused by the encounter of the wind with the upstream fire makes it difficult to extend the model to the downstream fire.

In the case of the upstream fire, the fire burning downstream tends to lift the tip of the upstream fire due to the nearly vertical flow of the gases resulting from the combustion gases rising from the downstream fire. In extending the model as shown in Figure 39B, it is assumed that the component of the "push" or "lift," caused by the downstream fire, along the horizontal can be expressed in terms of the undisturbed wind speed as

$$F_\ell = C_\ell \frac{\rho_a U^2}{2g_c} WL \cos\theta \qquad (95)$$

The equation of momentum balance along the x axis, neglecting the contribution of the gases entering the base of the flame, becomes

$$\frac{DWL}{2}\, g\rho_f\, \frac{T_f - T_a}{T_a} \sin\theta - C_f\, \frac{\rho_a U^2}{2}\, WL \cos\theta \cos\theta \qquad (96)$$

$$+ C_\ell\, \frac{\rho_a U^2}{2}\, WL \cos\theta \cos\theta = 0$$

Rearranging the terms, results in

$$\tan\theta = \frac{\left|C_f - C_\ell\right| \frac{\rho_a U^2}{2}\, WL \cos\theta}{\frac{DWL}{2}\, g\rho_f\, \frac{T_f - T_a}{T_a}} \qquad (97)$$

which reduces, by making use of Equation (94), to

$$\frac{\tan\theta}{\cos\theta} = \left|C_f - C_\ell\right| \frac{U^2}{Dg} \frac{T_f}{T_f - T_a} \qquad (61)$$

APPENDIX C

TABULAR SUMMARY OF DATA

TABLE 1

DENSITY AND MOISTURE CONTENT
OF THE WOOD IN THE CRIBS

Crib No.	Density lb/ft^{-3}	Moisture Content per cent
1	34.7	9.9
2	33.8	10.6
3	33.5	10.1
4	33.0	10.0
5	33.4	10.1
6	34.3	10.0
7	33.4	10.0
8	33.1	10.2
9	33.1	10.6
10	33.3	10.4
11	33.4	11.0
12	33.4	10.9
13	33.6	10.1
14	33.6	10.2
15	33.3	10.4
16	33.7	10.5
17	33.1	10.4
18	33.6	10.7
19	33.5	10.9
20	33.4	11.3
21	33.3	11.8
22	33.5	10.9
23	33.6	11.5
24	33.5	9.8
25	33.4	9.7
26	34.0	10.2
27	33.7	10.0
28	33.9	9.7
29	33.7	10.3
30	34.2	10.1
31	33.5	9.8
32	34.6	10.1
33	34.3	9.8
34	34.5	10.2
35	34.9	8.2
36	34.5	9.9
37	33.9	9.7
38	33.8	9.6
39	34.1	10.1
40	35.2	10.6

TABLE 2

SUMMARY OF TEMPERATURES (°F) DOWNSTREAM FROM THE SINGLE FIRE CHROMEL-ALUMEL THERMOCOUPLES

Run No.	Distance Downstream ft	Thermocouple Number and (x, t) Coordinate											
		1 (2,1)	2 (4,1)	3 (6,1)	4 (1,2)	5 (3,2)	6 (4,2)	7 (5,2)	8 (7,2)	9 (2,3)	10 (4,3)	11 (6,3)	12 (4,4)
030766-20-1A	3.75[a]	64	64	64	70	71	71	71	70	79	81	78	85
030766-20-2A	3.75	70	72	70	70	75	75	74	75	85	82	92	86
030766-20-3A	3.75	173	155	168	79	294	293	235	73	117	223	108	112
030766-22-4A	3.75	236	315	311	81	158	331	485	80	94	121	100	100
030866-25-5A	3.75	71	73	70	73	74	74	75	73	107	81	95	89
030866-25-6A	3.75	76	90	95	76	123	103	125	81	161	187	150	201
030866-26-7A	3.75	75	78	77	77	82	81	83	81	114	87	113	97
030866-26-8A	3.75	98	116	121	81	241	200	206	81	136	262	152	198
030966-37-9A	3.75	79	83	82	77	80	84	85	78	106	89	105	92
030966-37-10A	3.75	112	130	167	84	365	268	280	83	116	237	114	122
030966-36-11A	3.75	160	257	102	93	384	372	324	86	121	213	127	130
031566-40-12A	3.75	91	91	91	93	96	97	98	92	102	106	99	107
031566-40-13A	3.75	96	98	97	98	99	102	103	97	126	108	120	113
031566-40-14A	3.75	111	113	110	115	119	119	118	110	124	127	120	131

(a) The distance downstream was measured from the center of the depth of flaming zone to the position of the rack.

TABLE 3

SUMMARY OF TEMPERATURES (°F) DOWNSTREAM FROM THE SINGLE FIRE IRON-CONSTANTAN THERMOCOUPLES

Run No.	Distance Downstream From Centerline of the Fires ft	Thermocouple Number and (x,z) Coordinate										
		1 (1,4)	2 (7,4)	3 (2,5)	4 (4,5)	5 (6,5)	6 (1,6)	7 (4,6)	8 (7,6)	9 (2,7)	10 (4,7)	11 (6,7)
030766-20-1A	3.75[a]	74	74	78	85	78	90	91	100	98	99	97
030766-20-3a	3.75	102	106	98	91	104	105	100	110	105	108	110
030766-20-3A	3.75	80	75	99	112	102	128	132	126	154	161	150
030766-22-4A	3.75	86	81	90	100	88	87	97	81	100	97	95
030866-25-5A	3.75	104	107	114	97	106	116	114	119	119	122	126
030866-25-6A	3.75	118	118	154	183	162	168	193	168	172	183	170
030866-26-7A	3.75	103	101	116	111	--	117	120	123	121	126	132
030866-26-8A	3.75	122	122	160	182	--	180	197	181	191	170	164
030966-37-9A	3.75	116	118	129	106	--	130	121	129	129	129	130
030966-37-10A	3.75	95	98	126	138	--	164	146	143	160	167	161
030966-36-11A	3.75	95	90	99	108	--	102	109	99	143	143	138
031566-40-12A	3.75	120	121	116	111	--	128	120	128	129	129	128
031566-40-13A	3.75	127	133	133	119	--	138	130	149	140	141	152
031566-40-14A	3.75	121	125	126	136	--	158	150	159	153	157	153

[a] The distance downstream was measured from the center of the depth of flaming zone to the position of the rack.

TABLE 4

SUMMARY OF TEMPERATURES (°F) DOWNSTREAM FROM THE PROXIMATE FIRES
CHROMEL-ALUMEL THERMOCOUPLES

Run No.	Distance Downstream From Centerline of the Fires ft	Thermocouple Number and (x,z) Coordinate											
		1 (2,1)	2 (4,1)	3 (6,1)	4 (1,2)	5 (3,2)	6 (4,2)	7 (5,2)	8 (7,2)	9 (2,3)	10 (4,3)	11 (6,3)	12 (4,4)
120365-(4,1)-4	6.25[a]	86	86	86	93	93	94	94	92	99	100	100	107
120365-(4,1)-5	5.00	100	100	100	110	110	115	116	109	118	120	117	127
120365-(4,1)-6	3.75	98	116	112	133	130	129	125	102	132	129	130	138
120365-(4,1)-7	2.50	102	154	95	125	186	208	175	115	158	222	176	207
120865-(3,3)-8	4.00	131	1117	149	112	359	481	282	101	130	213	135	138
121465-(15,2)-9	8.75	81	81	81	82	82	82	82	82	87	87	88	103
121465-(15,2)-10	7.00	84	86	85	89	89	90	90	89	94	95	96	112
121465-(15,2)-11	5.25	91	97	97	102	102	104	104	103	113	113	113	122
121665-(13,16)-12	7.00	80	80	78	82	82	82	82	83	85	85	82	96
121665-(13,16)-13	5.25	92	92	88	100	100	100	95	93	108	109	105	119
121665-(13,16)-14	3.50	98	104	92	106	118	119	107	101	124	122	117	126
010766-(35,14)-15	4.50	117	119	106	117	134	142	128	116	128	151	131	151
010766-(35,14)-16	5.00	110	110	101	118	121	121	119	115	127	133	131	139
011166-(12,11)-17	6.00	84	85	83	89	89	89	89	79	94	95	96	104
011166-(12,11)-18	4.50	105	105	102	115	115	115	112	107	126	125	121	134
011466-(10,9)-19	5.00	80	92	80	87	124	106	114	108	157	139	148	179
012566-(8,7)-20	3.75	113	996	175	81	205	446	178	87	114	243	98	127
012866-(21,19)-21	6.25	87	81	72	87	87	85	88	87	156	99	139	132
012866-(21,19)-22	5.00	41	50	51	56	58	59	55	50	87	67	89	83
012866-(21,19)-23	5.00	96	135	102	64	188	297	272	74	75	251	80	170
030466-(24,23)-24	3.75	84	86	84	89	101	101	100	91	103	112	102	117
030466-(24,23)-25	3.00	83	88	74	100	100	107	117	95	131	153	155	184
031466-(38,39)-26	3.75	118	126	113	116	148	150	144	117	125	145	125	138
031466-(38,39)-27	3.00	141	167	136	128	168	188	166	120	149	187	143	170
031466-(38,39)-28	2.25	163	218	152	141	216	281	201	131	169	257	168	222
031766-(26,29)-29	3.75	158	156	115	149	301	266	301	123	173	291	195	257
031866-(30,31)-30	3.75	128	140	124	106	142	155	145	109	142	159	135	156
032166-(32,33)-31	5.50	193	333	165	126	317	546	354	156	188	429	196	255
032266-(34,27)-32	4.50	124	127	117	127	146	145	144	123	144	156	147	162
032266-(34,27)-33	2.70	139	198	108	115	169	309	195	116	181	300	205	270

[a] The distance downstream was measured from the centerline between the two fires to the position of the rack.

TABLE 5

SUMMARY OF TEMPERATURES (°F) DOWNSTREAM FROM PROXIMATE FIRES
IRON-CONSTANTAN THERMOCOUPLES

Run No.	Distance Downstream From Centerline of the Fires ft	Thermocouple Number and (x,z) Coordinate										
		1 (1,4)	2 (7,4)	3 (2,5)	4 (4,5)	5 (6,5)	6 (1,6)	7 (4,6)	8 (7,6)	9 (2,7)	10 (4,7)	11 (6,7)
120365-(4,1)-4	6.25[a]	110	109	118	122	118	147	129	144	148	139	149
120365-(4,1)-5	5.00	140	134	131	134	134	155	141	158	162	159	165
120365-(4,1)-6	3.75	151	159	156	158	175	179	177	196	189	192	198
120365-(4,1)-7	2.50	160	178	172	183	191	193	183	188	195	191	188
120865-(3,3)-8	4.00	143	137	185	201	198	218	235	213	233	239	235
121465-(15,2)-9	8.75	106	119	123	124	121	146	135	145	152	146	146
121465-(15,2)-10	7.00	111	114	129	132	124	155	143	155	162	155	154
121465-(15,2)-11	5.25	119	111	137	139	119	163	147	163	163	167	161
121665-(13,16)-12	7.00	100	96	113	115	104	145	127	138	153	149	140
121665-(13,16)-13	5.25	120	131	139	137	126	168	150	159	173	170	160
121665-(13,16)-14	3.50	128	130	145	139	139	172	157	169	178	182	173
010766-(35,14)-15	4.50	141	159	139	160	148	161	169	162	174	184	175
010766-(35,14)-16	5.00	137	157	151	159	154	177	170	177	187	182	181
011166-(12,11)-17	6.00	114	120	117	114	114	144	122	135	148	138	142
011166-(12,11)-18	4.50	129	130	145	149	137	164	152	163	173	165	165
011466-(10,9)-19	5.00	148	150	177	197	184	196	205	196	205	211	203
012566-(8,7)-20	3.75	68	60	73	79	71	135	131	128	176	184	176
012866-(21,19)-21	6.25	153	157	166	162	189	203	167	200	209	207	207
012866-(21,19)-22	5.00	103	99	106	104	114	123	127	134	134	143	144
012866-(21,19)-23	5.00	66	59	101	122	94	127	131	123	141	147	142
030466-(24,23)-24	3.75	118	113	129	123	124	151	140	148	158	156	156
030466-(24,23)-25	3.00	138	137	167	195	184	180	184	165	184	184	175
031466-(38,39)-26	3.75	129	120	133	136	136	156	142	150	163	160	159
031466-(38,39)-27	3.00	151	142	157	166	166	173	170	168	179	182	175
031466-(38,39)-28	2.25	167	161	179	206	206	190	205	187	201	213	194
031766-(28,29)-29	3.75	184	175	220	239	236	235	246	232	241	246	239
031866-(30,31)-30	3.75	181	156	177	163	163	195	179	186	199	201	203
032166-(32,33)-31	5.50	115	105	129	166	166	123	134	123	174	176	166
032266-(34,27)-32	4.50	165	160	167	172	172	185	181	182	190	191	220
032266-(34,27)-33	2.70	178	179	205	252	252	223	238	208	229	235	220

[a] The distance downstream was measured from the centerline between the two fires to the position of the rack.

TABLE 6

SUMMARY OF THE BURNING RATE DATA AND RESULTS -- SINGLE FIRE

Run No.	Burning Parameters			Surrounding Air Parameters		Dimensionless Groups	
	Fuel Burning Rate	Depth of the Flaming Zone	Fuel Burning Rate per Unit Area	Air Density	Air Viscosity	$\frac{qD}{\mu_a}$	$\frac{qD^3\rho_a^2}{\mu_a^2}$
	lb/sec	ft	lb/ft^2-sec	lb/ft^3	lb/ft-sec	dimensionless	dimensionless
030766-20-1A	0.00632	0.25	0.00867	0.075	1.17×10^{-5}	185.2	20.91×10^6
030766-20-2A	0.00783	0.50	0.00537	0.075	1.17×10^{-5}	229.4	166.70×10^6
030766-20-3A	0.02659	2.08	0.00438	0.075	1.18×10^{-5}	772.6	$11,709.24 \times 10^6$
030766-22-4A	0.03735	2.58	0.00496	0.074	1.19×10^{-5}	1075.8	$21,502.43 \times 10^6$
030866-25-5A	0.01014	0.50	0.00695	0.075	1.18×10^{-5}	294.6	163.95×10^6
030866-25-6A	0.02676	1.75	0.00524	0.075	1.18×10^{-5}	777.4	$7,047.96 \times 10^6$
030866-26-7A	0.00953	0.50	0.00653	0.074	1.18×10^{-5}	276.8	160.05×10^6
030866-26-8A	0.02658	2.00	0.00456	0.074	1.19×10^{-5}	765.7	$10.042.03 \times 10^6$
030966-37-9A	0.01135	0.58	0.00671	0.074	1.19×10^{-5}	327.1	242.95×10^6
030966-37-10A	0.03003	1.75	0.00588	0.073	1.20×10^{-5}	857.9	$6,457.09 \times 10^6$
030966-36-11A	0.04026	3.25	0.00425	0.073	1.20×10^{-5}	1150.2	$40,683.57 \times 10^6$
031566-40-12A	0.00712	0.33	0.00740	0.071	1.21×10^{-5}	201.9	40.14×10^6
031566-40-13A	0.00869	0.50	0.00596	0.071	1.22×10^{-5}	244.2	137.11×10^6
031566-40-14A	0.00820	0.33	0.00852	0.071	1.22×10^{-5}	230.5	39.38×10^6

TABLE 7

SUMMARY OF THE BURNING RATE DATA AND RESULTS -- UPSTREAM FIRE

Run No.	Burning Parameters			Surrounding Air Parameters		Dimensionless Groups	
	Fuel Burning Rate	Depth of the Flaming Zone	Fuel Burning Rate per Unit Area	Air Density	Air Viscosity	$\frac{\Delta Q}{\mu_a}$	$\frac{gD^3\rho_a^2}{\mu_a^2}$
	lb/sec	ft	lb/ft^2-sec	lb/ft^3	lb/ft-sec	dimensionless	dimensionless
120365-4-4	0.01575	0.87	0.00621	0.073	1.19×10^{-5}	453.7	806.82×10^{-6}
120365-4-5	0.01297	0.75	0.00593	0.074	1.19×10^{-5}	373.5	519.71×10^{-6}
120365-4-6	0.01712	1.25	0.00469	0.074	1.19×10^{-5}	493.1	$2,418.77\times10^{-6}$
120365-4-7	0.01120	0.87	0.00441	0.074	1.19×10^{-5}	322.6	822.42×10^{-6}
120865-3-8	0.01970	1.25	0.00540	0.073	1.20×10^{-5}	562.8	$2,302.03\times10^{-6}$
121465-15-9	0.01362	0.75	0.00622	0.074	1.17×10^{-5}	399.0	539.04×10^{-6}
121465-15-10	0.01352	0.67	0.00692	0.075	1.17×10^{-5}	396.0	393.73×10^{-6}
121465-15-11	0.01480	0.75	0.00676	0.075	1.17×10^{-5}	433.6	555.22×10^{-6}
121665-13-12	0.01703	1.00	0.00584	0.075	1.17×10^{-5}	499.1	$1,326.57\times10^{-6}$
121665-13-13	0.01837	1.12	0.00562	0.075	1.17×10^{-5}	538.2	$1,873.62\times10^{-6}$
121665-13-14	0.01237	0.62	0.00684	0.075	1.17×10^{-5}	362.3	317.80×10^{-6}
010766-35-16	0.01545	1.08	0.00490	0.075	1.18×10^{-5}	448.8	$1,625.99\times10^{-6}$
011166-12-18	0.01552	1.00	0.00532	0.073	1.19×10^{-5}	447.0	$1,225.24\times10^{-6}$
012566-8-20	0.02937	2.00	0.00503	0.077	1.15×10^{-5}	875.5	$11,673.84\times10^{-6}$
012866-21-21	0.02967	1.92	0.00530	0.075	1.17×10^{-5}	869.2	$9,489.25\times10^{-6}$
012866-21-22	0.02300	1.50	0.00526	0.079	1.12×10^{-5}	703.9	$5,477.08\times10^{-6}$
012866-21-23	0.02283	2.08	0.00376	0.079	1.12×10^{-5}	698.8	$14,603.76\times10^{-6}$
010466-24-24	0.01323	1.00	0.00454	0.076	1.16×10^{-5}	391.0	$1,367.18\times10^{-6}$
010466-24-25	0.01680	1.08	0.00533	0.075	1.17×10^{-5}	492.3	$1,688.86\times10^{-6}$
031466-38-26	0.00967	0.58	0.00571	0.073	1.20×10^{-5}	276.2	233.14×10^{-6}
031466-38-27	0.01065	0.67	0.00545	0.073	1.20×10^{-5}	304.2	359.45×10^{-6}
031466-38-28	0.01143	0.75	0.00523	0.073	1.20×10^{-5}	326.6	500.01×10^{-6}
031766-28-29	0.02847	2.92	0.00334	0.070	1.23×10^{-5}	793.4	$25,963.41\times10^{-6}$
031866-30-30	0.02075	1.75	0.00406	0.073	1.20×10^{-5}	592.8	$6,368.41\times10^{-6}$
032166-32-31	0.03367	3.50	0.00330	0.070	1.23×10^{-5}	938.4	$44,328.05\times10^{-6}$
032266-34-32	0.01190	0.83	0.00491	0.072	1.20×10^{-5}	339.9	661.04×10^{-6}
032266-34-33	0.01678	1.25	0.00460	0.072	1.19×10^{-5}	483.5	$2,328.17\times10^{-6}$

TABLE 8

SUMMARY OF THE BURNING RATE DATA AND RESULTS
DOWNSTREAM FLAME OF THE PROXIMATE FIRES

Run No.	Burning Parameters			Dimensionless Groups	
	Fuel Burning Rate	Depth of the Flaming Zone	Fuel Burning Rate per Unit Area	$\frac{\dot{m}D}{\mu_a}$	$\frac{gD^3\rho_a^2}{\mu_a^2}$
	lb/sec	ft	lb/ft^2-sec	dimensionless	dimensionless
120365-1-4	0.00559	0.50	0.00383	160.9	153.15×10^{-6}
120365-1-5	0.00751	0.50	0.00515	216.5	153.98×10^{-6}
120365-1-6	0.00774	0.62	0.00428	223.0	295.12×10^{-6}
120365-1-7	0.00842	0.50	0.00577	242.5	156.08×10^{-6}
120865-3-8	0.02028	1.50	0.00463	579.4	3977.96×10^{-6}
121465-2-9	0.00757	0.29	0.00895	222.0	31.17×10^{-6}
121465-2-10	0.00722	0.42	0.00589	211.5	96.99×10^{-6}
121465-2-11	0.00767	0.50	0.00526	224.7	164.50×10^{-6}
121665-16-12	0.00784	0.50	0.00537	229.6	165.82×10^{-6}
121665-16-14	0.00848	0.58	0.00501	248.4	260.19×10^{-6}
010766-14-15	0.00741	0.33	0.00770	213.5	45.19×10^{-6}
010766-14-16	0.00824	0.33	0.00856	239.3	46.34×10^{-6}
011166-11-18	0.00758	0.33	0.00787	218.3	43.99×10^{-6}
012866-19-21	0.01440	1.00	0.00494	422.0	1340.69×10^{-6}
012866-19-22	0.00791	0.58	0.00467	242.0	316.62×10^{-6}
012866-19-23	0.01620	1.67	0.00333	495.9	7558.37×10^{-6}
030466-23-24	0.00831	0.42	0.00678	245.6	101.31×10^{-6}
030466-23-25	0.00954	0.58	0.00564	279.5	261.57×10^{-6}
031466-39-26	0.00655	0.25	0.00898	187.0	18.64×10^{-6}
031466-39-27	0.00716	0.42	0.00584	204.6	88.55×10^{-6}
031466-39-28	0.00838	0.42	0.00684	239.5	87.82×10^{-6}
031766-29-29	0.01094	1.00	0.00375	305.0	1042.83×10^{-6}
031866-31-30	0.00774	0.33	0.00804	221.0	42.66×10^{-6}
032166-33-31	0.03294	3.25	0.00347	917.9	35491.49×10^{-6}
032266-27-32	0.00770	0.33	0.00800	219.9	41.50×10^{-6}
032266-27-33	0.01034	0.50	0.00709	298.0	149.00×10^{-6}

TABLE 9

SUMMARY OF THE FLAME LENGTH, FLAME HEIGHT AND RATE OF SPREAD DATA--SINGLE FLAME

Run No.	Flame Length ft	Flame Height ft	Experimental Rate of Spread ft/sec	Calculated Rate of Spread ft/sec
030766-20-1A	1.083	1.083	8.47×10^{-4}	9.14×10^{-4}
030766-20-2A	1.417	1.333	11.39×10^{-4}	11.33×10^{-4}
030766-20-3A	2.833	1.417	50.56×10^{-4}	38.47×10^{-4}
030766-22-4A	3.083	1.333	44.72×10^{-4}	54.02×10^{-4}
030866-25-5A	1.417	1.250	14.44×10^{-4}	14.67×10^{-4}
030866-25-6A	2.167	1.417	37.64×10^{-4}	38.71×10^{-4}
030866-26-7A	1.417	1.250	15.56×10^{-4}	13.78×10^{-4}
030866-26-8A	2.500	1.417	41.39×10^{-4}	38.45×10^{-4}
030966-37-9A	1.500	1.333	14.03×10^{-4}	16.42×10^{-4}
030966-37-10A	2.917	1.333	57.36×10^{-4}	43.44×10^{-4}
030966-36-11A	3.167	1.333	53.61×10^{-4}	58.24×10^{-4}
031566-40-12A	1.250	1.250	10.56×10^{-4}	10.31×10^{-4}
031566-40-13A	1.333	1.250	10.97×10^{-4}	12.57×10^{-4}
031566-40-14A	1.333	1.333	11.54×10^{-4}	11.85×10^{-4}

TABLE 10

SUMMARY OF FLAME LENGTH, FLAME HEIGHT, AND RATE OF SPREAD DATA--UPSTREAM FLAME OF THE PROXIMATE FIRES

Run No.	Flame Length ft	Flame Height ft	Experimental Rate of Spread ft/sec	Calculated Rate of Spread ft/sec
120365-4-4	2.000	1.500	16.11×10^{-4}	22.78×10^{-4}
120365-4-5	1.833	1.500	19.03×10^{-4}	18.76×10^{-4}
120365-4-6	1.917	1.667	19.31×10^{-4}	24.76×10^{-4}
120365-4-7	--	--	12.78×10^{-4}	16.20×10^{-4}
120865-3-8	2.417	1.333	22.50×10^{-4}	28.50×10^{-4}
121465-15-9	1.667	1.500	16.11×10^{-4}	19.70×10^{-4}
121465-15-10	1.667	1.500	20.14×10^{-4}	19.55×10^{-4}
121465-15-11	2.083	1.583	15.56×10^{-4}	21.41×10^{-4}
121665-13-12	1.917	1.417	21.94×10^{-4}	24.64×10^{-4}
121665-13-13	1.917	1.500	17.64×10^{-4}	26.57×10^{-4}
121665-13-14	1.750	1.333	13.89×10^{-4}	17.89×10^{-4}
010766-35-15	1.750	1.500	15.42×10^{-4}	14.34×10^{-4}
010766-35-16	2.250	1.500	20.42×10^{-4}	22.35×10^{-4}
011166-12-17	2.083	1.417	16.39×10^{-4}	14.25×10^{-4}
011166-12-18	1.917	1.500	17.36×10^{-4}	22.44×10^{-4}
011466-10-19	3.167	1.417	25.28×10^{-4}	27.41×10^{-4}
012566-8-20	2.250	1.417	28.06×10^{-4}	42.48×10^{-4}
012866-21-21	3.000	1.417	34.30×10^{-4}	42.91×10^{-4}
012866-21-22	2.417	1.417	25.83×10^{-4}	33.27×10^{-4}
012866-21-23	2.500	1.417	----	33.03×10^{-4}
030466-24-24	1.750	1.333	17.36×10^{-4}	19.14×10^{-4}
030466-24-25	1.750	1.167	$24.30 \times .0^{-4}$	24.30×10^{-4}
031466-38-26	1.583	1.333	12.22×10^{-4}	13.98×10^{-4}
031466-38-27	1.417	1.250	13.06×10^{-4}	15.40×10^{-4}
031466-38-28	1.417	1.167	13.33×10^{-4}	16.54×10^{-4}
031766-28-29	2.750	1.167	38.33×10^{-4}	41.17×10^{-4}
031866-30-30	1.917	1.417	26.25×10^{-4}	30.02×10^{-4}
032166-32-31	3.167	1.333	39.72×10^{-4}	48.70×10^{-4}
032266-34-32	1.583	1.417	15.97×10^{-4}	17.21×10^{-4}
032266-34-33	1.833	1.417	19.44×10^{-4}	24.28×10^{-4}

TABLE 11

SUMMARY OF THE FLAME LENGTH, FLAME HEIGHT, AND RATE OF SPREAD DATA--DOWNSTREAM FLAME OF THE PROXIMATE FIRES

Run No.	Flame Length ft	Flame Height ft	Experimental Rate of Spread ft/sec	Calculated Rate of Spread ft/sec
120365-1-4	1.417	1.417	7.50×10^{-4}	8.08×10^{-4}
120365-1-5	1.583	1.583	8.47×10^{-4}	10.87×10^{-4}
120365-1-6	1.333	1.333	9.03×10^{-4}	11.20×10^{-4}
120365-1-7	1.500	1.500	3.89×10^{-4}	12.17×10^{-4}
120865-3-8	2.667	1.750	42.36×10^{-4}	29.33×10^{-4}
121465-2-9	1.667	1.667	11.11×10^{-4}	10.96×10^{-4}
121465-2-10	1.500	1.500	10.00×10^{-4}	10.44×10^{-4}
121465-2-11	1.417	1.417	11.94×10^{-4}	11.09×10^{-4}
121665-16-12	1.583	1.583	11.94×10^{-4}	11.33×10^{-4}
121665-16-13	1.333	1.333	9.72×10^{-4}	12.28×10^{-4}
121665-16-14	1.750	1.750	12.78×10^{-4}	12.26×10^{-4}
010766-14-15	1.417	1.417	10.42×10^{-4}	10.72×10^{-4}
010766-14-16	1.500	1.500	11.39×10^{-4}	11.91×10^{-4}
011166-11-17	1.333	1.333	8.33×10^{-4}	----
011166-11-18	1.583	1.583	11.11×10^{-4}	10.96×10^{-4}
011466-9-19	1.833	1.750	14.03×10^{-4}	15.39×10^{-4}
012566-7-20	2.250	1.333	----	27.83×10^{-4}
012866-19-21	1.583	1.333	13.33×10^{-4}	20.83×10^{-4}
012866-19-22	1.417	1.417	11.80×10^{-4}	11.44×10^{-4}
012866-19-23	2.083	1.417	----	23.44×10^{-4}
030466-23-24	1.417	1.417	10.14×10^{-4}	12.02×10^{-4}
030466-23-25	1.750	1.417	12.92×10^{-4}	13.80×10^{-4}
031466-39-26	1.250	1.250	8.19×10^{-4}	9.47×10^{-4}
031466-39-27	1.250	1.250	9.17×10^{-4}	10.36×10^{-4}
031466-39-28	1.417	1.417	10.00×10^{-4}	12.12×10^{-4}
031766-29-29	1.583	1.333	18.33×10^{-4}	15.83×10^{-4}
031866-31-30	1.417	1.417	11.39×10^{-4}	11.19×10^{-4}
032166-33-31	2.500	1.417	34.30×10^{-4}	47.64×10^{-4}
032266-27-32	1.500	1.500	10.97×10^{-4}	11.13×10^{-4}
032266-27-33	1.500	1.417	12.92×10^{-4}	14.96×10^{-4}

TABLE 12

SUMMARY OF FLAME BENDING DATA--
SINGLE FIRES

Run No.	Wind Velocity ft/sec	Air Temperature °R	Flame Optical Temperature °R	Flame Angle degrees	Flame Model Coefficient
030766-20-1A	0.00	507	2400	0	--
030766-20-2A	1.43	508	2495	18	2.14
030766-20-3A	2.33	510	2540	59	31.87
030766-22-4A	4.09	516	2530	64	18.49
030866-25-5A	1.77	509	2455	32	3.00
030866-25-6A	2.53	508	2570	49	12.39
030866-26-7A	1.64	514	2470	31	3.32
030866-26-8A	2.55	515	2555	56	22.36
030966-37-9A	1.65	517	2465	26	2.94
030966-37-10A	2.77	521	2560	62	23.41
030966-36-11A	2.98	525	2600	65	47.75
031566-40-12A	1.26	530	2395	8	0.74
031566-40-13A	1.46	531	2415	24	2.87
031566-40-14A	0.84	531	2390	7	1.45

TABLE 13

SUMMARY OF FLAME BENDING DATA--UPSTREAM FLAME OF THE PROXIMATE FIRES

Run No.	Wind Velocity ft/sec	Air Temperature °R	Flame Optical Temperature °R	Flame Angle degrees	Flame Model Coefficient
120365-4-4	2.08	520	2435	42	6.17
120365-4-5	2.51	519	2479	34	2.46
120365-4-6	2.50	517	2484	31	3.57
120365-4-7	2.61	515	2410	--	--
120865-3-8	3.53	524	2540	57	7.25
121465-15-9	1.07	507	2450	25	8.60
121465-15-10	0.75	506	2515	27	17.58
121465-15-11	0.70	505	2495	40	43.04
121665-13-12	2.53	505	2535	41	4.64
121665-13-13	2.57	504	2600	40	4.82
121665-13-14	2.46	504	2515	41	3.04
010766-35-15	1.61	514	2500	31	7.47
010766-35-16	1.33	512	2560	48	26.09
011166-12-17	1.99	514	2600	47	11.08
011166-12-18	1.92	515	2610	38	6.95
011466-10-19	4.07	514	2600	63	18.53
012566-8-20	4.33	493	2600	55	6.93
012866-21-21	5.13	504	2580	62	7.58
012866-21-22	3.45	478	2540	55	8.20
012866-21-23	4.31	478	2600	57	8.32
030466-24-24	2.81	502	2582	39	3.43
030466-24-25	2.96	509	2540	50	5.90
031466-38-26	2.19	523	2460	32	2.26
031466-38-27	2.08	523	2505	31	2.76
031466-38-28	1.97	525	2500	34	4.00
031766-28-29	4.15	538	2520	65	21.80
031866-30-30	3.91	521	2610	43	3.76
032166-32-31	6.20	538	2600	65	--
032266-34-32	1.79	522	2540	29	4.20
032266-34-33	3.00	518	2570	38	3.54

TABLE 14

SUMMARY OF FLAME BENDING DATA--DOWNSTREAM FLAME OF THE PROXIMATE FIRES

Run Number	Flame Optical Temperature °R	Flame Angle degrees	Distance Between Centers of the Fires ft
120365-1-4	2410	2	5
120365-1-5	2410	6	4
120365-1-6	2426	11	3
120365-1-7	2380	5	2
120865-3-8	2460	49	2
121465-2-9	2405	6	5
121465-2-10	2425	9	4
121465-2-11	2420	7	3
121665-16-12	2460	3	4
121665-16-13	2552	4	3
121665-16-14	2500	8	2
010766-14-15	2480	7	5
010766-14-16	2490	13	4
011166-11-17	2480	0	4
011166-11-18	2520	2	3
011466-9-19	2490	15	4
012566-7-20	2550	54	3.75
012866-19-21	2520	31	5
012866-19-22	2520	13	4
012866-19-23	2495	48	4
030466-23-24	2444	-2	4.16
030466-23-25	2465	36	3.33
031466-39-26	2385	-1	4.16
031466-39-27	2405	0	3.33
031466-39-28	2450	7	2.50
031766-29-29	2470	32	4.16
031866-31-30	2530	3	4.16
032166-33-31	2500	56	5
032266-27-32	2500	-2	5
032266-27-33	2460	19	3

INTERACTION EFFECTS OF WIND-BLOWN PROXIMATE FLAMES FROM BURNING WOOD CRIBS

By Joe Rios

Major Professor: C. M. Sliepcevich

Research on characteristics of free-burning fires has been increasing during recent years. Most of the studies have utilized single flames from solid, liquid or gaseous fuels. However, the largest amount of destruction and loss of life is usually caused by mass fires, i.e., fires made up of several separate units of fuel burning simultaneously. Some studies have been carried out to gain an insight of the phenomena occurring during the mass fires.

The present lack of basic information hinders the study of the effects of mass fires. The object of this study was to contribute such information. The case of two proximate fires burning under the action of wind was considered. Single fires were also burned under windy conditions to relate their behavior with that of the proximate fires. Wood cribs were utilized as the fuel. A weighing system was designed and built into the test section of a wind tunnel to use in recording burning rates. Essentially, the spacing between the two fires and the wind speed were varied. The size and arrangement of the fuel in the crib, its moisture content and the type of wood (yellow pine) were the same for all experiments.

As a result of these studies, it was concluded that: 1) the burning rate per unit area of the single fire as well as for each of two proximate fires can be correlated in terms of the depth of flaming zone only, irrespective of wind velocity and spacing between the fires; 2) total burning rate, flame length and propagation rates for single fires or each flame of proximate fires can also be correlated in terms of the depth of the flaming zone; 3) the rate of propagation can be predicted satisfactorily from burning rate and depth of flaming zone data for either single or proximate fires; 4) the burning rate correlation of this study is in reasonable agreement with a previous correlation for wood cribs burning in still air after correcting for differences in initially exposed surface area of the fuel and the fuel loading between the studies; 5) the burning rate correlation for wood cribs is approximately the same as for liquid fires reported by others, except that the latter has a larger exponent; 6) the mathematical model for flame bending of wind-blown fires can be applied to single fires

and the upstream flame of proximate fires by using the coefficients derived experimentally in this study; 7) the data on temperatures in the wake of the gases indicated that the wind tunnel walls, and particularly the ceiling, exerted a pronounced effect on the temperature profiles; and 8) steady state was not achieved with respect to radiation from the fires, even after steady state was reached in burning rate, temperature of the wake gases and rate of fire spread in that order.